

**STUDY ON THE PURIFICATION OF LIPID MEMBRANES
OF GIANT UNILAMELLAR VESICLES USING A LOCALLY
DEVELOPED LOW COST TECHNIQUE**

*A dissertation submitted to the Department of Physics, Bangladesh University of Engineering
and Technology, Dhaka in partial fulfillment of the requirements for the degree of*
MASTER OF SCIENCE (M.Sc.) IN PHYSICS

by

Mostafizur Rahman

Student ID.: 0417142519 F

Session: April, 2017



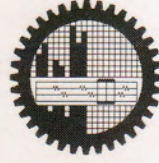
Department of Physics

BANGLADESH UNIVERSITY OF ENGINEERING AND TECHNOLOGY

DHAKA – 1000, BANGLADESH

July, 2019

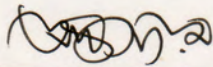
BANGLADESH UNIVERSITY OF ENGINEERING & TECHNOLOGY (BUET), DHAKA
DEPARTMENT OF PHYSICS



Certification of Thesis

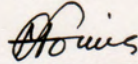
The thesis titled “**STUDY ON THE PURIFICATION OF LIPID MEMBRANES OF GIANT UNILAMELLAR VESICLES USING A LOCALLY DEVELOPED LOW COST TECHNIQUE**” submitted by **Mostafizur Rahman**, Roll No. 0417142519F, Session: April/2017, has been accepted as satisfactory in partial fulfillment of the requirement for the degree of **Masters of Science (M.Sc.)** in Physics on 20 July, 2019.

BOARD OF EXAMINERS



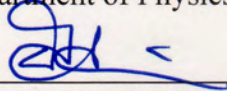
Dr. Mohammad Abu Sayem Karal (Supervisor)
Associate Professor
Department of Physics, BUET, Dhaka-1000

Chairman



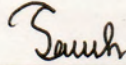
Dr. Md. Forhad Mina
Professor and Head
Department of Physics, BUET, Dhaka-1000

Member (Ex-Officio)



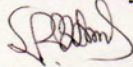
Dr. Md. Rafi Uddin
Professor
Department of Physics, BUET, Dhaka-1000

Member



Dr. Muhammad Samir Ullah
Assistant Professor
Department of Physics, BUET, Dhaka-1000

Member



Dr. Md. Mizanur Rahman
Professor
Department of Physics
University of Dhaka, Dhaka-1000

Member (External)

CANDIDATE'S DECLARATION

It is hereby declared that this thesis or any part of it has not been submitted elsewhere for the award of any degree or diploma.

Signature of the candidate

A rectangular box containing a handwritten signature in black ink. The signature appears to be 'M. Fiz' or similar, written in a cursive style.

Mostafizur Rahman

Student ID.: 0417142519 F

Session: April, 2017

DEDICATED
TO
MY BELOVED PARENTS
AND TEACHERS

ACKNOWLEDGEMENTS

First of all, I would like to convey my humble thanks to Almighty Allah for enabling me to complete this thesis with sound mind and health and I would appreciably like to acknowledge those who have contributed to complete my thesis within the time frame.

Foremost, I wish to express my heartfelt gratitude and sincere thanks to my honorable supervisor Dr. Mohammad Abu Sayem Karal, Associate Professor, Department of Physics, Bangladesh University of Engineering and Technology (BUET), Dhaka-1000, Bangladesh for giving me an opportunity to perform such a thesis work under his guidance. Throughout my MS study, his continuous guidance, encouragement, surveillance and kind attention have greatly changed me into hard worker and self-confident.

I am thankful to Prof. Dr. Md. Forhad Mina, Head, Department of Physics, BUET for providing me necessary facilities to carry out this research work. I am also thankful to Prof. Dr. Jiban Podder, Prof. Dr. Md. Feroz Alam Khan, Prof. Dr. A. K. M. Akther Hossain, Prof. Dr. Md. Mostak Hossain, Prof. Dr. Afia Begum, Prof. Dr. Md. Rafi Uddin, Prof. Dr. Nasreen Akter, Prof. Dr. Mohammed Abdul Basith for their inspiration and constructive suggestions.

I am extremely grateful to other teachers of Department of Physics, BUET, Dhaka-1000, Bangladesh, for their intellectual help and continuous inspiration throughout my research work. I would like to give special thanks to my friends Md. Kabir Ahamed, Marzuk Ahmed for their invaluable direct mental and physical help during research work. I would like to give cordial thanks to lab mates Md. Sayful Islam, Md. Mehedi Hasan, Shamor Kanti Roy, Mohammad Moniruz Zaman, Md. Kamrul Hasan, Md. Shareef Ahammed, Md. Mostofa Shakil, for their help and support.

I am also grateful to the authority of Department of Physics, BUET for providing me the logistic supports for this thesis work. Sincere acknowledgement to the Ministry of Science and Technology, Ministry of Education, University Grants Commission (UGC), Bangladesh and the Committee for Advanced Studies and Research (CASR),

BUET for granting the funds to carry out this research. Highly acknowledged to the Ministry of Science and Technology of Bangladesh for providing me the National Science and Technology Fellowship (NST) for the fiscal year 2018-2019 to carry out the research smoothly.

At last, I would like to thank and acknowledge my parents whose unlimited love and blissful inspiration were always with me, to lead me to success in my life. I am also thankful to my siblings, family members and relatives for their constant inspiration, support, sacrifices and help to complete the thesis successfully.

Mostafizur Rahman

July, 2019

ABSTRACT

Lipid membranes of giant unilamellar vesicles (GUVs) with diameters greater than 10 μm are promising model membranes for investigating the physical and biological properties of biomembranes of cells. To study the interaction of various membranes active agents like nanoparticles and peptides, elasticity of membrane, shape change, phase change, membrane rupture, electroporation, purified and similar-sized oil-free GUVs are necessary. In the proposed technique, the gravitational energy is used to continue the flow of buffer and a locally available low cost roller clamp regulator, which is used in medical sector to give saline into human body, is used to control the flow rate of buffer with GUVs suspension. This technique has been characterized in terms of size distribution, average size, flow rate and efficiency of dioleoylphosphatidylglycerol (DOPG)/dioleoylphosphatidylcholine (DOPC)-GUVs prepared by the natural swelling method. The GUVs were purified using three different flow rates 1.0, 1.5 and 2.0 mL/min. After purification of GUVs, the diameters of 300-400 GUVs have been measured and plotted a histogram. The histograms are fitted with a theoretical equation and the fitting is evaluated by the co-efficient of determination (R^2). In each case, the values of R^2 were more than 0.90. The average diameter of unpurified and purified GUVs is calculated by taking mean and variance from the histogram. Before purification, the average sizes of GUVs of two independent experiments are $10. \pm 0.7$, 11.2 ± 3.7 and $8.8 \pm 0.4 \mu\text{m}$. Whereas the average sizes of purified GUVs of two independent experiments are 16.9 ± 0.8 , 18.7 ± 0.3 and $20.0 \pm 0.1 \mu\text{m}$ for the flow rates 1.0, 1.5 and 2.0 mL/min. respectively. After purification, the average sizes of GUVs are increased because the smaller GUVs are passed away through the filter during the purification. In well reported membrane filtering method, the average sizes of unpurified GUVs of two independent experiments are 8.1 ± 0.8 , 11.3 ± 4.3 and $7.7 \pm 0.3 \mu\text{m}$ and the average sizes of purified GUVs of two independent experiments are 17.6 ± 2.1 , 19.7 ± 1.2 and $20.0 \pm 0.1 \mu\text{m}$ for the flow rates 1.0, 1.5 and 2.0 mL/min. respectively. It illustrates that the new technique gives the similar results within the error bar to that of membrane filtering method. So, it can be declared that this technique can perform the purification of GUVs using only gravity without any electromechanical devices and the apparatuses are repeatedly usable. This technique is ecofriendly, time saving and cost effective. Therefore, it will be a low cost non-electromechanical future tool for the purification of GUVs with using gravity.

CONTENTS	Page No.
ACKNOWLEDGEMENTS	iv
ABSTRACT	vi
LIST OF FIGURES	xi
LIST OF TABLES	xiii
LIST OF ABBREVIATIONS	xiv

INDEX

CHAPTER 1 INTRODUCTION

1.1	Background of the Study	01
1.2	Objectives of the Thesis	05
1.3	Outline of the Thesis	05

CHAPTER 2 THEORETICAL BACKGROUND

2.1	Biomembrane	07
2.2	Lipid Molecule	08
2.3	Lipid Membrane	10
2.4	Liposomes	11
2.4.1	Classification of liposomes	12
2.5	Method of GUV Synthesis	13
2.5.1	Electroformation	13
2.5.2	Solid hydration method	15
2.5.3	Emulsion droplets transfer	16
2.5.3.1	Water-in Oil (W/O) emulsion droplets formed by vortexing	17
2.5.3.2	Microfluidics to produce uniform W/O emulsion	18

2.5.3.3	Transferring emulsion droplets to GUVs	19
2.5.4	Inverted emulsion droplets method	19
2.5.5	Lipid coated ice droplet hydration	22
2.6	Literature review	24
2.7	Purification	25
2.7.1	Necessity of purification	25
2.8	Purification Techniques	26
2.8.1	Dialysis	26
2.8.2	Centrifugation	27
2.8.3	Microfiltration technique	28
2.8.4	Membrane filtering method	30

CHAPTER 3

EXPERIMENTAL TECHNIQUES

3.1	Chemicals and Reagents	32
3.2	Preparation of Buffer and Solution	35
3.2.1	Physiological buffer	35
3.2.2	Internal solution of the GUVs	35
3.2.3	External solution of the GUVs	35
3.3	Synthesis of Lipid Membranes of GUVs	35
3.3.1	Schematic representation of GUV synthesis	36
3.3.2	Flow chart of GUV preparation	37
3.3.3	Preparation of 1mM 40%DOPG + 60%DOPC	38
3.3.4	Dry with N ₂ stream	38
3.3.5	Fine dry at vacuum desiccator	39
3.3.6	Pre-hydration at 45 °C	39

3.3.7	Incubation at 37 °C for 2.5 to 3 h	40
3.3.8	Centrifugation at 13000 RCF	40
3.4	Equipment for Purification	41
3.4.1	Syringe	41
3.4.2	Regulators	41
3.4.3	Pipe	42
3.4.4	Fittings	42
3.4.5	Filter holder	43
3.4.6	Filter paper	43
3.4.7	Stop cock	44
3.4.8	Peristaltic pump	44
3.5	Method of Purifying Lipid Membranes of GUVs	45
3.5.1	Non-electromechanical method	45
3.5.2	Membrane filtering method	47
3.6	Observation of GUVs	49
3.6.1	GUVs suspension in microchamber	49
3.6.2	Inverted phase contrast microscope (IX-73)	49
3.7	Statistical Analysis using Lognormal Distribution	51

CHAPTER 4

RESULTS AND DISCUSSION

4.1	Effects of filtering on the size distribution and average size of GUVs at flow rate 1.0 mL/min using non-electromechanical technique	53
4.2	Effects of filtering on the size distribution and average size of GUVs at flow rate 1.0 mL/min using membrane filtering method	56
4.3	Effects of filtering on the size distribution and average size of GUVs at flow rate 1.5 mL/min using non-electromechanical technique	58
4.4	Effects of filtering on the size distribution and average size of GUVs at flow rate 1.5 mL/min using membrane filtering method	60
4.5	Effects of filtering on the size distribution and average size of GUVs at flow rate 2.0 mL/min using non-electromechanical technique	62
4.6	Effects of filtering on the size distribution and average size of GUVs at flow rate 2.0 mL/min using membrane filtering method	64

4.7	Effects of second purification on the size distribution and average size of GUVs using non-electromechanical technique	66
4.8	Effects of flow rate on the size distribution and average size of GUVs	68
4.9	Effects of higher flow rate on the size distribution and average size of GUVs in the non-electromechanical technique	71
4.10	Flow rate dependent efficiency of the purification of GUVs	73
4.11	Direct comparison of the present technique with other methods	74

CHAPTER 5 CONCLUSIONS

5.0	Conclusions	77
5.1	Recommendations	80

CHAPTER 6 REFERENCES

6.0	References	81
	Appendix	

LIST OF FIGURES

Fig. 2.1	Biomembrane	07
Fig. 2.2	Lipid molecule and molecular structure of lipid	09
Fig. 2.3	Lipid membrane	10
Fig. 2.4	Unilamellar and multilamellar vesicles	12
Fig. 2.5	Different types of unilamellar vesicles	12
Fig. 2.6	GUV formation in a chamber	14
Fig. 2.7	Schematic representation of formation of GUVs in solid hydration method	15
Fig. 2.8	Emulsion droplets transfer	16
Fig. 2.9	W/O emulsion droplets formed by vortexing	17
Fig. 2.10	Microfluidics to produce uniform W/O emulsion	18
Fig. 2.11	Transferring emulsion droplets to GUVs	19
Fig. 2.12	Inverted emulsion droplets method	20
Fig. 2.13	Schematic diagram of lipid coated ice droplet hydration	23
Fig. 2.14	Schematic diagram of dialysis	26
Fig. 2.15	Centrifugation	27
Fig. 2.16	Purification of giant vesicles by microfiltration	29
Fig. 2.17	The apparatus for the membrane filtering method	31
Fig. 3.1	Schematic diagram of GUV synthesis	36
Fig. 3.2	Preparation of 1mM 40%DOPG + 60%DOPC	38
Fig. 3.3	Dry with N ₂ stream	38
Fig. 3.4	Fine dry at vacuum desiccator	39
Fig. 3.5	Pre-hydration at 45 °C	39
Fig. 3.6	Incubation at 37 °C for 2.5 to 3 h	40
Fig. 3.7	Centrifugation at 13000 RCF	40
Fig. 3.8	Syringe	41
Fig. 3.9	Regulators	41
Fig. 3.10	Pipe	42
Fig. 3.11	Fittings	42
Fig. 3.12	Filter holder	43
Fig. 3.13	Filter paper	43

Fig. 3.14	Stop cock	44
Fig. 3.15	Double headed peristaltic pump	44
Fig. 3.16	Set-up for the purification of GUVs using a locally developed low cost non-electromechanical technique	46
Fig. 3.17	Set-up of membrane filtering method	48
Fig. 3.18	GUVs suspension in microchamber	49
Fig. 3.19	Observation of GUVs suspension under inverted phase contrast microscope (IX-73)	50
Fig. 3.20	Lognormal distribution	51
Fig. 4.1	Effects of filtering on the size distribution and average size of the GUV _S at flow rate 1.0 mL/min. using non-electromechanical technique	54
Fig. 4.2	Effects of filtering on the size distribution and average size of the GUV _S at flow rate 1.0 mL/min. using membrane filtering method	57
Fig. 4.3	Effects of filtering on the size distribution and average size of the GUV _S at flow rate 1.5 mL/min. using non-electromechanical technique	59
Fig. 4.4	Effects of filtering on the size distribution and average size of the GUV _S at flow rate 1.5 mL/min. using membrane filtering method	61
Fig. 4.5	Effects of filtering on the size distribution and average size of the GUV _S at flow rate 2.0 mL/min using non-electromechanical technique	63
Fig. 4.6	Effects of filtering on the size distribution and average size of the GUV _S at flow rate 2.0 mL/min. using membrane filtering method	65
Fig. 4.7	Effects of second purification on the size distribution and average size of the GUVs	67
Fig. 4.8	Effects of flow rate on the size distribution and average size of the GUVs	69
Fig. 4.9	Flow rate dependent average size of purified GUVs	71
Fig. 4.10	Effects of filtering on size distribution histogram of the GUVs at flow rate 3.0 mL/min	72
Fig. 4.11	Bar diagram of the average size of the unpurified and flow rate dependent purified GUVs	75

LIST OF TABLES

Table 1	Flow rate dependent average size of GUVs	73
Table 2	Flow rate dependent efficiency of the purification of GUVs	74
Table 3	Comparison of methods for the purification of GUVs	76

LIST OF ABBREVIATIONS

SYMBOL	ABBREVIATION
GUV	Giant Unilamellar Vesicle
LUV	Large Unilamellar Vesicle
SUV	Small Unilamellar Vesicle
DOPC	1, 2-Dioleoyl-sn-glycero-3-phosphocholine
DOPG	1, 2-dioleoyl-sn-glycero-3-phospho-(1'-rac-glycerol)
POPC	1-palmitoyl-2-oleoyl-sn-glycero-3-phosphocholine
DMPC	1,2-Dimyristoyl-sn-glycero-3-phosphocholine
POPG	2-oleoyl-1-palmitoyl-sn-glycero-3-glycerol
DMPC	1,2-dimyristoyl-sn-glycero-3-phosphocholine
Chol.	Cholesterol
Tris.	Trisaminomethane
SA	Stearylamine
PDMS	Polydimethylsiloxane
EGTA	Ethyleneglycol- N, N, N', N',-tetraacetic acid
BSA	Bovine serum albumin
ITO	Indium Tin Oxide
PEG-6000	Polyethylene Glycol-6000
KOH	Potassium Hydroxide
W/O	Water-in-Oil
RCF	Relative Centrifugal Force
GV	Giant Vesicle
O-Solution	Outer Solution
I-Solution	Inner Solution
CCD	Charge-Coupled Device
d_{ave}	Average diameter of GUV
\overline{d}_{ave}	Average size of GUV

CHAPTER 1

INTRODUCTION

1.1 Background of the Study

All living creatures are made of cells. One cellular component, the membrane, plays a crucial role in almost all cellular activities. The primary function of all cell membranes is to act as barriers between the intracellular and extracellular environments, and as sites for diverse biochemical activities. The cell itself is encapsulated by its own membrane, the plasma membrane. Although the composition of membranes varies, in general, lipid molecules make up approximately 40 percent of their dry weight; proteins, approximately 60 percent. The lipids and proteins are held together by noncovalent interactions.

Among several possible stable arrangements of protein and lipid molecules in membranes, the bilayer model, first described over seventy years ago, characterizes most biological membranes. An important feature of this model is that the hydrophilic groups of the lipid molecules are oriented toward the surfaces of the bilayer, and the hydrophobic groups toward the interior. In 1972 Jonathan Singer and Garth Nicolson postulated a unified theory of membrane structure called the fluid-mosaic model. They proposed that the matrix, or continuous part, of membrane structure is a fluid bilayer, and that globular amphiphilic proteins are embedded in a single monolayer, with some proteins spanning the thickness of both monolayers. Both proteins and lipids are mobile and, thus, the membrane can be viewed as a two-dimensional solution of proteins in lipids. In addition to phospholipids, two other kinds of lipids are found in the membranes of animal cells: glycolipids and cholesterol. Glycolipids usually make up only a small fraction of the lipids in the membrane but have been shown to possess many biological functions, one of which is their capacity to function as recognition sites. Cholesterol is an important component of plasma membranes and has been shown to play a key role in the control of membrane fluidity. The lipid membrane is a thin polar membrane made of two layers of phospholipid molecules. These membranes are flat sheets that form a continuous barrier around all cells. For avoiding complexity of biomembranes, the scientists use lipid membranes to

study the different biophysical properties and interactions. When a lipid membrane forms a spherical compartment in aqueous solution then it is known as vesicles. [20]. Vesicles are used as mimic of living cell to study biological systems, physical and chemical properties [21]. Vesicles are mainly two types: a) unilamellar vesicle which contains only one bilayer of lipid molecules and b) multi-lamellar vesicle which contains more than one bilayer of lipid molecules like as onion. Again, unilamellar vesicles are of three types:

- a) Small Unilamellar Vesicle (SUV) (size 20-100 nm)
- b) Large Unilamellar Vesicle (LUV) (size 100-1000 nm)
- c) Giant Unilamellar Vesicle (GUV) (size 1-200 μ m)

Vesicles are usually used to study the elasticity of membranes, shape change of vesicles by different membrane active agents, rupture formation by electroporation and mechanical tension, protein-membrane interactions, nanoparticles-membrane interactions, membrane permeability, drug delivery system, antimicrobial test, antibacterial test and many other cases.

Artificially synthesized lipid membranes have been considered as a mimic of biological membranes and therefore giant unilamellar vesicles (GUVs) with diameters equal to 10 μ m or more have been extensively used to investigate the biological and physical properties of membranes. Due to their cell-mimicking properties, GUVs are greatly used in different fields of biomimetic chemistry, biomembranes physics and artificial cell synthesis. Many studies focusing the mimicking biological membranes, for example by reconstituting membrane components of bilayers of GUVs, the preparation of giant vesicles with thin unilamellar walls and a defined size and shape is often required [9]. One of the most important applications of GUVs is that, these are used as a simple model systems for investigating certain physicochemical properties of biological membranes such as mechanical properties of the entire vesicle [10] or of the membrane, lipid domain formation, lipid dynamics, membrane growth [11–14]. The changes in the structure and physical properties of GUVs due to the interactions of antimicrobial peptides [21-23], cell penetrating peptides [24-26], toxics [27] and nanoparticles [28] have been observed as a function of temporal and spatial coordinates [29]. Now a days GUVs are intensively used for studying the interaction of different nano-particles and salts with the membrane of GUVs. Further again permeabilization

of GUVs applying electric field i.e the electroporation is interesting application of GUVs. Among the various methods for the preparation of GUVs [9], a novel technique called the “lipid-coated ice droplet hydration method” is synthesized of giant vesicles with a controlled size between 4 and 20 μm and entrapment yields for water-soluble molecules of up to about 30%. The method consists of three main steps. In the first step, a monodisperse water-in-oil emulsion with a predetermined average droplet diameter between 4 and 20 μm is prepared by microchannel emulsification, using sorbitan monooleate (Span 80) and stearylamine (SA) as emulsifiers and hexane as oil. In the second step, the water droplets of the emulsion are frozen and separated from the supernatant hexane solution by precipitation, followed by a removal of the supernatant and followed by the replacement of Span 80 by using a hexane solution containing egg yolk phosphatidylcholine, cholesterol, and stearylamine (5:5:1, molar ratio). This procedure is performed at $-10\text{ }^{\circ}\text{C}$ to keep the water droplets of the emulsion in a frozen state and thereby to avoid extensive water droplet coalescence. In the third step, hexane is evaporated at -4 to $-7\text{ }^{\circ}\text{C}$ and an external water phase is added to the remaining mixture of lipids and water droplets to form giant vesicles that have an average size in the range of that of the initial emulsion droplets (4-20 μm). This method can synthesize purified similar sized GUVs [30]. Water droplet transfer method or technique forms vesicles from lipids, mixed lipid and surfactant systems, and diblock copolymers. The stability of lipid-stabilized emulsions limits the range of sizes that can be produced and the vesicle yield; nevertheless, there are several advantages with this emulsion-based technique: It is possible to make unilamellar vesicles with sizes ranging from 100 nm to 1 μm . Moreover, the process allows for efficient encapsulation and ensures that the contents of the vesicles remain isolated from the continuous aqueous phase [31]. However, these methods contain significant amounts of hydrocarbon-oils which greatly affects the physicochemical properties and prevents to get actual biophysical properties of the lipid membranes [30]. On the other hand, in electroformation method, liposome formation and lipid swelling on platinum electrodes in distilled water and water solutions in d.c. electric fields have been inspected for unlike amounts of a negatively charged lipid, and a neutral lipid 1,2-dimyristoyl-sn-glycero-3-phosphocholine (DMPC). Negatively charged lipids do not form liposomes without field when the thickness of the dried lipid layer is of the order or less than that corresponding to 90

bilayers. The rate and extent of swelling of layers thicker than 90 bilayers is largest on the cathode, smaller without fields and smallest on the anode [32]. In the natural swelling method, GUVs are formed by rehydrating charged or neutral lipid or mixer of both in chloroform reagent [3,9]. Both the methods are highly popular for synthesis of GUVs because these can synthesize different sized oil-free GUVs with some non-entrapped solutes. Irrespective of the methods of GUVs preparation, the purification of GUVs is needed. Purification is the process of rendering something pure, i.e. clean of foreign elements and/or pollution. Besides this, purification means to remove the unwanted things from the desired sample. In case of the lipid membrane of GUVs, purification is to remove smaller GUVs, LUVs, lipid aggregates and various water-soluble substances like proteins and fluorescent probes. To investigate the elasticity, shape change, rupture formation and electroporation similar and cell sized GUVs are necessary. So, to get required quality of GUVs, purification is important. GUVs can generally be purified using dialysis [33] and differential centrifugation techniques. Dialysis works on the principles of the diffusion of solutes and ultrafiltration of fluid across a semi-permeable membrane. Diffusion is a property of substances in water; substances in water tend to move from an area of high concentration to an area of low concentration [7]. A semipermeable membrane is a thin layer of material that contains holes of various sizes, or pores. Smaller solutes and fluid pass through the membrane, but the membrane blocks the passage of larger substances. In the dialysis, a large volume of external solution has been needed to flow for several hours. Therefore, it is a time-consuming technique which hinder to get the high-quality purified GUVs suspension. The differential centrifugation generally takes 10 to 15 min, but it is required a high concentration of sucrose and glucose in the inside and the outside of GUVs, respectively. Therefore, more centrifugation rounds are necessary for getting the required GUVs suspension, which ultimately increase the overall purification time. To obtain the oil-free and similar sized GUVs, membrane filtering method is currently used [34]. In this method, peristaltic pump is necessary for controlling the flow and flow rate of buffer along with GUVs suspension. Very recently, a microfiltration technique has been developed for the rapid purification of GUVs in which a vacuum pump with a pressure regulator is connected to the flask for generating the pressure difference for the microfiltration [35]. Since these purification systems need

electromechanical devices, they have required a continuous supply of electricity during the purification. In this respect, a modification is applied in the membrane filtering method so that the system does not require any electrical or mechanical devices as well as electricity. The flow of the buffer in the purification unit is maintained using the gravity and the flow rate is controlled with a locally available roller clamp regulator. The new technique can purify GUVs without electricity and the apparatus can be used repeatedly. The technique has been characterized using size distribution, average size and efficiency of purifying GUVs at different flow rates. In addition, the results of the new technique have been compared to the membrane filtering method. Therefore, this simple and low cost non-electromechanical technique will be a promising future tool for the purification of lipid membranes of GUVs.

1.2 Objectives of the Thesis:

The objectives of this research project are as follows:

- i. Synthesis of lipid membranes of GUVs.
- ii. Development of low cost non-electromechanical technique for the purification of GUVs.
- iii. Effects of purification of GUVs suspension on the size distribution of GUVs.
- iv. Dependency of the efficiency of the purification of GUVs on the flow rate.
- v. Effects of double purification on the size distribution and average size of GUVs.
- vi. Comparison of the results of present work with that obtained from membrane filtering method.

1.3 Outline of the Thesis

The overall goal of the thesis work is to synthesis the GUVs using the natural swelling method and purifying them using low cost non-electromechanical purification technique.

Chapter 1: The introduction, motivation and outline of the thesis are discussed in this chapter.

Chapter 2: In this chapter, at first literature review of purification technique has been discussed and then describes the results of different purification techniques in details.

Chapter 3: The experimental setup for the synthesis process of GUVs using natural swelling method and the development of low cost non-electromechanical purification technique is described in detail here.

Chapter 4: The experimental results and discussions are presented here. A comparative study among different flow rates is discussed in this chapter. The statistical analysis of size distribution of unpurified and purified GUVs is also present here.

Chapter 5: The overall conclusion on the purification of GUVs by the low cost non-electromechanical technique is discussed here.

CHAPTER 2

THEORITICAL BACKGROUND

2.1 Biomembrane

Biomembrane is chemical and electrical enclosing or separating membrane that acts as a selectively permeable barrier within living things. Biological membranes, in the form of eukaryotic cell membranes, consist of a phospholipid bilayer with embedded integral and peripheral proteins used in communication and transportation of chemicals and ions. Glycoproteins, glycolipids and cholesterol are embedded with biomembrane bilayer. The bulk of lipid in a cell membrane provides a fluid matrix for proteins to rotate and laterally diffuse for physiological functioning. Proteins are adapted to high membrane fluidity environment of lipid bilayer with the presence of an annular lipid shell, consisting of lipid molecules bound tightly to surface of integral membrane proteins [36].

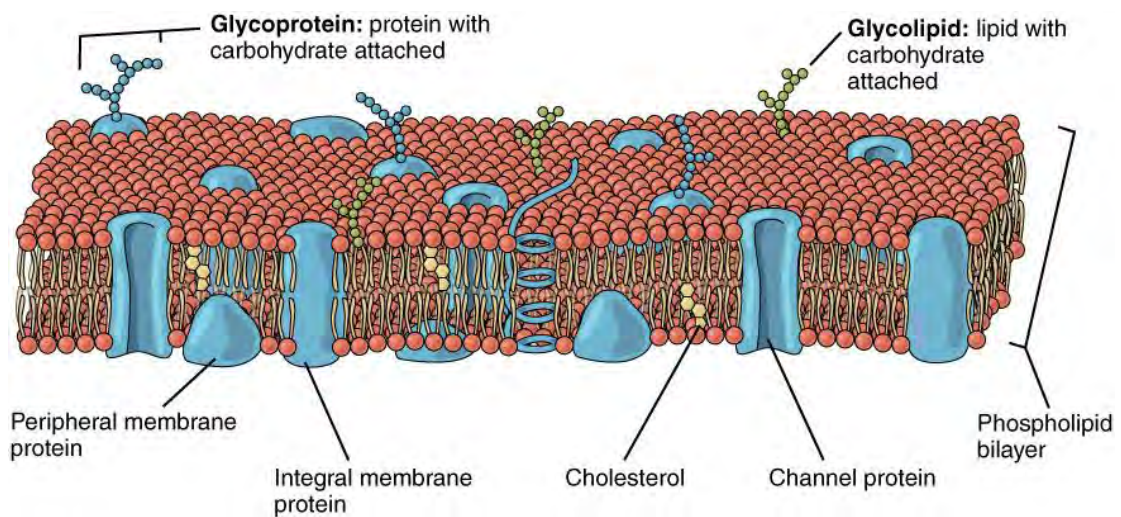


Fig. 2.1 Biomembrane [37]

Biomembrane is permeable only to very small molecules like water, oxygen and carbon dioxide and to a very small degree to polar compounds of hydrophobic molecules (e.g. amino acids, DNA, RNA, carbohydrates, proteins and ions). These molecules are either

transported into the cell via endo-cytosis or through membrane proteins that allow a controlled carriage through pores and channels or by active transport. The transmembrane transport of essential ions like Na^+ , K^+ , Ca^{2+} and Cl^- is largely controlled by the cell with ion pumps and exchangers. These enable the cell to build up chemical and electrical gradients. Under physiological conditions the cell keeps chemical gradients for Na^+ and K^+ across the cell membrane to facilitate the membrane potential that is vital to many cellular functions. The majority of cellular reactions is controlled by the Ca^{2+} signaling system and the concentration of free Ca^{2+} in the cytoplasm is under strict control. It is kept very low ($\sim 0.1 \mu\text{M}$) inside the cell, while the outside concentrations of free Ca^{2+} are multifold higher ($\sim 1.3 \text{ mM}$). High levels of intracellular ATP entertain the different active ports that maintain these gradients and sustain the energy-dependent cellular processes which the cell integrity depends on.

2.2 Lipid Molecule

Lipids form a major component of all types of biological membranes. The cytoplasmic membrane which is the limiting layer isolating the biological cell from the outer environment is present universally in all organisms. It consists mainly of a lipoprotein bilayer [9]. On the basis of chemical structure and constitution, lipids are broadly classified into two categories: i. simple lipids and ii. complex lipids. Simple lipids contain a trihydric alcohol, glycerol and long chain fatty acids. The carboxyl groups of the fatty acids are ester-linked to the hydroxyl groups of glycerol. The fatty acids present in simple lipids have generally 16 or 18 carbon atoms and they may be saturated or unsaturated. The unsaturated fatty acids, usually have one or two double bonds. Such lipids having three molecules of fatty acids esterified to glycerol are called triglycerides. It is important to note that the hydrophobic nature of fats and oils is due to the long-chain fatty acids which are highly insoluble in water and are strongly hydrophobic, though glycerol itself is a hydrophilic compound [38]. The lipid molecules are oriented in such a manner that the hydrophilic glycerol moieties remain in contact with water, while the fatty acid tails project inward to build a compact hydrophobic central zone. The same principle applies also in the formation of biological membranes in which the hydrophilic glycerol and protein molecules form a layer towards the outside and the lipid-tails remain inside. Thus, in a bilayer membrane, lipids

form the middle hydrophobic layer and glycerol and protein remain on two sides facing the outer and inner aqueous environment [39].

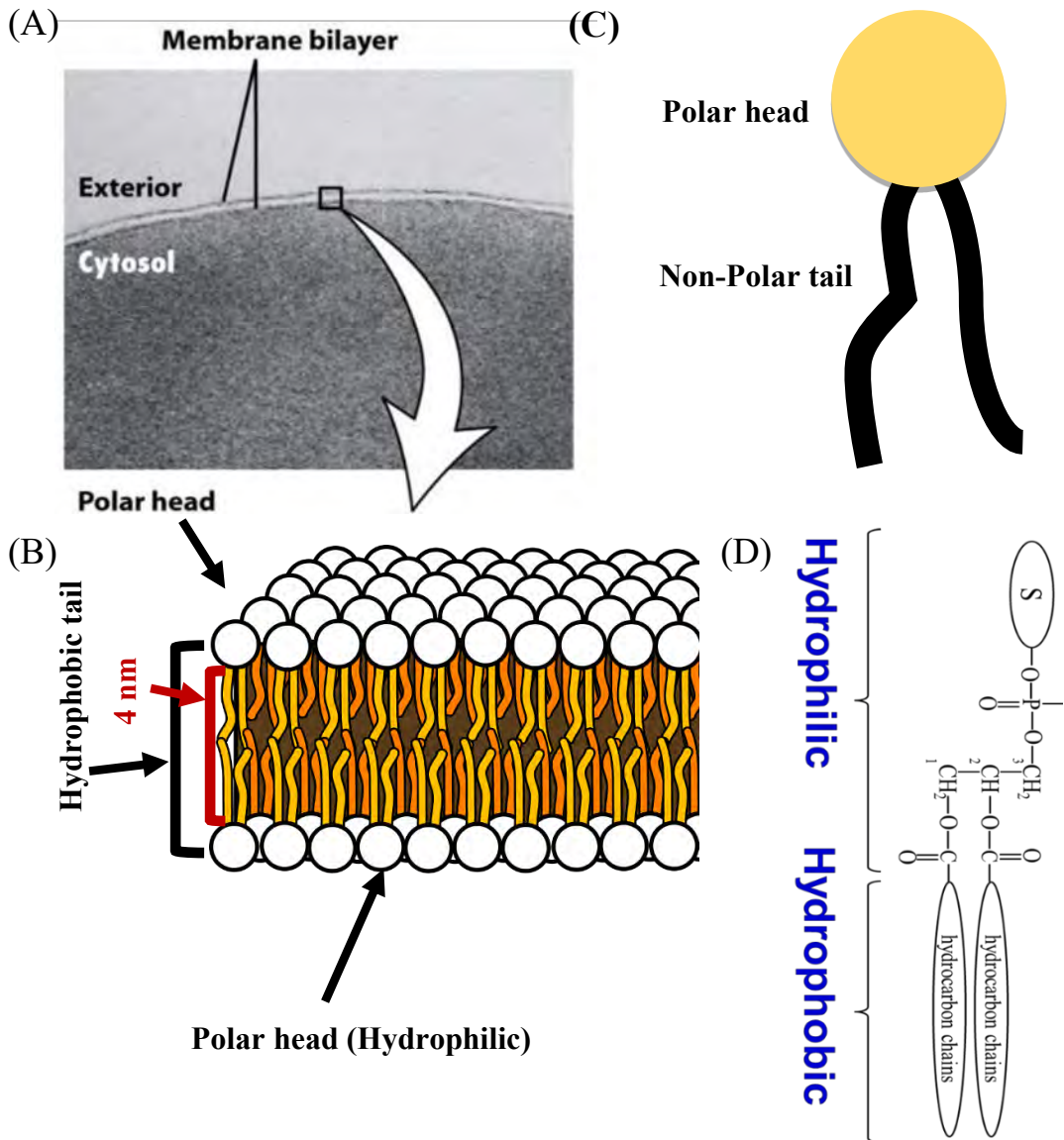


Fig. 2.2 A) Cell membrane. B) Lipid bilayer. C) Lipid molecule. D) Molecular structure of lipid molecule.

In contrast to simple lipids, the complex lipids contain elements like phosphorus, sulfur, nitrogen etc., besides carbon, hydrogen and oxygen which are present in all lipids. Phospholipids are a major constituent of the cell membranes of most of the organisms.

In a phospholipid molecule, two hydroxyl groups of glycerol are esterified with carboxyl groups of long chain fatty acids as in case simple lipids, while the third hydroxyl group of glycerol is esterified with phosphoric acid. Such a lipid is called a phosphatide. In most of the phospholipids, phosphoric acid is further linked to an organic group. Another group of complex lipids are steroids which are quite different in chemical structure from simple lipids [31]. The steroid nucleus contains three 6-membered and one 5-membered carbon rings. Steroids having an alcoholic (OH) group attached to one of the rings are known as sterols, e.g. cholesterol. Sterols are widely distributed in the plasma membranes of animals, plants and fungi, but not in bacteria.

2.3 Lipid Membrane

The lipid bilayer (or phospholipid bilayer) is a thin polar membrane made of two layers of lipid molecules. These membranes are flat sheets that form a continuous barrier around all cells. The cell membranes of almost all living organisms and many viruses are made of a lipid bilayer, as are the membranes surrounding the cell nucleus and other sub-cellular structures. The lipid bilayer is the barrier that keeps ions, proteins and other molecules where they are needed and prevents them from diffusing into areas where they should not be.

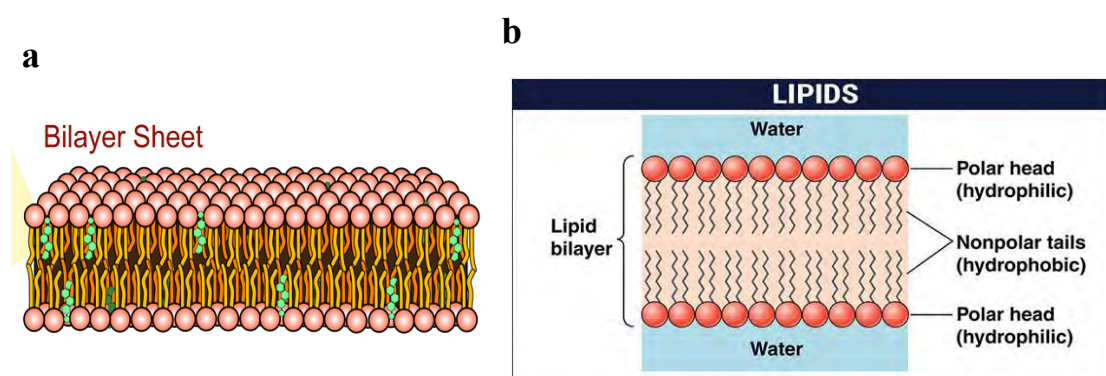


Fig. 2.3 a. 3D view of lipid bilayer b. 2D schematic diagram of lipid bilayer [40]

Lipid bilayers are ideally suited to this role, even though they are only a few nanometers in width, they are impermeable to most water-soluble (hydrophilic) molecules. Bilayers are particularly impermeable to ions, which allows cells to regulate salt concentrations

and pH by transporting ions across their membranes using proteins called ion pumps. Biological bilayers are usually composed of amphiphilic phospholipids that have a hydrophilic phosphate head and a hydrophobic tail consisting of two fatty acid chains. Phospholipids with certain head groups can alter the surface chemistry of a bilayer and can, for example, serve as signals as well as "anchors" for other molecules in the membranes of cells [29]. Just like the heads, the tails of lipids can also affect membrane properties, for instance by determining the phase of the bilayer. The bilayer can adopt a solid gel phase state at lower temperatures but undergo phase transition to a fluid state at higher temperatures, and the chemical properties of the lipids' tails influence at which temperature this happens. The packing of lipids within the bilayer also affects its mechanical properties, including its resistance to stretching and bending. Many of these properties have been studied with the use of artificial "model" bilayers produced in a lab. Vesicles made by model bilayers have also been used clinically to deliver drugs. Biological membranes typically include several types of molecules other than phospholipids. A particularly important example in animal cells is cholesterol, which helps strengthen the bilayer and decrease its permeability. Cholesterol also helps regulate the activity of certain integral membrane proteins. Integral membrane proteins function when incorporated into a lipid bilayer, and they are held tightly to lipid bilayer with the help of an annular lipid shell. Because bilayers define the boundaries of the cell and its compartments, these membrane proteins are involved in many intra- and inter-cellular signaling processes. Certain kinds of membrane proteins are involved in the process of fusing two bilayers together. This fusion allows the joining of two distinct structures as in the fertilization of an egg by sperm or the entry of a virus into a cell. Because lipid bilayers are quite fragile and invisible in a traditional microscope, they are a challenge to study. Experiments on bilayers often require advanced techniques like electron microscopy and atomic force microscopy.

2.4 Liposomes

A liposome is a spherical chamber/vesicle, bounded by bilayer of an amphiphilic lipids or a mixture of such lipids, containing aqueous solution inside the chamber [41]. Liposomes are used as mimic of living cell to study biological systems, physical and chemical properties [8]. Liposomes are also known as vesicles.

2.4.1 Classification of vesicle

Vesicles are two types based on their structure.

- 1) Unilamellar vesicle which contains only one bilayer of lipids.
- 2) Multilamellar vesicle which contains more than one lipid bilayers as like as onion.

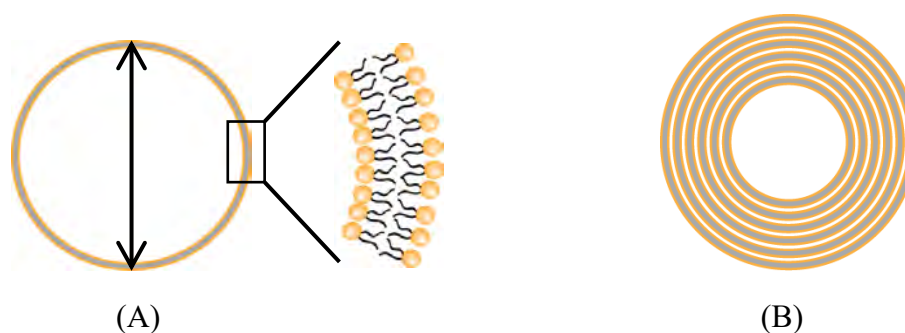


Fig. 2.4 (A) Unilamellar vesicle (B) Multilamellar vesicle

Again, unilamellar vesicles are classified into three types based on their sizes.

- 1) Small Unilamellar Vesicle (SUV) with size range of 20-100 nm
- 2) Large Unilamellar Vesicle (LUV) with size range of 100-1000 nm
- 3) Giant Unilamellar Vesicle (GUV) with size range of 1-200 μm .

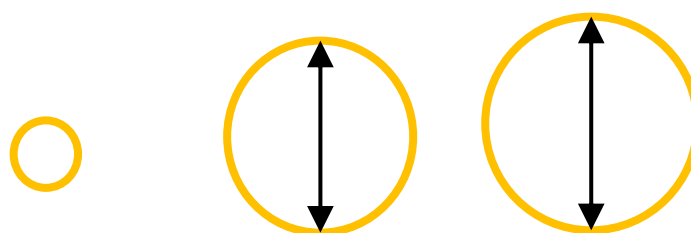


Fig. 2.5 Different types of unilamellar vesicles

GUVs are mostly used as models for biological membranes in research work [42]. The size of the animal and plant cells are typically 10–30 μm and 10–100 μm , respectively. Even the cell organelles of mitochondria are typically 1-2 μm . Therefore, an appropriate model membrane should consider for the size of the specimen being studied. In addition, the vesicles size indicates their membrane curvature which is a major factor for studying fusion proteins [10]. Smaller sized vesicles have a higher

membrane curvature and vesicles with high membrane curvature can prefer membrane fusion faster to vesicles with lower membrane curvature like GUVs [43]. The ingredients and properties of the cell membrane changes with different cells (plant cells, mammalian cells, bacterial cells, etc). In a membrane bilayer, often the formation of the phospholipids is different between the inner and outer leaflets. Some of the most common lipids of animal cell membranes are phosphatidylcholine, phosphatidylethanolamine, phosphatidylserine, phosphatidylinositol, and sphingomyelin. These lipids are extensively different in charge, length, and saturation state [1]. The presence of unsaturated bonds (carbon carbon double bonds) in lipids creates a kink in acyl chains which alters the lipid packing and results in a looser packing. Therefore, the compositions and sizes of the unilamellar vesicles must be chosen carefully based on the subject of the study.

2.5 Method of GUV Synthesis

There are many established methods for synthesizing GUVs. Some well reputed methods of them are elaborately described below.

2.5.1 Electroformation

Electroformation of GUVs is the process allowing the reproducible production of giant liposomes and therefore is quite often used in laboratories performing studies on model bilayers. This experimental set-up consists of the elements that are typically also used in other laboratories: the chamber with a temperature- controlling unit, AC electric generator and a confocal microscope. The chamber (see Fig 2.6A, B) and the temperature-controlling unit were designed and manufactured in laboratory. GUV preparation begins with covering the platinum electrodes with chloroform (or chloroform/methanol) solution of the appropriate lipid mixture, also containing the fluorescent dye. Typically, 1.3 mM lipid concentration is used and the solution contains 0.1 mol% of the fluorescent probe. The electrodes are then dried using nitrogen gas, and the remaining chloroform is also dried by placing the chamber in vacuum desiccator for at least 1 h. The temperature of the chamber is set to approximately 10 °C higher than the temperature of the main phase transition of the highest-melting lipid

used in the experiment [44]. GUVs are produced using sinusoidal wave of 10 Hz frequency and 3 V amplitude (peak-to-peak) which applied for at least one hour to two parallel platinum-wire electrodes (diameter 0.1 mm, placed at a distance of 2 mm) situated at the bottom of the Teflon cylindrical chamber presented in Fig. 2.6C.

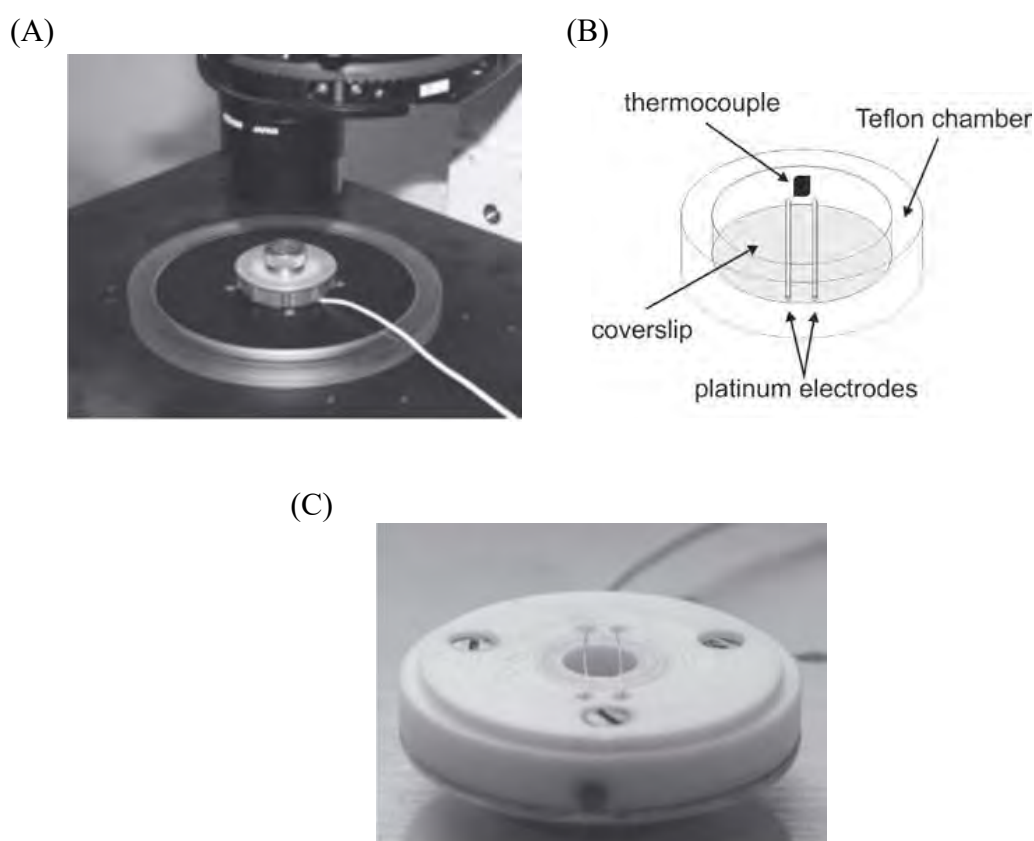


Fig. 2.6 GUV formation chamber. **A.** chamber placed on the support of an inverted microscope. **B.** scheme of the chamber. **C.** Teflon part of chamber (note that the chamber is turned upside-down) [44].

A thermocouple is placed in the wall of chamber, close to the electrodes [45]. The temperature of the chamber is controlled with 0.2 °C precision. Anyone can use indium tin oxide (ITO)-covered glass instead of the platinum electrodes. After the production of GUVs, the chamber temperature is lowered to the value at which the microscopic observations are carried out.

2.5.2 Solid hydration method

The GUV is the most desirable type of giant vesicle owing to its single bilayer shell. Multilamellar (“onion-like”) vesicles are more complicated and less amenable to theoretical analysis. Classical methods for preparing GUVs all have disadvantages including an unwanted production of multilamellar vesicles, fibers, “sausages”, and undefined lipid clumps. Among several published methods such as drying-rehydration [46], dialysis [47], freeze-thaw [48] and solid hydration [49], initially selected for studies. Since GUV photographs given herein have been prepared by solid hydration, the details of this particular procedure are presented. In the solid hydration method, a phospholipid or phospholipid mixture is dissolved in chloroform or methanol ($\text{CHCl}_3/\text{MeOH}$), whereupon the solvent is removed under reduced pressure. Adding deionized water to the dry film and vortexed it. Subsequent freezing and lyophilization affords a white fluffy powder. Giant vesicle synthesis is initiated by smearing 0.1 mg or less of the powder inside a Teflon outer-ring cemented onto a microscope slide. Approximately 0.5 mL of water is used to cover the powder, and the sample is allowed to hydrate for at least 30 min at 20 °C [50].

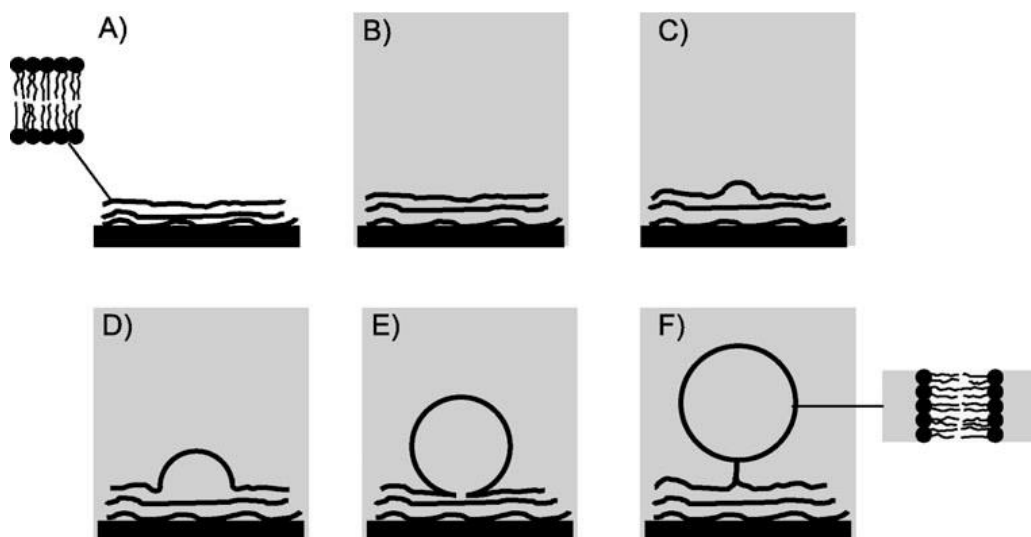


Fig. 2.7 Schematic representation of formation of GUVs in solid hydration method [50]

Solid hydration has three appealing attributes: (a) It is simple and requires no special equipment. (b) In our hands it produces fewer “unidentified swimming objects” than do many other methods. (c) Vesicles are confined to a small region near the bottom of the slide from where they originate.

2.5.3 Emulsion droplets transfer

Aqueous solution of the water phase of the emulsion droplets (inner solution) constitutes of 100 mM Hepes-KOH (pH 7.6), 150 mM sucrose, 350 mM glucose and 2.5 wt.% Polyethylene Glycol-6000 (PEG-6000), whereas that of the continuous aqueous phase of the GUV suspension (outer solution) contains 100 mM Hepes-KOH (pH 7.6) and 500 mM glucose. The specific density of the inner solution (1.08 g/cm^3) is slightly heavier than the outer solution (1.05 g/cm^3) to isolate the transferring process across the oil/water interface. PEG-6000 is included in the inner solution to get a better contrast during microscopic observation [51]. For the oil phase of the emulsion, liquid paraffin containing phospholipids and detergents is prepared.

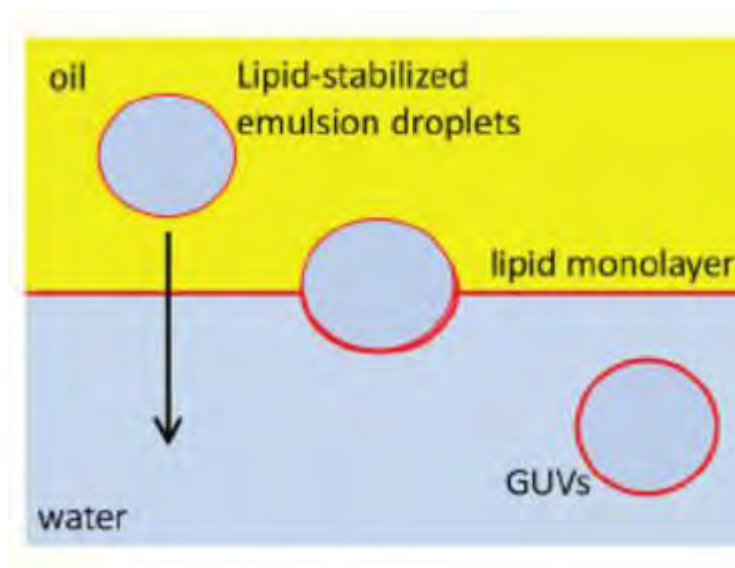


Fig. 2.8 Emulsion droplets transfer [51]

In the following text, oil 1 and oil 2 refer to the liquid paraffin containing detergents (1–5%v/v, Span 80 and Tween 80 at 9:1 volume ratio) and lipids (5 mg/mL, 1-

palmitoyl-2-oleoyl-sn-glycero-3-phosphocholine (POPC): 2-oleoyl-1-palmitoyl-sn-glycero-3-glycerol (POPG): Cholesterol (Chol) at 9:1:1 weight ratio), respectively. This lipid composition is used because a large number of dispersed GUVs are formed. The interfacial tension between the aqueous buffer and the paraffin with amphiphiles used in the experiment is measured by the pendant drop technique.

2.5.3.1 Water-in Oil (W/O) emulsion droplets formed by vortexing

For observing the basic aspects in vesicle formation at various compositions and conditions, the emulsion droplets prepared by the conventional vortexing method, which have broader size distribution than the droplets formed by the microfluidics, were used. For these experiments, a W/O emulsion was prepared by adding 100 μL of oil 1, 500 μL of oil 2, and 4 μL of the inner solution into a tube, which was then subjected to vortex agitation for 30 s using a vortex mixer (Vortex Genie 2, Scientific Industries, Inc.)

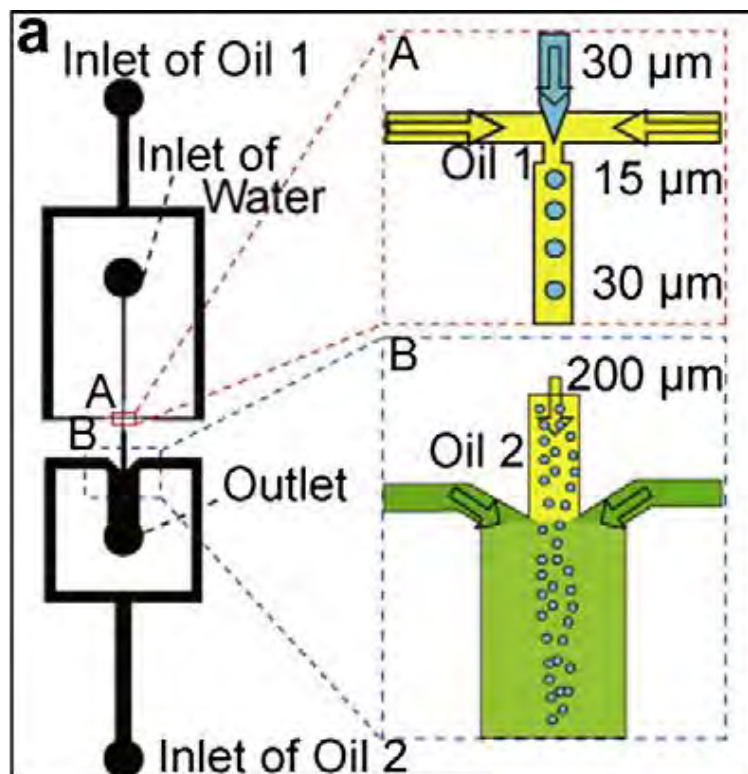


Fig. 2.9 W/O emulsion droplets formed by vortexing [52]

2.5.3.2 Microfluidics to produce uniform W/O emulsion

The microfluidic device was fabricated to produce W/O emulsion droplets at a uniform size that were stabilized by phospholipids as an emulsifier. The microchannel device was made of Polydimethylsiloxane (PDMS) using the standard soft lithography process. In short, the master mold with a height of 30 μm was made of SU-8 photoresist (MicroChem Corp.) on a 2-inch silicon wafer according to the manufacturer's protocol. PDMS mixed with the curing agent was poured over the mold and was removed after curing for 2 h on a 75 $^{\circ}\text{C}$ hot plate.

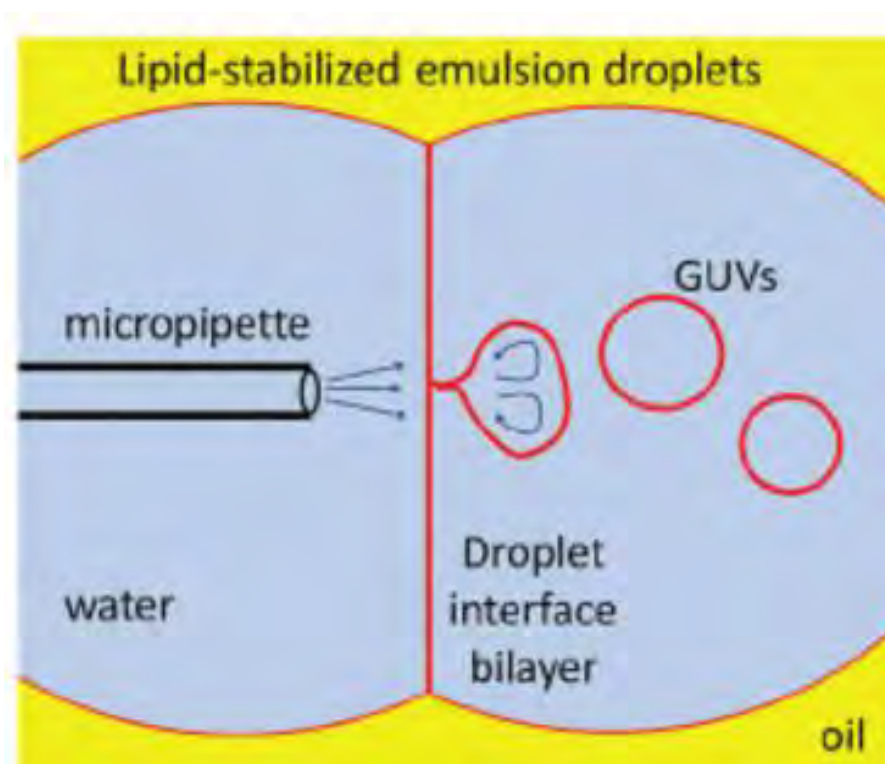


Fig. 2.10 Microfluidics to produce uniform W/O emulsion [52]

The PDMS slab with the channel structure was bonded onto a glass slide after applying an oxygen plasma. Subsequently, inlet and outlet tubes were mounted, which were then connected to syringes filled with the oil and water phases. The PDMS microfluidic channel was mounted on a microscope stage to monitor the formation process of the emulsion droplets. Emulsion droplets formed were retrieved from the outlet tubes.

2.5.3.3 Transferring emulsion droplets to GUVs

Emulsion droplets were transformed into GUVs by forcing them to pass across the amphiphile-saturated O/W interface via centrifugation. The emulsion suspension (100 μL) was placed on 50 μL of the outer solution in a 200 μL test tube. This tube was then centrifuged at various relative centrifugal force (RCF) for 30 min at 4 $^{\circ}\text{C}$ and the precipitated GUVs were collected through a hole opened by a needle after centrifugation at the bottom of the test tube.

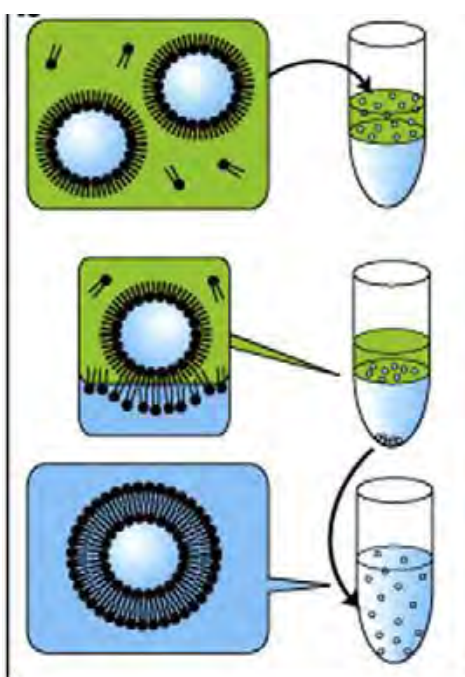


Fig. 2.11 Transferring emulsion droplets to GUVs [53]

2.5.4 Inverted emulsion droplets method

The choice of the organic phase used to make the inverted emulsion is dictated by the balance between the solubility of the lipid in oil, the stability of the inverted emulsion, and the possible presence of oil in the final bilayer. Unlike previous attempts to use similar techniques, a sufficiently long-chain alkane is used to ensure that the alkane molecules are not incorporated into the final bilayer [54] and that a stable, inverted macroemulsion is formed. The use of alkanes with chains shorter than 10 carbons resulted in a microemulsion where no longer able to control the size of the water

droplets. Dodecane, a 12-carbon alkane was most suitable for applications, but a variety of oils can be used. Alkanes with chain lengths ranging from 12 to 17 carbons resulted in stable macroemulsions. The composition of the bilayer has checked by making a thin layer chromatography analysis of the final vesicles and comparing this to that of pure lipids and pure alkane samples. This is the sensitivity limit of this technique; other techniques were not pursued. The best alkane for an oil-free bilayer is squallene, which has the advantage that it is immiscible in lipid bilayers. while still providing a good continuous phase for emulsion preparation. A wide variety of surfactants can be used to stabilize an inverted emulsion. Here nonionic surfactants, lipids, and diblock copolymers are chosen according to geometrical arguments [55] such that

$$(v/a_0l_c) \geq 1 \quad \dots \quad \dots \quad \dots \quad (2.1)$$

where v is the volume of the hydrocarbon chain, a_0 is the surface area of the polar head, and l_c is the chain length. When this ratio is greater than one, the area of the hydrophobic part of the molecule is larger than that of the hydrophilic part, which favors the stabilization of an inverted emulsion. Lipids have a ratio only slightly higher or lower than one depending on the polar headgroup and salt conditions; this fact makes them a poor surfactant with which to stabilize an emulsion. The inverted emulsion was usually prepared by first dispersing the surfactant in the oil phase.

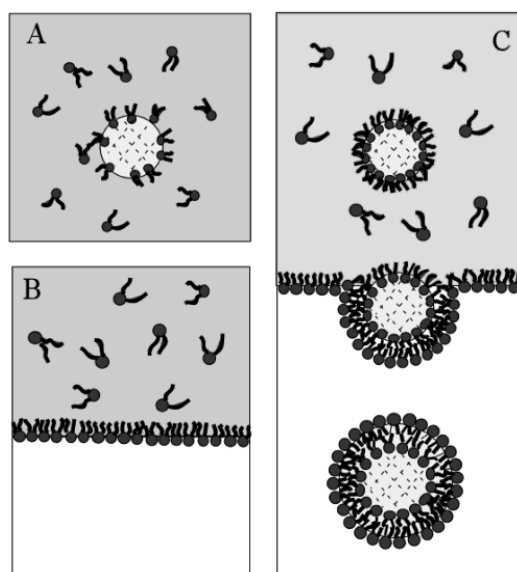


Fig. 2.12 Inverted emulsion droplets method [55]

For multicomponent lipid mixtures, the lipids were first dissolved together in chloroform to obtain a homogeneous dispersion. The chloroform was then evaporated under a stream of nitrogen to form a dry thin film on the surface of a glass vial, which swelled easily when dodecane was added. To fully disperse the lipid molecules in dodecane, the suspension was placed in a sonication bath overnight at 25 °C. Surfactants in liquid form, a nonionic surfactant, were added directly to the dodecane. Finally, for samples prepared with the diblock copolymer was more convenient to dissolve the powder directly in the aqueous solution at 0.1 wt % to prepare the inverted emulsion. The emulsification of the aqueous solution and surfactant saturated dodecane can be achieved by various methods. The amount of shear and the method by which it is applied to the suspension are responsible for the mean size and polydispersity of the emulsion produced. Four different emulsification techniques were used: shear by gentle stirring, shear using a mixer, extrusion, and sonication. For lipids and nonionic surfactants, a crude inverted emulsion was prepared either by vortexing the solution for several minutes or by gently stirring the suspension with a magnetic stir bar for 1-3 h. The emulsion produced was very polydisperse with a mean size around 1 μm . More controlled preparation was achieved by using a shear mixer with variable rotation speed or extrusion of the suspension through a narrow pore size polycarbonate filter. Extrusion was also used to reduce the polydispersity and the size of the droplets in an emulsion produced by other techniques. Further purification steps are then required to extract the inverted emulsion [56]. Finally, in some cases, such as the diblock copolymer, the best results were obtained by sonicating the suspension. Unless otherwise specified, the emulsified aqueous solution consisted of 100 mM NaCl and 5 mM Tris buffered at pH 7.4. The volume fraction of the aqueous solution was 0.5% of the total volume. To prepare for the final step in the assembly, 3mL of aqueous buffer was placed in a centrifuge tube and then gently poured about 2mL of dodecane containing amphiphilic molecules for the outer monolayer on top of the buffer. Some of these molecules diffused to cover the oil-water interface. For most surfactants, adsorption at an interface is diffusion limited [57] and full coverage should occur in only a few minutes. The adsorption mechanism for lipids appears to be more complex; it takes from 30min for charged lipids up to 90 min for zwitterionic ones to achieve full coverage. Once the interface was fully covered, the inverted emulsion was added to the

Falcon tube. The volume of the emulsion added was varied from 0.1 mL to 1 mL to ensure that the total area of the emulsion did not exceed the total area of the monolayer available to supply the outer leaflet. After the three layers were assembled, the tube was placed in a spin-bucket centrifuge and spun at 120g for 5-10 min. Since water is denser than oil, the water droplets sediment toward the oil-buffer interface. Centrifugation was used to enhance the rate of sedimentation, decreasing the time required to transfer the droplets from several hours to a few minutes.

2.5.5 Lipid coated ice droplet hydration

Figure 2.13 illustrates the procedure that was applied for preparing size-controlled oligo or multilamellar GVs from a W/O emulsion. In a first step, a monodisperse W/O emulsion containing calcein was prepared by microchannel (MC) emulsification using Span 80 and Stearylamine (SA) as surfactant (Fig. 2.13a). Subsequently, the Span 80 and SA molecules that covered the dispersed water droplets in the emulsion were replaced by a bilayer-forming lipid mixture at 10 °C, under conditions that kept the water droplets in a frozen state, to avoid their coalescence. The lipid mixture was composed of egg PC, Chol, and SA at a molar ratio of 5:5:1. The water droplets in the W/O emulsion were frozen by cooling with liquid nitrogen; the surfactant replacement process was performed at 10 °C in a cold room. The frozen water droplets were precipitated by sedimentation for 30 min at 10 °C, and 9 mL of the supernatant was removed by suction. Then, 19 mL of the hexane solution containing 0.16 mg of lipid/mL at an egg PC:Chol:SA molar ratio of 5:5:1 was added. The system was mixed with a Pasteur pipet, followed by a sedimentation of the frozen water droplets for 30 min at 10 °C. During all this procedure, the water droplets remained frozen. Afterward, 18 mL of the supernatant was removed by suction, followed by the addition of 18 mL of hexane solution containing egg PC:Chol:SA (5:5:1, molar ratio).

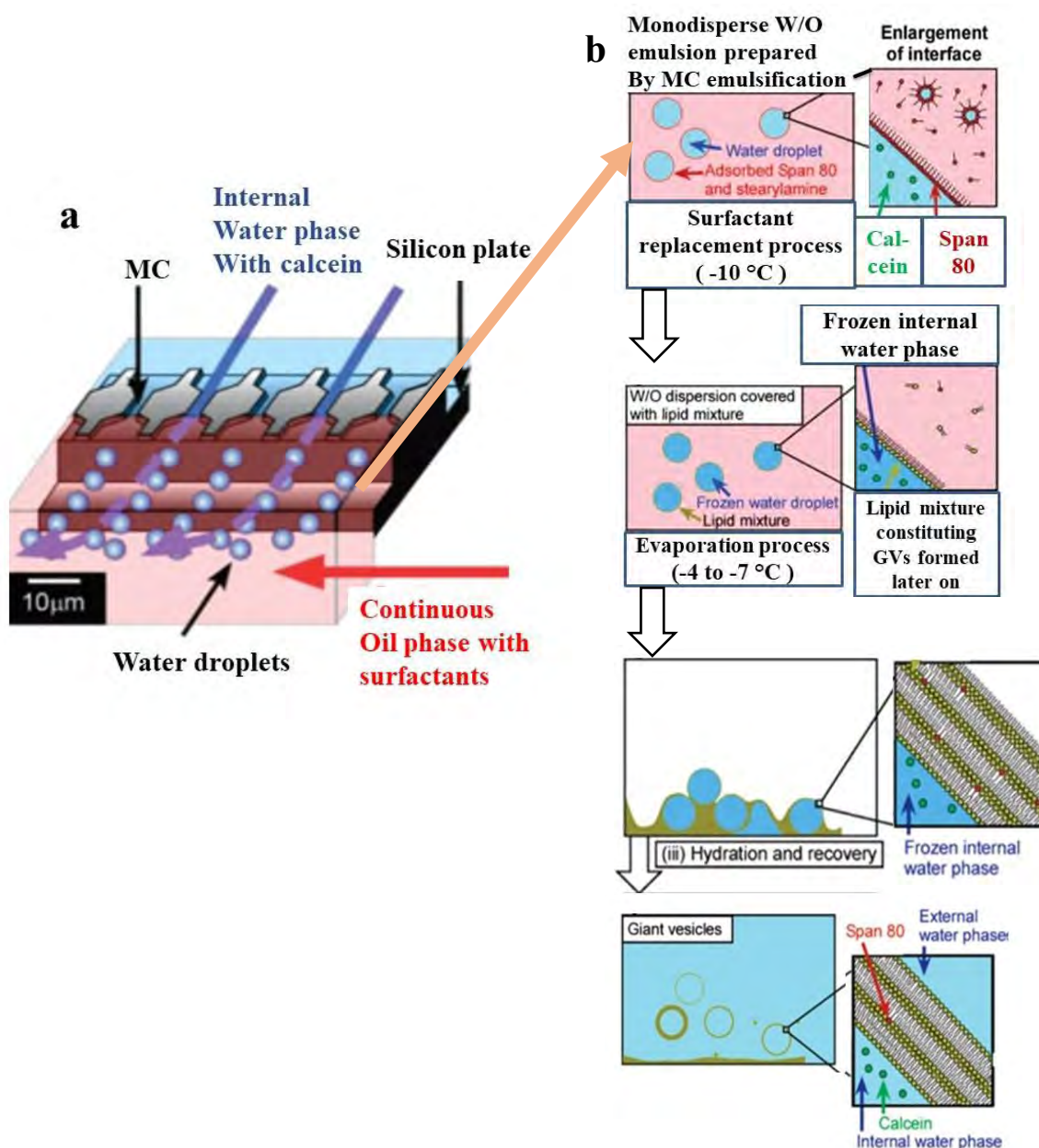


Fig. 2.13 Schematic representation of lipid coated ice droplet hydration [58]

After being mixed with a Pasteur pipet, followed by water droplet sedimentation as described above, 12 mL of the supernatant was removed and replaced by 12 mL of hexane solution containing egg PC:Chol:SA (5:5:1, molar ratio). At this stage, the water content of the system was determined by withdrawing 2 mL of the suspension [58]. On the basis of these water determinations, the water content in the suspension was adjusted to 20 mg/mL suspension by removing supernatant. The resulting suspension

was diluted by adding an equal volume of hexane solution containing egg PC:Chol:SA (5:5:1, molar ratio). From this diluted suspension, 0.1 mL was transferred into an empty test tube and 0.9 mL of hexane solution containing egg PC:Chol:SA (5:5:1, molar ratio) was added to yield a volume of 1mL containing 1mg of water and 0.16mg of lipid mixture. The Span 80 concentration was reduced during the entire procedure to 0.01% of the initial concentration [30]. After this surfactant replacement step, hexane was evaporated by rotatory evaporation (from 1 mL of W/O suspension) at 15 hPa and a temperature of -4 to -7 °C to keep the water droplets frozen. After solvent evaporation, 50-1000 μ L of 50 mM Tris-HCl buffer (pH 9.0), which had been kept at 4 °C, was added for lipid hydration and for the formation of GVs at 4 °C. Finally, additional external water phase could be added to further disperse and dilute the GVs if this was desired; typically, 5 mL of 50 mM Tris-HCl buffer (pH 9.0) was added, and the sample was warmed up to room temperature.

2.6 Literature review

F. M. Menger and Kurt Gabrielson [12] observed molecular assemblies of membrane by optical microscope in a study of chemically-induced aggregation, budding, and fusion in giant vesicles. In the ensuing paper, they first described a new and efficient way to prepare giant unilamellar vesicles (GUVs) from a synthetic lipid. In that way, vesicles were 1-100 μ m in diameter.

D.P. Pantazatos, R.C. MacDonald [19] were developed a novel method for the direct examination of pairwise encounters between positively and negatively charged phospholipid bilayer vesicles. Giant bilayer vesicles of 4–20 μ m in diameter were prepared in that method.

M. Z. Islam, et al. [29] recently developed the single giant unilamellar vesicle (GUV) method for investigating the functions and dynamics of biomembranes. The single GUV method can provide detailed information on the elementary processes of physiological phenomena in biomembranes, such as their rate constants .

Dmitri Fayolle et al. [35] explored a novel methodology of GV purification by microfiltration under reduced pressure, operated by a simple apparatus. This method purifies the inner and outer solution of GUVs. Where a vacuum pump was used to

induce pressure difference across the filter paper during purification. In this method, recovery rate of purified vesicles is very low.

Yukihiro Tamba et al. [34] developed a new technique for the purification of GUVs to obtain a large population of similar-sized GUVs composed of oil-free membranes for investigating the properties of biomembranes. In this method, similar-sized GUVs with diameters of 10–30 μm were obtained. Moreover, this method enabled GUVs to be separated from water soluble fluorescent probes and LUVs. The membrane filtering method can be applied to purify GUVs prepared by other methods. This method provides the desired results but it needs two peristaltic pumps and continuous supply of electricity during purification.

2.7 Purification

Purification is the process of rendering something pure, i.e. clean of foreign elements and/or pollution. It may also refer to that purification means to remove the unwanted things from the desired sample. In case of the lipid membrane of GUVs, purification is to remove smaller GUVs, LUVs, lipid aggregates and various water-soluble substances like proteins and fluorescent probes. This process can also be used for concentration of dilute GUVs suspensions.

2.7.1 Necessity of purification of GUVs

Among above mentioned GUVs synthesis methods, some methods produce similar sized GUVs containing significant amounts of hydrocarbon-oils which greatly affects the physicochemical properties and prevents to get actual biophysical properties of the lipid membranes. On the other hand, some other methods prepare oil free vesicles of various sizes like GUVs, LUVs, SUVs along with lipid aggregates and various water-soluble substances. When we want to study the biophysical properties of lipid membranes or to develop a mechanism for different membrane active agents (proteins, peptides, nanoparticles etc) then a lot of LUVs, SUVs and lipid aggregates interrupt with the results. For this reason, LUVs, SUVs and lipid aggregates should be removed from the GUVs suspension. Another fact is that our target is to study the different biophysical properties of biomembranes/cell membranes. The structure of a cell

membrane is complex and to grow a cell with cell culture in a laboratory is very difficult. For avoiding the above-mentioned difficulties, artificially synthesized lipid membranes of GUVs are used to investigate the different biophysical properties of membrane and interactions of membrane active agents with GUVs. To get proper membrane interaction and biological properties, cell sized GUVs which can get using purification should be used.

2.8 Purification Techniques

2.8.1 Dialysis

In research fields, dialysis process can be used to isolate molecules based on their size. In addition, it can be used to balance buffer between a sample and the solution "dialysis bath" or "dialysate" that the sample is in. For dialysis in a laboratory, a tubular semipermeable membrane made of cellulose acetate or nitrocellulose is used [59]. Pore size is changed according to the size separation required with larger pore sizes allowing larger molecules to pass through the membrane. Solvents, ions and buffer can pass easily across the semipermeable membrane, but larger molecules are unable to pass through the membranes.

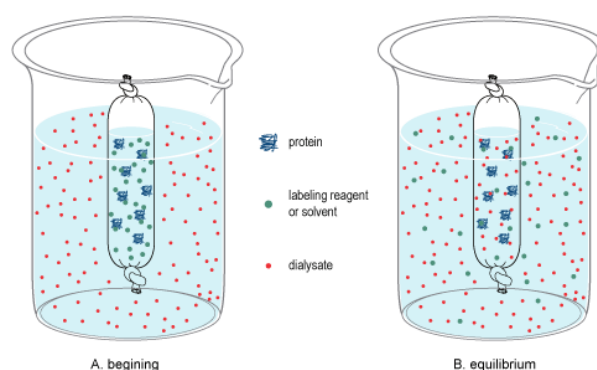


Fig. 2.14 Schematic diagram of dialysis [59]

This can be used to purify proteins of interest from a complex mixture by eliminating smaller proteins and molecules. Dialysis treatments replace some of these functions through diffusion (waste removal) and ultrafiltration (fluid removal). Highly purified

(also known as "ultrapure") water used in dialysis techniques. Dialysis works on the principles of the diffusion of solutes and ultrafiltration of fluid across a semi-permeable membrane. Diffusion is a property of substances in water; substances in water tend to move from an area of high concentration to an area of low concentration. A semipermeable membrane is a thin layer of material that contains holes of various sizes, or pores. Smaller solutes and fluid pass through the membrane, but the membrane blocks the passage of larger substances.

2.8.2 Centrifugation

Biological centrifugation is a technique that uses centrifugal force to isolate and purify mixtures of biological particles according to their size, shape, density, viscosity of the medium and rotor speed in a liquid medium [60]. It is a key process for separating and analyzing cells, subcellular fractions, supramolecular complexes and isolated macromolecules such as proteins or nucleic acid.

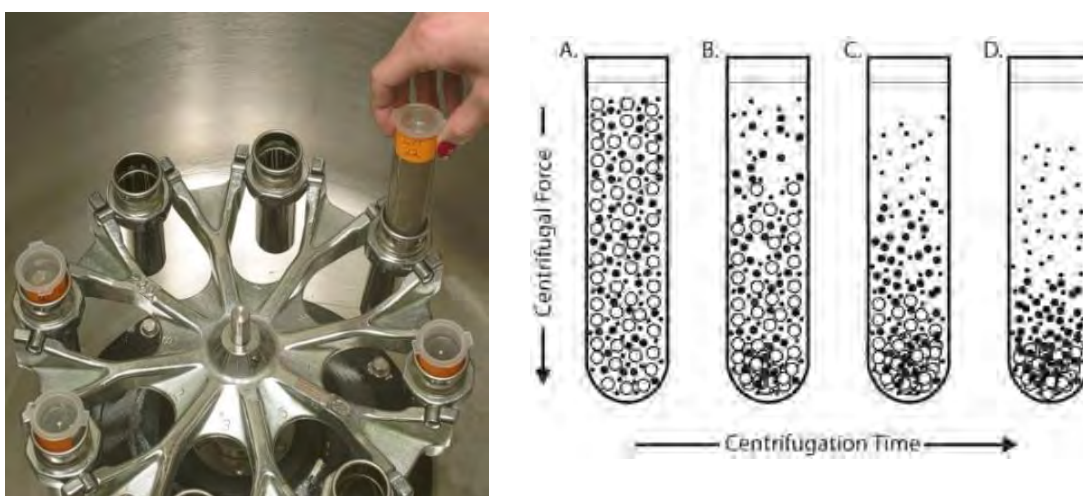


Fig. 2.15 Centrifugation [60]

More-dense components of the mixture migrate away from the axis of the centrifuge (move to the outside), while less-dense components of the mixture migrate towards the axis, i. e., move to the center. Researcher may increase the effective gravitational force on a test tube so as to more rapidly and completely cause the precipitate (pellet) to gather on the bottom of the tube. The rest of the solution (supernatant) may be discarded

with a pipette. Centrifugation of protein solution, for example, allows elimination of impurities into the supernatant. Differential Centrifugation is a type of centrifugation in which one selectively spins down components of a mixture by a series of increasing centrifugation forces. This technique is generally used to distinct organelles and membranes found in cells. Organelles normally differ from each other in density in size, making the use of differential centrifugation, and centrifugation in general, possible. The organelles can then be recognized by testing for indicators that are unique to the specific organelles.

2.8.3 Microfiltration technique

The removal of the exterior solution from a GV suspension by microfiltration needs a selective passage of solutes through the pores of the filter while GVs are retained in the retentate [35]. To this end, nylon filters of a microscopic sponge-like structure with 0.2 μm average pore size have been used. GV microfiltration was done on a simple apparatus that can be easily accumulated in most of laboratories (Fig 2.16 b). It contains a small filter holder, which is funnel-shaped, connected to a vacuum Erlenmeyer flask. A pump with a pressure regulator is connected to the flask, to generate a pressure difference ($\Delta P = P_{\text{atm}} - P_{\text{pump}}$) across the filter, which drives the microfiltration. Unlike centrifugation, GV filtration does not need any density difference between the lumen and outside solution, so in principle no GV pre-treatment is needed. It is however convenient to dilute the crude GVs with outer solution, in order to progress the purification efficiency and avoid filter obstruction.

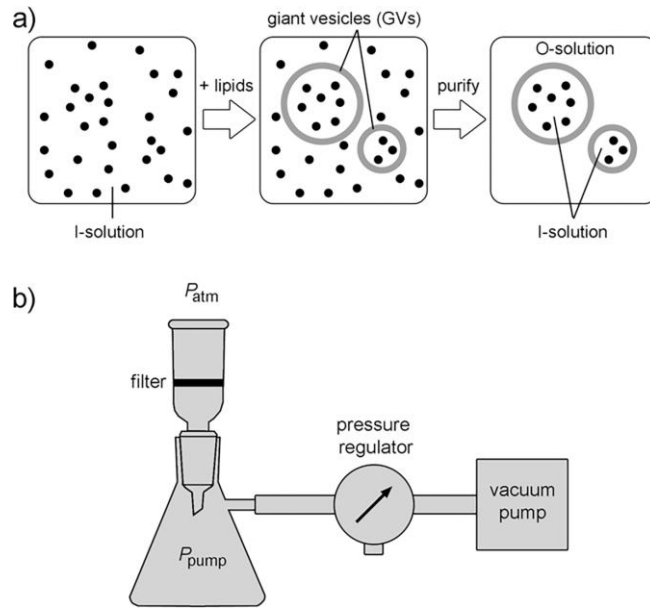


Fig 2.16 a) Purification of giant vesicles by microfiltration. b) Schematic drawing of microfiltration apparatus. Nylon filters with 0.2 μm pores have been used in this work.

Note that $\Delta P = P_{atm} - P_{pump} \approx 1000 \text{ mbar} \pm P_{pump}$ [35].

When a volume V of the GV suspension is diluted with a volume V_o of outer solution, the concentration of non-entrapped solutes reduced by a factor b ,

$$b = \frac{V+V_o}{V} \quad \dots \quad \dots \quad \dots \quad (2.2)$$

Although this procedure does not change the intra-vesicle solute concentration, it decreases the GV concentration. When a diluted GV suspension $V + V_o$ is filtered, the GVs are retained by the filter and become concentrated in the retentate by a factor β ,

$$\beta = \frac{V+V_o}{V_{ret}} \quad \dots \quad \dots \quad \dots \quad (2.3)$$

where V_{ret} is the volume of the retentate. During purification, small external solutes maintain their concentration, but are reduced in number. It follows that combining a preliminary GV dilution with a consequent GV microfiltration is an optimum and rapid route to effectively purify GVs. However, the GV recovery in the retentate is lower than the expected because of vesicle adsorption/rupture on the filter.

2.8.4 Membrane filtering method

In this method, for the purification of GUVs, a centrifuged GUV suspension containing supernatant is filtered through a nucleopore polycarbonate membrane with 12 μm diameter pores (Nomura Micro Science, Atsugi, Japan) using a homemade apparatus (Fig. 2.17A) [34]. In this apparatus, the nucleopore membrane is clamped in a polypropylene filter holder (Swinnex, = 25 mm, Millipore Co., Billerica, MA), and then the upper and lower side of the filter holder are connected to a 10 mL plastic (polypropylene) syringe (Top Co., Tokyo, Japan, or Terumo Co., Tokyo, Japan) (syringe A in Fig. 2.17A) and a tube made of polypropylene (inner diameter 5 mm and length 11 cm) (tube in Fig. 2.17A), respectively. The other end of the tube is associated to another 10 mL plastic syringe (syringe B in Fig. 2.17A). After the apparatus was filled with buffer A containing 0.1 M glucose, all the air bubbles were carefully removed. Then, after removing the buffer from syringe B (~ 1 mL buffer should remain), a GUV suspension in buffer A containing 0.1 M sucrose was added to syringe B. After diluting the GUV suspension with buffer A containing 0.1 M glucose in syringe B, buffer A containing 0.1 M glucose was added to syringe B at a constant velocity using a peristaltic pump (SJ-1220, Atto Co., Tokyo, Japan), and simultaneously the buffer in syringe A was removed at the same constant velocity using another peristaltic pump. The direction of the flow of buffer at the filter was from the bottom to the top, shown in Fig. 2.17A, so the smaller vesicles passed through the filter into the upper syringe (syringe A). After filtering for a definite time, the addition of buffer A containing 0.1 M glucose to syringe B was stopped, and then the buffer inside syringe A was removed by the pump at the same flow rate. Finally, the suspension in the tube and the filter holder was collected and used as a purified GUV suspension.

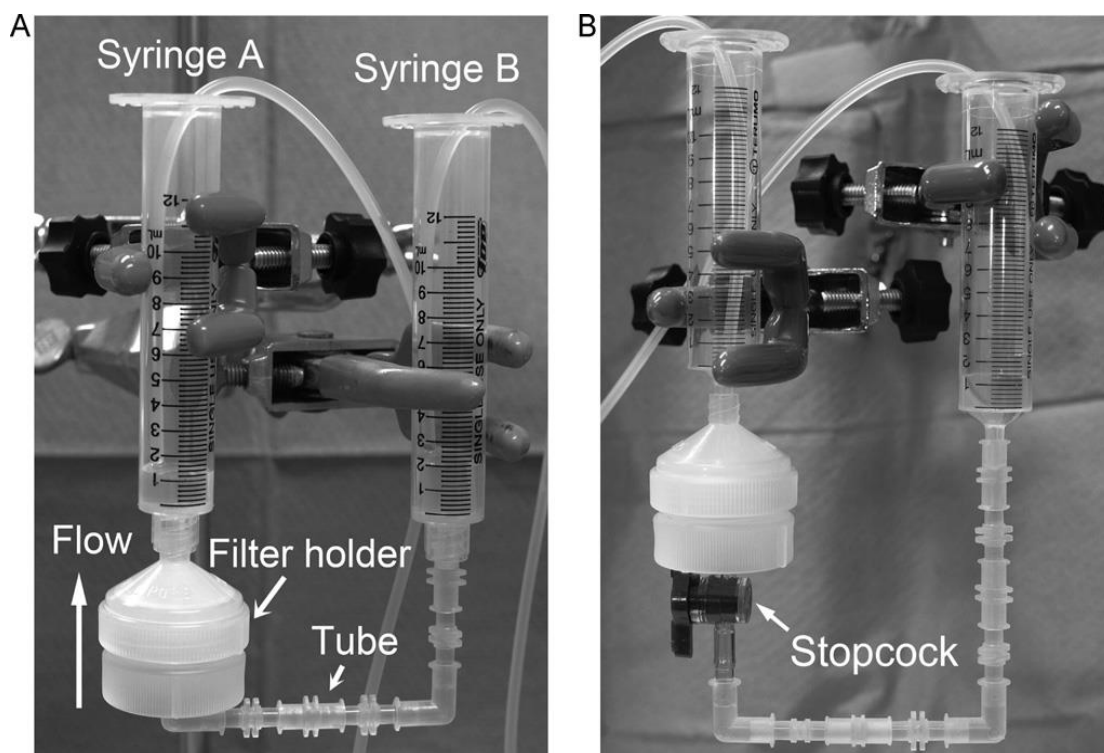


Fig. 2.17 (A) The apparatus for the membrane filtering method. (B) The apparatus with a stopcock for the membrane filtering method.

For the experiments to confirm the location of GUVs in the apparatus following purification and those of the concentration of GUVs, a 1-way luer stopcock made of polycarbonate (VXB1055, ISIS Co., Ltd., Osaka, Japan) was used, which was introduced between the filter holder and the tube (Fig. 2.17B).

A GUV suspension was filtered using the apparatus (Fig. 2.17B) while the stopcock was open, and after the filtering the stopcock was closed. Then the solutions above the stopcock (i.e., in the space under the filter membrane) and in the tube below the stopcock were collected. Purified GUV solution (300 μL) was taken to a handmade microchamber [2]. A glass slide was coated with 0.1% (w/v) BSA in buffer A containing 0.1 M glucose. GUVs in the chamber were observed using an inverted fluorescence phase contrast microscope (IX-71, Olympus, Tokyo, Japan).

CHAPTER 3

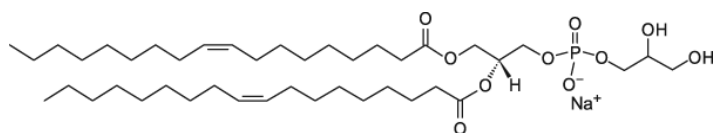
EXPERIMENTAL TECHNIQUE

3.1 Chemicals and Reagents

The chemicals and reagents that are used in this study are listed below along with their molecular weight and chemical formula and chemical structure.

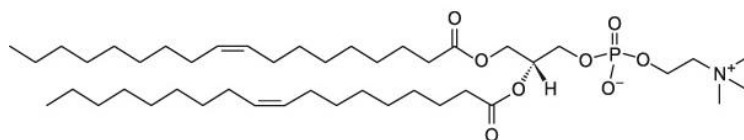
1) 1, 2-dioleoyl-sn-glycero-3-phospho-(1'-rac-glycerol) (sodium salt) (DOPG) [61].

Molecular weight: 797 g/mol Chemical formula: $C_{42}H_{78}NaO_{10}P$



2) 1, 2-Dioleoyl-sn-glycero-3-phosphocholine (DOPC) [62].

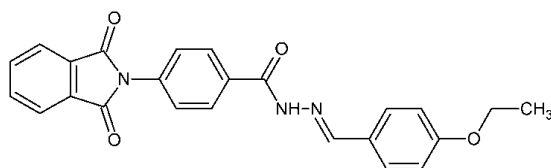
Molecular weight: 786.1 g/mol Chemical formula: $C_{44}H_{84}NO_8P$



These lipids were purchased from Avanti Polar Lipids Inc. (Alabaster, AL).

3) Bovine serum albumin (BSA), Piperazine-1, 4-bis (2-ethanesulfonic acid) [63].

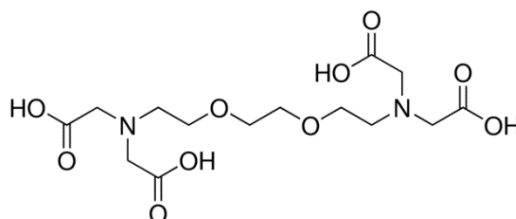
Molecular weight: 66430.3 g/mol. Chemical formula: $C_{123}H_{193}N_{35}O_{37}$



- 4) O, O'-Bis (2-aminoethyl) ethyleneglycol- N, N, N', N',-tetraacetic acid (EGTA) [64]

Molecular weight: 380.35 g/mol.

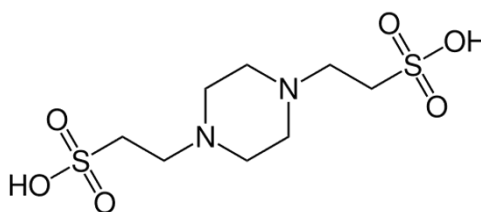
Chemical formula: $C_{14}H_{24}N_2O_{10}$



- 5) 1,4-Piperazinediethanesulfonic acid (PIPES) [65].

Molecular weight: 302.4 g/mol

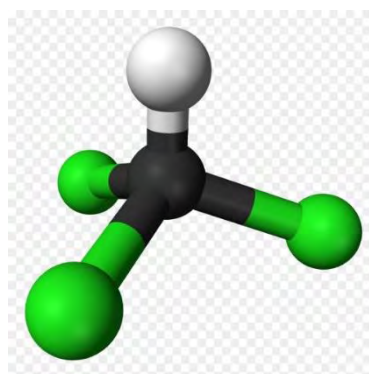
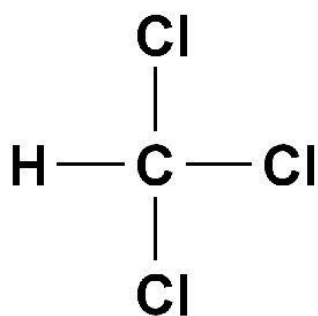
Chemical formula: $C_8H_{18}N_2O_6S_2$



- 6) Chloroform [66].

Molecular weight: 119.37 g/mol

Chemical formula: $CHCl_3$

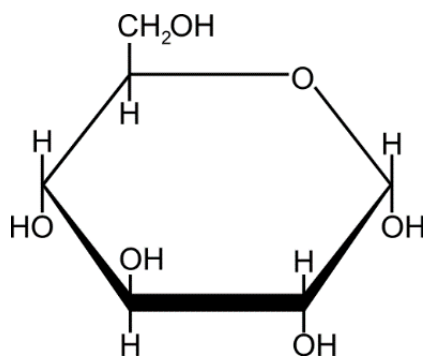


BSA, EGTA and PIPES were purchased from Sigma-Aldrich (Germany). These chemicals were used without further purification.

7) Glucose

Molecular weight: 180.156 g/mol

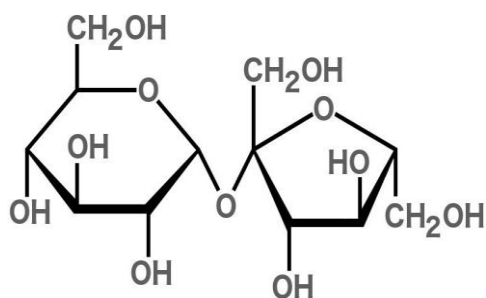
Chemical formula: $C_6H_{12}O_6$



8) Sucrose

Molecular weight: 342.3 g/mol

Chemical formula: $C_{12}H_{22}O_{11}$



Sucrose and Glucose were purchased from Mark, Germany.

3.2 Preparation of Buffer and Solution

3.2.1 Physiological buffer

In our experiment, a buffer of 10 mM PIPES, 150 mM sodium chloride (NaCl) and 1 mM EGTA is used where pH of the buffer remains fixed at 7.0. If pH of the buffer remains below 7.0 then we control pH at 7.0 adding some sodium hydroxide (NaOH).

3.2.2 Internal solution of the GUVs

We have taken milliQ water at polypropylene pot and added sucrose of measured amount such that its concentration be 0.1 M. Internal solution is prepared by adding buffer with 0.1 M sucrose. 0.1 M sucrose solution is used as internal solution because its molecular weight is greater than that of glucose which helps to settle down the vesicles in hand made microchamber during observation under microscope.

3.2.3 External solution of the GUVs

Firstly, we have taken milliQ water at polypropylene pot and added glucose of measured amount such that its concentration be 0.1 M. External solution is prepared by adding buffer with 0.1 M glucose. Low molecular weight external solution creates a phase contrast with high molecular weight sucrose.

3.3 Synthesis of Lipid Membranes of GUVs

40%DOPG/60%DOPC-GUVs (% indicates mole %) were synthesized by the natural swelling method. At first, 80 μ L DOPG and 120 μ L DOPC (concentration of DOPG and DOPC was 1 mM) in chloroform were taken into a 4.5 mL glass vial and dried with a gentle flow of nitrogen gas to produce a thin homogeneous lipid film. The residual chloroform in the film was removed by placing the vial in a vacuum desiccator overnight (12 h). 20 μ L MilliQ water was added into the vial and then pre-hydrated at 45 °C for 8 min. After pre-hydration, the sample was incubated with 1 mL of buffer (10 mM PIPES, pH 7.0, 150 mM NaCl and 1 mM EGTA) containing 0.10 M sucrose for 3.5 h at 37 °C to produce GUVs suspension.

3.3.1 Schematic representation of GUV Synthesis

The following figures show the schematic representation of the synthesis of lipid membranes of GUVs using the natural swelling method.

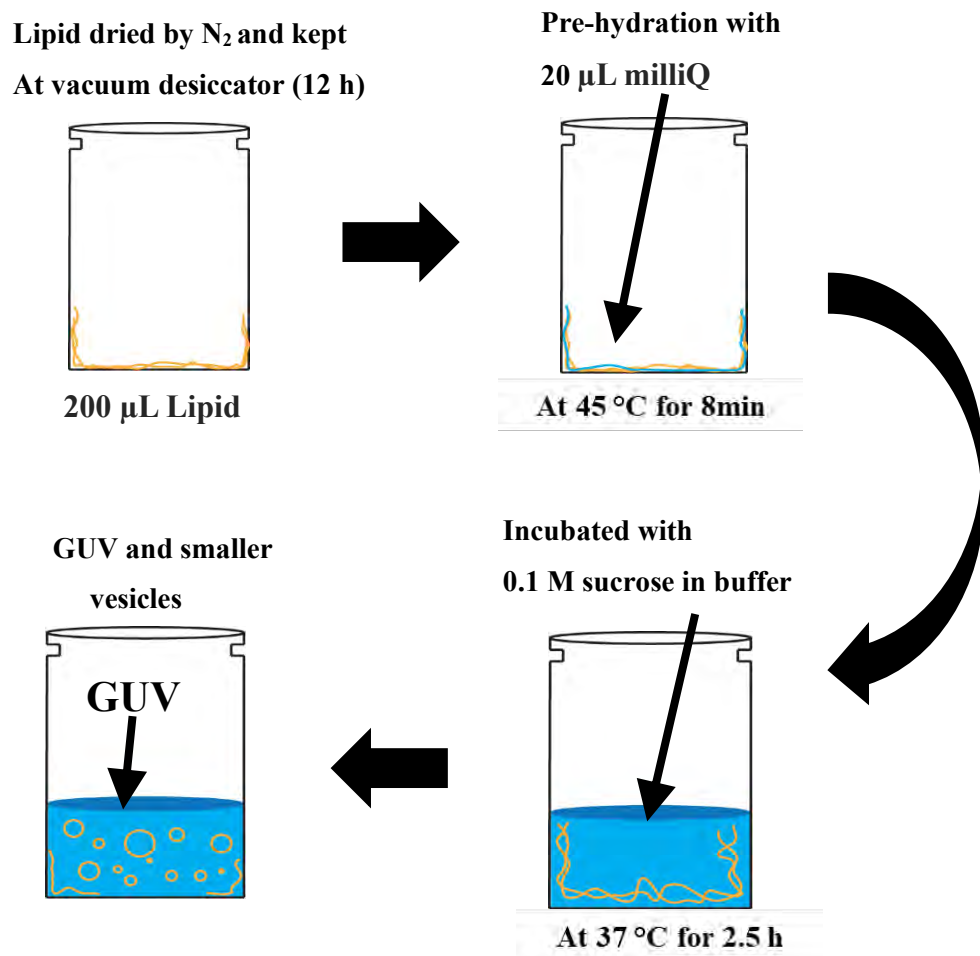
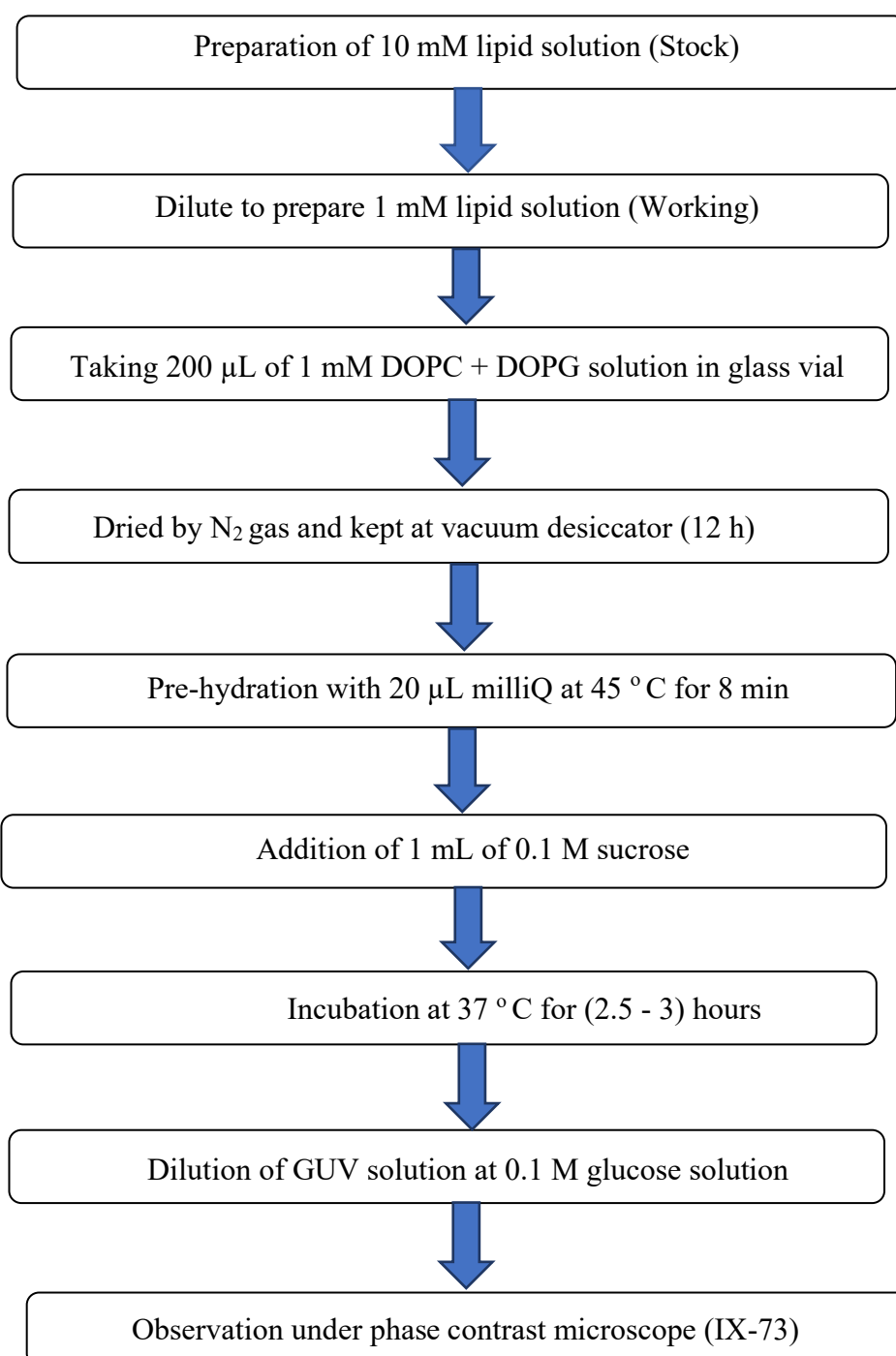


Fig. 3.1 Schematic diagram of GUV synthesis

3.3.2 Flow chart of GUV preparation

The GUV synthesis method is described in the following flow chart.



3.3.3 Preparation of 1mM 40%DOPG + 60%DOPC

At first, 80 μL DOPG and 120 μL DOPC (concentration of DOPG and DOPC was 1 mM) in chloroform were taken into a 4.5 mL glass vial. It is defined as 40% DOPG/60%DOPC-GUVs.

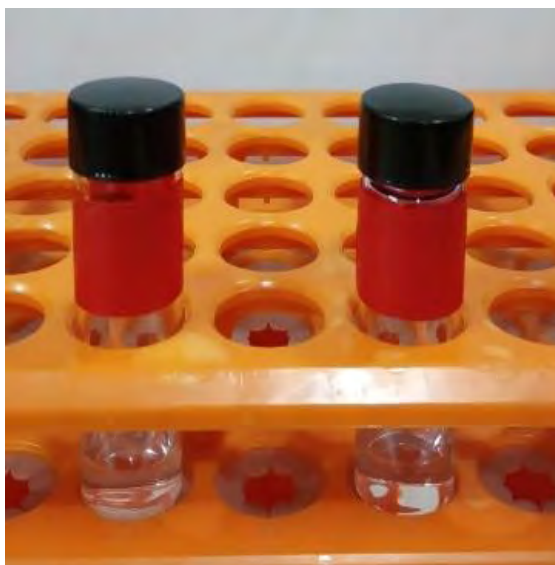


Fig. 3.2 Preparation of 1mM 40%DOPG/60%DOPC-GUVs

3.3.4 Dry with N_2 stream

200 μL lipid solution (80 μL DOPG and 120 μL DOPC) in glass vial was dried with a gentle flow of nitrogen gas to produce a thin homogeneous lipid film of lipid.



Fig. 3.3 Dry with N_2 stream

3.3.5 Fine dry at vacuum desiccator

The residual chloroform in the film of lipid in the glass vial was removed by placing the vial in a vacuum desiccator overnight (12 h).



Fig. 3.4 Fine dry at vacuum desiccator

3.3.6 Pre-hydration at 45 °C for 8 min

20 μ L MilliQ water was added in the fine dried lipid film into the glass vial and then lipid film was pre-hydrated by sinking the glass vial in a water fill beaker at 45 °C for 8 min.



Fig. 3.5 Pre-hydration at 45 °C for 8 min

3.3.7 Incubation at 37 °C for 2.5 to 3 h

After pre-hydration the sample was incubated with 1 mL of buffer (10 mM PIPES, pH 7.0, 150 mM NaCl and 1 mM EGTA) containing 0.1 M sucrose for 2.5 to 3 h at 37 °C to produce GUVs suspension.



Fig. 3.6 Incubation at 37 °C for 2.5 to 3 h

3.3.8 Centrifugation at 13000 rpm

After incubation, the GUVs suspension was taken in a 1.5 mL eppendorf tube using 1000 μ L micropipette. Eppendorf tube was carefully put on the centrifuge head such that the balance was maintained. Finally the sample in Eppendorf tube was centrifuged at 13,000 \times g for 20 min at 20 °C using a refrigerated centrifuge (NF 800R, NUVE, Turkey)



Fig. 3.7 Centrifugation at 13000 rpm

3.4 Equipment for Purification

3.4.1 Syringe

Two plastic (polypropylene) syringes (JMI Syringes and Medical Devices Ltd. Bangladesh) of 10 mL which contains GUVs suspension during the purification are clamped in a stand at a fixed height from the surface of the earth.



Fig. 3.8 Syringe

3.4.2 Regulators

The fine roller clamp regulator (JMI Syringes and Medical Devices Ltd. Bangladesh) was controlled flow rate (mL/min) when GUVs suspension passed away through the pipe.



Fig. 3.9 Regulators

3.4.3 Pipe for buffer flow

The plastic tube of inner diameter 3 mm (JMI Syringes and Medical Devices Ltd. Bangladesh) is used for transferring internal solution to first syringe from a buffer filled glass beaker maintained at a finite height.



Fig. 3.10 Pipe for buffer flow

3.4.4 Fittings for purification tube

A tube made by three different type polypropylene fittings (Luer fittings VRFE6, VRFC6, VRSC6; AS-ONE, Japan) of inner diameter 3 mm.



Fig. 3.11 Different types of fittings

3.4.5 Filter holder

It is a polypropylene filter holder (Swinnex, $\phi = 25$ mm, Millipore Co., Billerica, MA). A 10 μm diameter pores nucleopore polycarbonate membrane (Whatman® Nucleopore™ Track-Etched Membranes, UK) is clamped inside it during purification.



Fig. 3.12 Filter holder

3.4.6 Filter paper

10 μm diameter pores nucleopore polycarbonate membrane (Whatman® Nucleopore™ Track-Etched Membranes, UK) was used in the investigation.



Fig. 3.13 Filter paper

3.4.7 Stop cock

1-way polycarbonate stopcock (Luer stopcock VXB1055, AS-ONE, Japan) was used in the purification which was inserted between the filter holder and the polypropylene tube.



Fig. 3.14 Stop cock

3.4.8 Peristaltic pump

The following figure shows a compact double headed peristaltic pump. The range of flow rate of this pump is 0.0024-190 ml/min



Fig 3.15 Double headed peristaltic pump

3.5 Method of Purifying Lipid Membranes of GUVs

3.5.1 Non-electromechanical method

After incubation, the GUVs suspension was centrifuged at $13,000\times g$ (gravitational acceleration) for 20 min at 20 °C using a refrigerated centrifuge (NF 800R, NUVE, Turkey) and then the supernatant containing GUVs was filtered through a 10 μm diameter pores nuclepore polycarbonate membrane (Whatman® Nuclepore™ Track-Etched Membranes, UK) clamped in a polypropylene filter holder (Swinnex, $\phi = 25$ mm, Millipore Co., Billerica, MA). The arrangement of the purification technique is depicted in Fig. 3.16. The upper end of the filter holder was connected with a 10 mL plastic (polypropylene) syringe 2 (JMI Syringes and Medical Devices Ltd. Bangladesh) and the lower end was connected with a tube containing three different types of polypropylene fittings (Luer fittings VRFE6, VRFC6, VRSC6; AS-ONE, Japan) having inner diameter 3 mm as shown in Fig. 3.16. In this case, the tube contains a total number of 11 fittings instead of 9 that was used in the membrane filtering method [42]. The other end of the tube was connected to syringe 1 having the same volume of 10 mL. The GUVs suspension in buffer (external solution) containing 0.1 M glucose was added to syringe 1 where the buffer was continuously flowing due to gravity through a plastic tube of inner diameter 3 mm (JMI Syringes and Medical Devices Ltd. Bangladesh) from a buffer filled glass beaker maintained at a finite height. Before starting the flow of buffer from beaker to syringe 1, the air bubbles were carefully removed from the polypropylene tube and filter holder. In this case, the syringe 1 was filled with 7-9 mL buffer containing 0.1 M glucose and then alternately pushed and pulled the buffer using a pasteur pipette so that buffer can pass through the polypropylene tube. To initiate the flow of buffer from beaker to syringe 1, a pasteur pipette was used for the suction of buffer. The pasteur pipette was removed after starting the continuous flow of buffer from the beaker to syringe 1. The flow rate (mL/min) was controlled by a fine roller clamp regulator 1 (JMI Syringes and Medical Devices Ltd. Bangladesh).

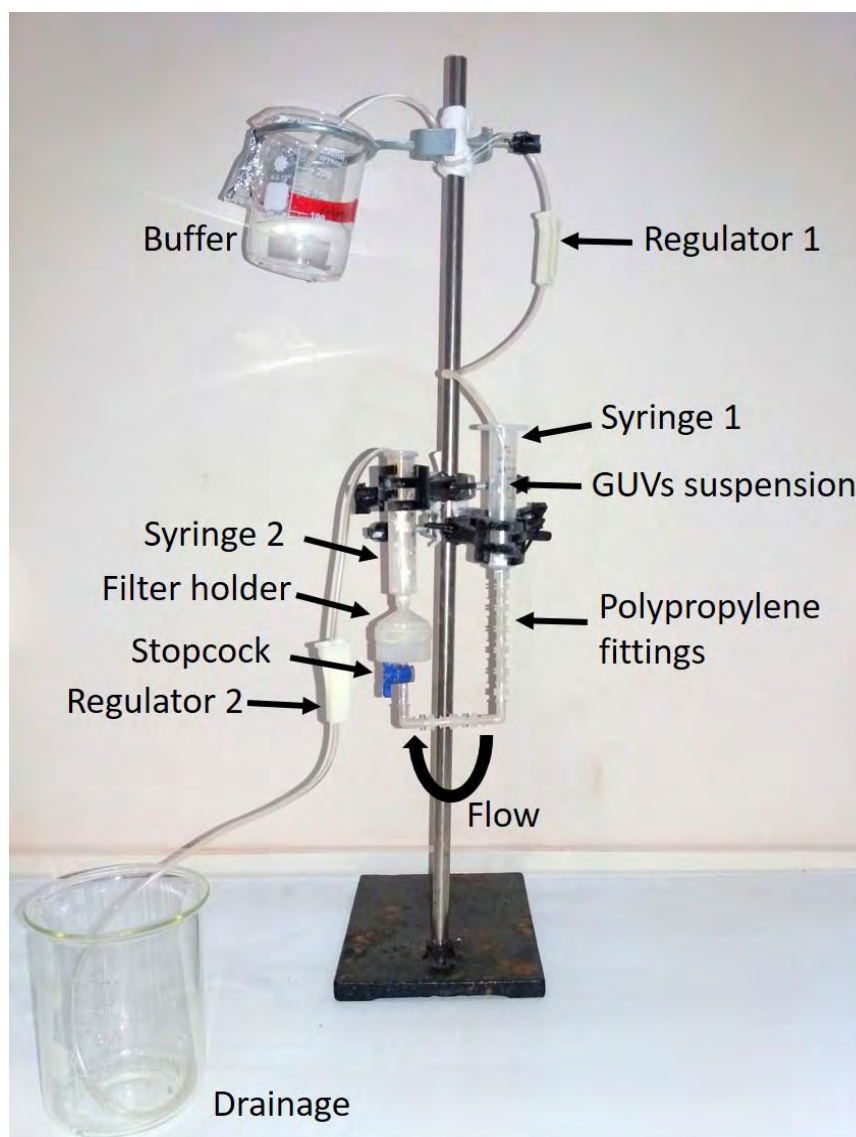


Fig. 3.16 Set-up for the purification of GUVs using a locally developed low cost non-electromechanical technique [42].

The drainage rate of buffer from syringe 2 to drain was kept at the same flow rate of buffer flowing from beaker to syringe 1. In this regard, after calibrating the roller clamp regulators, the positions of roller for different flow rates were marked on the surface of roller clamp regulators. When the buffer started to flow at a constant rate, the GUVs suspension was added to the syringe 1. If the beaker is kept at a height, h from the ground, the potential energy of the buffer in the beaker, $P.E. = h\rho g$, where, ρ is the density of buffer and g is the acceleration due to gravity. During the flow of buffer from

beaker to syringe 1, the potential energy of buffer changes to kinetic energy, $K.E.=1/2 \cdot mv^2$, where m is the mass of buffer and v is the velocity of flow of buffer to the syringe 1. The flow of buffer due to gravity is controlled by the roller clamp regulator 1. The similar physical equation is also applied for removing the buffer from the syringe 2 to drainage. The direction of the flow of buffer through the polycarbonate membrane was from bottom to top as shown in Fig. 3.16. The smaller vesicles passed through the pores of polycarbonate membrane to the syringe 2. For getting the similar size concentrated GUVs suspension from the purification, a 1-way polycarbonate stopcock (Luer stopcock VXB1055, AS-ONE, Japan) was inserted between the filter holder and the polypropylene tube as shown in Fig. 3.16. After filtering the GUVs suspension for a certain time, stopcock was closed and the solution in the space under the filter holder was collected and used as a purified GUVs suspension.

3.5.2 Membrane filtering method

To compare the experimental results, a compact double-headed peristaltic pump (CPP-SP2, Shenchen, China) was used to flow and to control the flow rate of buffer in the membrane filtering method. In the standard membrane filtering method, a double-headed peristaltic pump is used for the continuous flow of buffer and the controlling of flow rate of buffer with GUVs suspension. In this case, polypropylene tube contains a total number of 9 fittings instead of 11 used in the new purification technique. To perform the experiment, it requires continuous supply of electricity during purification. After incubation, the GUVs suspension was centrifuged at $13,000 \times g$ for 20 min at $20^\circ C$ using a refrigerated centrifuge (NF 800R, NUVE, Turkey) and then the supernatant containing GUVs was filtered through a $10 \mu m$ diameter pores nucleopore polycarbonate membrane (Whatman® Nucleopore™ Track-Etched Membranes, UK) clamped in a polypropylene filter holder (Swinnex, $\phi = 25$ mm, Millipore Co., Billerica, MA). The arrangement of the purification technique is depicted in Fig. 3.17. The upper end of the filter holder was connected with a 10 mL plastic (polypropylene) syringe 2 (JMI Syringes and Medical Devices Ltd. Bangladesh) and the lower end was connected with a tube containing three different types of polypropylene fittings (Luer fittings VRFE6, VRFC6, VRSC6; AS-ONE, Japan) having inner diameter 3 mm as shown in Fig. 3.17. In this case, the tube contains a total number of 9 fittings instead of 11 that

was used in non-electromechanical technique [34]. The other end of the tube was connected to syringe 1 having the same volume of 10 mL. The GUVs suspension in buffer containing 0.1 M glucose was added to syringe 1 at a certain flow rate which is control by peristaltic pump. Before starting the flow of buffer through syringe 1 to syringe 2, the air bubbles were carefully removed from the polypropylene tube and filter holder. In this case, the syringe 1 was filled with 7-9 mL buffer containing 0.1 M glucose and then alternately pushed and pulled the buffer using a pasteur pipette so that buffer can pass through the polypropylene tube.

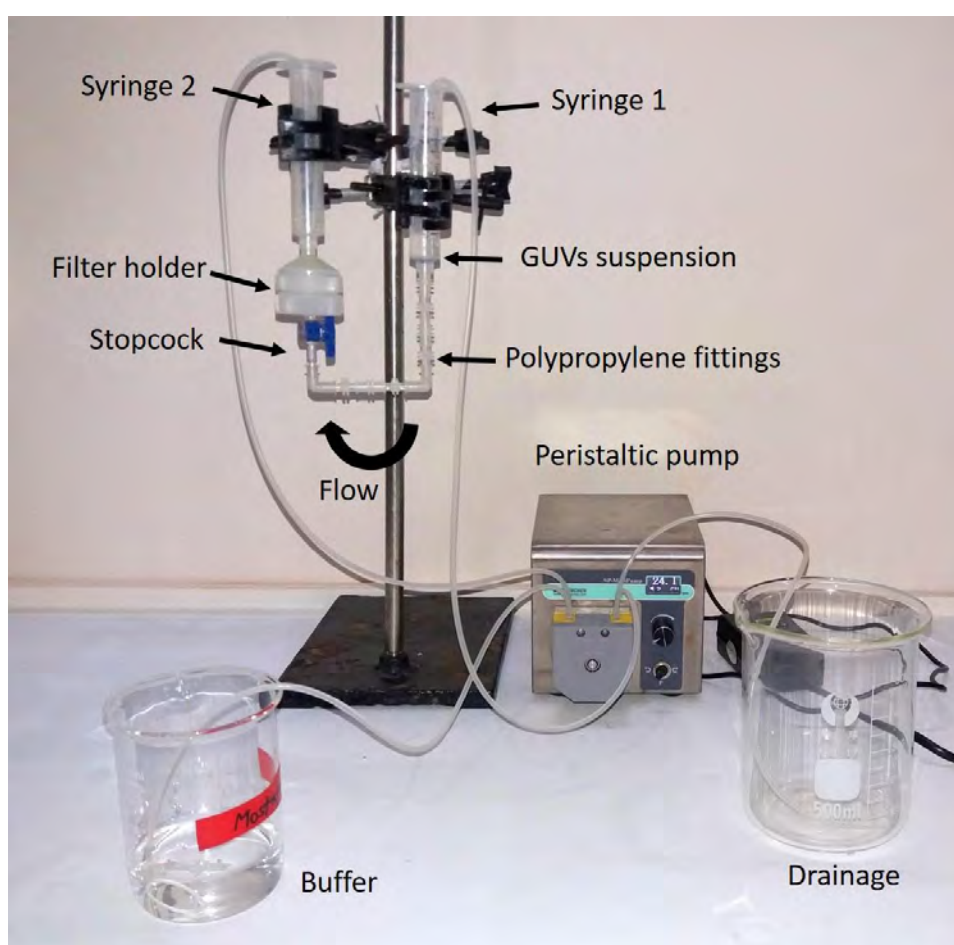


Fig. 3.17 Set-up of membrane filtering method.

The set-up of membrane filtering method is shown in Fig. 3.17. The detail of this method is described in the published paper [34]. The drainage rate of buffer from syringe 2 to drain was kept at the same flow rate using peristaltic pump. The direction of the flow of buffer with GUVs suspension through the polycarbonate membrane was from bottom to top as shown in Fig. 3.17. The smaller vesicles passed through the pores

of polycarbonate membrane to the syringe 2. For getting the similar size concentrated GUVs suspension from the purification, a 1-way polycarbonate stopcock (Luer stopcock VXB1055, AS-ONE, Japan) was inserted between the filter holder and the polypropylene tube as shown in Fig. 3.16. After filtering the GUVs suspension for a certain time, stopcock was closed and the solution in the space under the filter holder was collected and used as a purified GUVs suspension.

3.6 Observation of GUVs

3.6.1 GUVs suspension in a microchamber

After the purification, 300 μL GUVs suspension was taken into a handmade microchamber which was prepared on a glass slide by inserting a U-shaped silicone rubber spacer between the cover slip and the glass slide. To prevent the strong interaction between the glass surface and GUVs, the inside of the microchamber was coated with 0.10% (w/v) BSA dissolved in the buffer containing 0.1 M glucose.

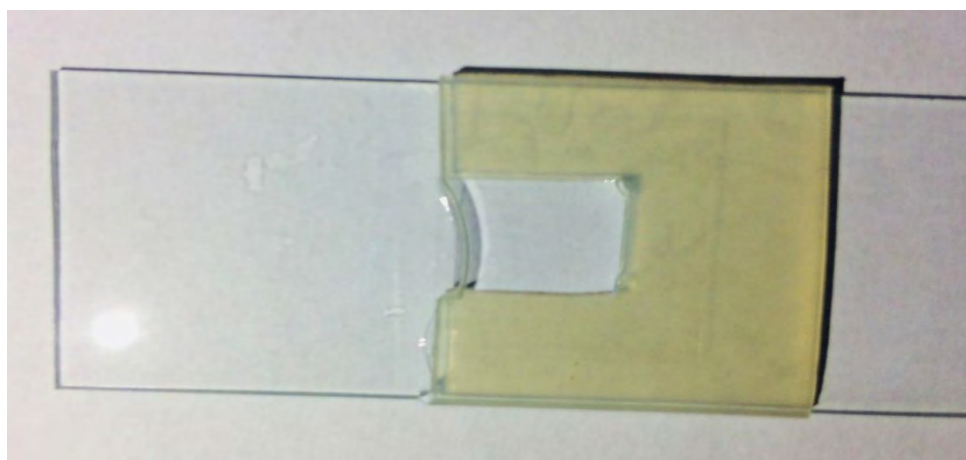


Fig. 3.18 GUVs suspension in a microchamber

3.6.2 Inverted phase contrast microscope (IX-73)

Phase contrast microscopy is used for observing colorless and transparent specimens and living cells. It utilizes the difference between light rays propagating directly from the light source and light rays refracted by the specimen when light passes through it to add bright/dark contrast to images of transparent specimens. The microscope is fitted

with a phase-contrast objective and a condenser for observations. Specimens may be made to appear dark against a bright background (positive contrast) or bright against a dark background (negative contrast). The borders of images are surrounded by a characteristic bright “halo.” To observe the GUVs in the suspension, it is very important to create sugar asymmetry between the inside and the outside of GUVs. Therefore, the solution densities between inside and outside of GUVs have to be different. The GUVs were settled down at the bottom of the microchamber due to this density difference. The difference in refractive indices of the sugar solution enhanced the contrast of GUVs during the observation in the phase contrast microscope. For this reason, 0.1 M sucrose was used in the buffer as the internal solution and 0.1 M glucose in the buffer as the external solution of GUVs.



Fig. 3.19 Observation of GUVs suspension under Inverted phase contrast microscope (IX-73)

The GUVs were observed using an inverted phase contrast microscope (IX-73, Olympus, Japan) with 20× objective at 25 ± 1 °C and phase contrast image of GUVs was recorded with CCD camera (DP22 Olympus, Japan).

3.7 Statistical Analysis using Lognormal Distribution

The lognormal distribution has been used as a model for empirical data generating processes in a wide variety of disciplines. In portfolio analysis and in statistical studies of the deposition of mineral resources of lognormal random variables are of central interest. Lognormal distributions are widely and increasingly used to fit data from radar, physical and biological lifetimes, incomes, stock market prices, geography and geology [67]. In probability theory, a lognormal distribution is a continuous probability distribution of a random variable whose logarithm is normally distributed. Thus, if the random variable d is log-normally distributed, then $f(d) = \ln d$ has a normal distribution. If $f(d)$ has a normal distribution, then the exponential function of $f(d)$, $d = \exp[f(d)]$ has a log-normal distribution.

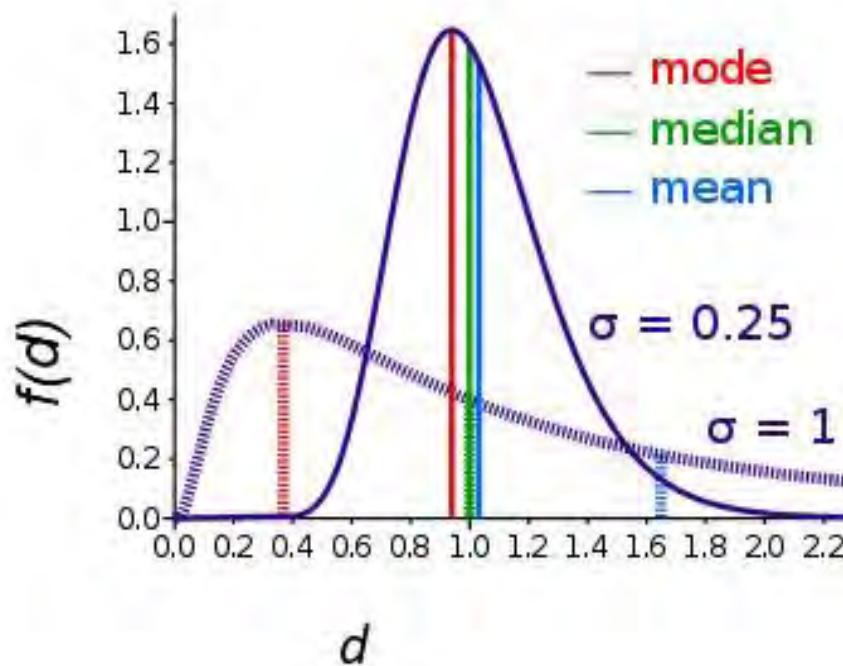


Fig. 3.20 Lognormal distribution

A random variable which is log-normally distributed takes only positive real values [68]. The lognormal distribution is defined as follows,

$$f(d) = \frac{1}{d \cdot \sigma \sqrt{2\pi}} \exp\left(-\frac{(\ln d - \mu)^2}{2\sigma^2}\right) \quad \dots \quad \dots \quad \dots \quad (3.1)$$

$f(d)$ = Probability distribution function of GUVs with diameter d .

Average diameter of the distribution is,

$$\mu_{ave} = \exp\left(\mu + \frac{\sigma^2}{2}\right) \quad \dots \quad \dots \quad \dots \quad (3.2)$$

μ = Mean of the lognormal distribution

σ^2 = Variance of the lognormal distribution

CHAPTER 4

RESULTS AND DISCUSSION

4.1. Effects of filtering on the size distribution and average size of GUVs at flow rate 1.0 mL/min using non-electromechanical method

To investigate the effects of filtering on the size distribution and average size of GUVs, 40%DOPG/60%DOPC-GUVs (% indicates mole %) in buffer were purified using the apparatus shown in Fig. 3.16. Fig. 4.1A shows a typical experimental result of a phase contrast image of a GUVs suspension before purification, showing GUVs with different diameters. After measuring the diameters of 485 GUVs (i.e. number of observed GUVs, $N = 485$) from several phase contrast images, a histogram of the distribution of GUVs was prepared as shown in Fig. 4.1B. From the histogram, a small number of GUVs with diameters greater than 10 μm , and a large number of GUVs with diameters less than 10 μm was observed. A similar result was also obtained from two independent experiments (i.e. number of independent experiments, $n = 2$). The vesicle with diameters less than 2 μm was eliminated because they were too many to count. In contrast, after 45 min purification of a GUV suspension at flow rate 1.0 mL/min, a typical phase contrast image of the preparation is shown in Fig. 4.1C. The histogram using $N = 317$ of the purified suspension is shown in Fig. 4.1D, in which a small number of GUVs with diameters smaller than 10 μm and a large number of GUVs with diameters 10–30 μm is observed. A similar result is also obtained from $n = 2$. Therefore, these results indicate that the purified suspension of GUVs contains mainly similar-size GUVs with diameters 10–30 μm .

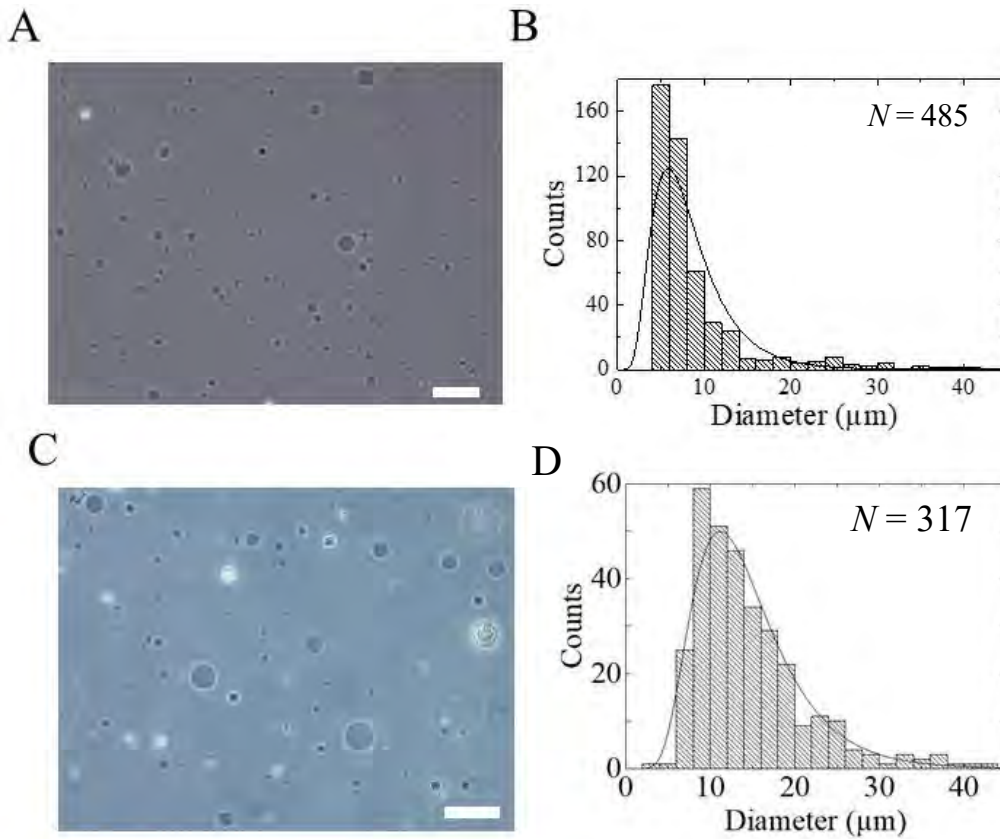


Fig. 4.1 Effects of filtering on the size distribution and average size of the 40%DOPG/60%DOPC-GUVs using non-electromechanical technique. (A) and (B) show a typical phase contrast image and a size distribution histogram of the GUVs suspension before the purification, respectively. (C) and (D) show a typical phase contrast image and a size distribution histogram of the GUVs suspension after the purification with flow rate 1.0 mL/min for 45 min, respectively. The bar in the images corresponds to 30 μm. The solid line of Fig. B and D corresponds to the lognormal distribution fit of eq. 1. N = Number of observed GUVs.

It turned out that all obtained histograms were asymmetric by form. It is well known that such distributions are described mathematically by a lognormal distribution as follows:

$$f(d) = \frac{1}{d} \cdot \frac{1}{\sigma\sqrt{2\pi}} \exp\left(-\frac{(\ln d - \mu)^2}{2\sigma^2}\right) \quad \dots \quad \dots \quad \dots \quad (4.1)$$

where, $f(d)$ indicates the normalized counts of GUVs with diameter d . Here, μ is the mean and σ^2 is the variance of the lognormal distribution.

These are determined from the real distribution. Then the average value of the distribution is as follows:

$$d_{ave} = \exp\left(\mu + \frac{1}{2}\sigma^2\right) \quad \dots \quad \dots \quad \dots \quad (4.2)$$

A lognormal distribution was previously used to fit the histogram of the persistence length of the endoplasmic reticulum found from a combination of fixed and live cells (human MRC5 lung cells) [69]; and based on energetic and thermodynamic analyses a distribution function has been developed that fitted experimental results on the size distribution of egg lecithin vesicles prepared by sonication [70], a distribution quite similar to a lognormal distribution function. Therefore, the histograms of Fig. 4.1B and 4.1D were fitted with equation (4.1) from which the average values of the GUVs were obtained. From the fitted curves, the average values of the GUVs using equation (4.2) are 10.5 and 17.5 μm for the unpurified and purified GUVs suspension, respectively. The best fit of the lognormal distribution was evaluated from the coefficient of determination, R^2 . The values of R^2 were 0.87 and 0.95 for the unpurified and purified GUVs, respectively. The average sizes of the GUVs, $\overline{d_{ave}}$, from two independent experiments were (10.0 ± 0.7) and (16.9 ± 0.8) μm (\pm indicating the standard deviation) for the unpurified and purified GUVs suspension, respectively. These results can be explained in the following way: that during purification most of the vesicles with diameters less than 10 μm pass through the pores of a polycarbonate membrane and therefore the average size of the GUVs is increased after purification. However, in Fig. 4.1D, some GUVs with diameters less than 10 μm are observed, perhaps because lipid aggregates have obstructed their passage through the pores of the polycarbonate membrane.

4.2 Effects of filtering on the size distribution and average size of GUVs at flow rate 1.0 mL/min using membrane filtering method

A similar size distribution of GUVs is also observed in the pump-driven membrane filtering method [34]. To compare with the results of our new technique, an experiment was therefore performed using a compact mini peristaltic pump [34]. It is to be noted that 9 polypropylene fittings are used instead of 11 in the pump-driven standard membrane filtering method and the flow of buffer is controlled by a peristaltic pump, with the buffer sucked from syringe 1 to 2 using the pump. In our technique, the flow of buffer in the purification unit is due to gravity. If 9 propylene fittings were used in our case then about 2 mL buffer would remain in syringe 1 at the end of purification. To remove the entire buffer containing GUVs suspension from syringe 1 to the polypropylene tube owing to gravity, syringe 1 was kept slightly higher than syringe 2 by employing 11 polypropylene fittings instead of 9. A typical phase contrast image of unpurified GUVs and their corresponding histogram of $N = 506$ with fitting (solid line) of equation (4.1) are presented in Fig. 4.2A and 4.2B, respectively. Similarly, a typical phase contrast image of a GUV suspension purified using pump-driven membrane filtrated and their corresponding histogram of $N = 325$ with fitting (solid line) of equation 1 are presented in Fig. 4.2C and 4.2D, respectively. From the fitting shown in Fig. 4.2B and 4.2D, the average values of the GUVs were 8.7 and 17.1 μm for the unpurified and purified suspensions of GUVs, respectively using equation (4.2). The values of R^2 are found to be 0.89 and 0.91 for the unpurified and purified GUV suspensions, respectively. The average sizes of the GUVs obtained from two independent experiments are (8.1 ± 0.8) and (17.6 ± 2.1) μm for the unpurified and purified GUV suspensions, respectively.

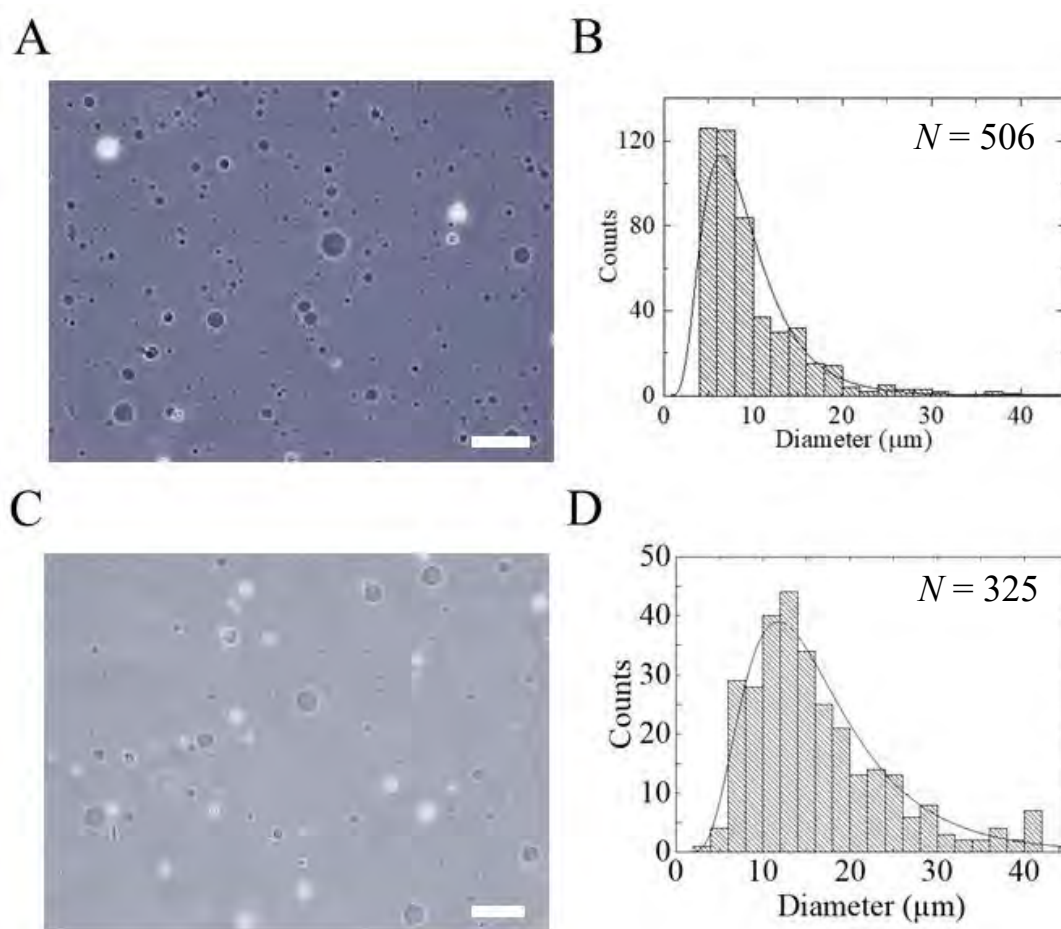


Fig.4.2 Effects of filtering on the size distribution and average size of the 40%DOPG/60%DOPC-GUVs using membrane filtering method. (A) and (B) show a typical phase contrast image and a size distribution histogram of the GUVs suspension before the purification, respectively. (C) and (D) show a typical phase contrast image and a size distribution histogram of the GUVs suspension after the purification with a flow rate 1.0 mL/min for 45 min, respectively. The bar in the images corresponds to 30 μm . The solid line of Fig. B and D corresponds to the lognormal distribution fit of eq. 1. N = Number of observed GUVs.

Therefore, the results from the new technique exhibit a high degree of similarity to that of the pump-driven membrane filtering method. The key point of this technique is that it provides a way to obtain enough GUVs of more or less similar size for subsequent experiments. In the gravity-based membrane filtering technique which is discussed here, the average size of the GUVs increases compared to the initial GUV preparation

while its dispersion decreases. Therefore, an asymmetrical distribution of GUV sizes was obtained that could be described mathematically as a lognormal distribution. By removing from the initial preparation vesicles with diameters less than 10 μm , we increased the average size of GUVs on the one hand and decreased the dispersion (i.e. constricted the width of the distribution) on the other hand. This seems a good approach if a narrow range of GUV distributions such as 10–20 μm is desired. Since the single GUV method requires various similar size GUVs such as 10–15, 16–20, 21–25 μm etc, the new purification technique has provided the required distribution as shown in Fig. 4.1(D). Without purification the size distribution width is also probably narrow enough as shown in Fig. 4.1B, but the presence of many small vesicles of sizes 2–10 μm and lipid aggregates in the observation chamber create challenges for studying membrane-active agents (peptides, proteins, nanoparticles, surfactants) interacting with single GUVs and suspensions of GUVs. Therefore, it is important to remove the smaller vesicles and lipid aggregates from the GUVs suspension.

4.3 Effects of filtering on the size distribution and average size of GUVs at flow rate 1.5 mL/min using non-electromechanical method

To observe the effects of filtering on the size distribution and average size of GUVs, 40%DOPG/60%DOPC-GUVs in buffer were purified using the apparatus shown in Fig. 3.16. Fig. 4.3A shows a typical experimental result of a phase contrast image of a GUVs suspension before purification, showing GUVs with different diameters. After measuring the diameters of 505 GUVs (i.e. number of observed GUVs, $N = 505$) from several phase contrast images, a histogram of the distribution of GUVs was prepared as shown in Fig. 4.3B. From the histogram, a small number of GUVs with diameters greater than 10 μm , and a large number of GUVs with diameters less than 10 μm was observed. A similar result was also obtained from two independent experiments (i.e. number of independent experiments, $n = 2$). The vesicle with diameters less than 2 μm was eliminated because they were too many to count. In contrast, after 45 min purification of a GUV suspension at flow rate 1.5 mL/min, a typical phase contrast image of the preparation is shown in Fig. 4.3C. The histogram using $N = 310$ of the

purified suspension is shown in Fig. 4.3D, in which a small number of GUVs with diameters smaller than 10 μm and a large number of GUVs with diameters 10–30 μm is observed. A similar result is also obtained from $n = 2$. Therefore, these results indicate that the purified suspension of GUVs contains only similar-size GUVs with diameters 10–30 μm .

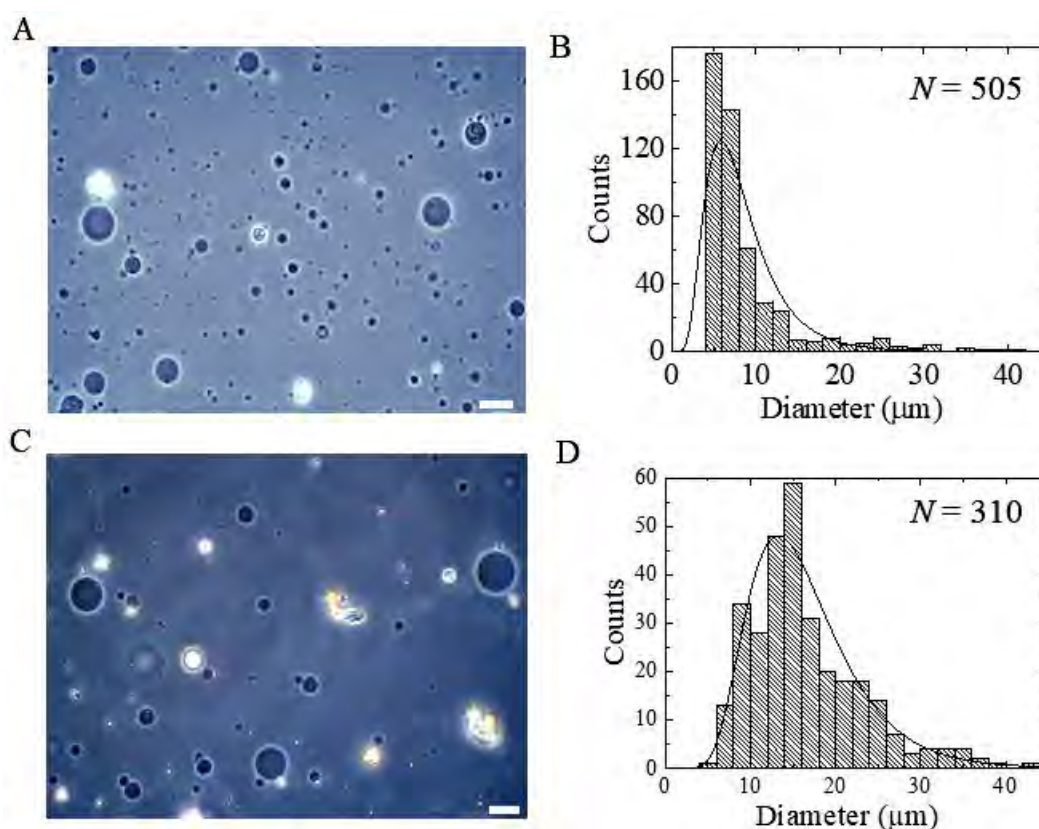


Fig. 4.3 Effects of filtering on the size distribution and average size of the 40%DOPG/60%DOPC-GUVs using non-electromechanical technique. (A) and (B) show a typical phase contrast image and a size distribution histogram of the GUVs suspension before the purification, respectively. (C) and (D) show a typical phase contrast image and a size distribution histogram of the GUVs suspension after the purification with flow rate 1.5 mL/min for 45 min, respectively. The bar in the images corresponds to 30 μm . The solid line of Fig. B and D corresponds to the lognormal distribution fit of eq. 1. N = Number of observed GUVs.

The histograms of Fig. 4.3B and 4.3D were fitted with equation (4.1) from which the average values of the GUVs were obtained. From the fitted curves, the average values of the GUVs using equation (4.2) are 8.6 and 18.5 μm for the unpurified and purified GUVs suspension, respectively. The best fit of the lognormal distribution was evaluated from the coefficient of determination, R^2 . The values of R^2 were 0.87 and 0.89 for the unpurified and purified GUVs, respectively. The average sizes of the GUVs, $\overline{d_{\text{ave}}}$, from two independent experiments were (11.2 ± 3.7) and (18.7 ± 0.3) μm (\pm indicating the standard deviation) for the unpurified and purified GUVs suspension, respectively. These results can be set forth in the following way: that during purification most of the vesicles with diameters less than 10 μm pass through the pores of a polycarbonate membrane and therefore the average size of the GUVs is increased after purification. However, in Fig. 4.3D, some GUVs with diameters less than 10 μm are observed, perhaps because lipid aggregates have obstructed their passage through the pores of the polycarbonate membrane.

4.4 Effects of filtering on the size distribution and average size of GUVs at flow rate 1.5 mL/min using membrane filtering method

An identical size distribution of GUVs is also revealed in the pump-driven membrane filtering method. To compare with the results of our new technique for 1.5 mL/min flow rate, an experiment was therefore performed using a compact mini peristaltic pump. A typical phase contrast image of unpurified GUVs and their corresponding histogram of $N = 506$ with fitting (solid line) of equation 1 are presented in Fig. 4.4A and 4.4B, respectively. Similarly, a typical phase contrast image of a GUV suspension purified using pump-driven membrane filtrated and their corresponding histogram of $N = 325$ with fitting (solid line) of equation (4.1) are presented in Fig. 4.4C and 4.4D, respectively. From the fitting shown in Fig. 4.4B and 4.4D, the average values of the GUVs were 8.2 and 18.8 μm for the unpurified and purified suspensions of GUVs, respectively using equation (4.2). The values of R^2 are found to be 0.91 and 0.90 for the unpurified and purified GUV suspensions, respectively. The average sizes of the GUVs obtained from two independent experiments are (11.3 ± 4.3) and (19.7 ± 1.2) μm for the unpurified and purified GUV suspensions, respectively.

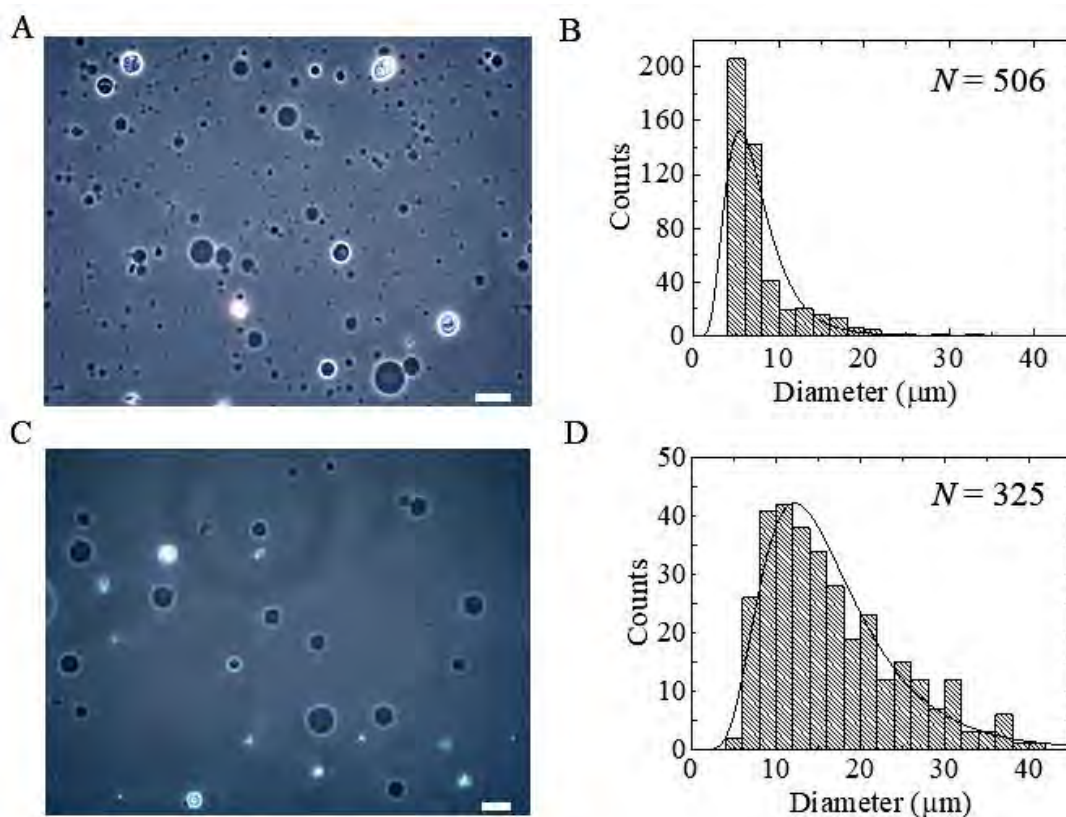


Fig. 4.4 Effects of filtering on the size distribution and average size of the 40%DOPG/60%DOPC-GUVs using membrane filtering method. (A) and (B) show a typical phase contrast image and a size distribution histogram of the GUVs suspension before the purification, respectively. (C) and (D) show a typical phase contrast image and a size distribution histogram of the GUVs suspension after the purification with a flow rate 1.5 mL/min for 45 min, respectively. The bar in the images corresponds to 30 μm . The solid line of Fig. B and D corresponds to the lognormal distribution fit of eq. 1. N = Number of observed GUVs.

Therefore, the results from the new technique exhibit a high degree of similarity to that of the pump-driven membrane filtering method. The key point of this technique is that it provides a way to obtain enough GUVs of more or less similar size for subsequent experiments. In the gravity-based membrane filtering technique which is discussed here, the average size of the GUVs increases compared to the initial GUV preparation while its dispersion decreases. The new purification technique has provided the

required distribution as shown in Fig. 4.4D. Without purification the size distribution width is also probably narrow enough as shown in Fig. 4.4B, but the presence of many small vesicles of sizes 2–10 μm and lipid aggregates in the observation chamber create challenges for studying membrane-active agents (peptides, proteins, nanoparticles, surfactants) interacting with single GUVs and suspensions of GUVs. Therefore, it is important to remove the smaller vesicles and lipid aggregates from the GUVs suspension.

4.5 Effects of filtering on the size distribution and average size of GUVs at flow rate 2.0 mL/min using non-electromechanical method

To investigate the effects of filtering on the size distribution and average size of GUVs, 40%DOPG/60%DOPC-GUVs in buffer were purified using the apparatus shown in Fig. 3.16. Fig. 4.5A and Fig. 4.5C show the typical experimental result of phase contrast images of GUVs suspension before and after purification respectively, showing GUVs with different diameters. After measuring the diameters of 503 GUVs (i.e. number of observed GUVs, $N = 503$) from several phase contrast images of unpurified GUVs suspension, a histogram of the distribution of GUVs was prepared as shown in Fig. 4.5B. From the histogram, a small number of GUVs with diameters greater than 10 μm , and a large number of GUVs with diameters less than 10 μm was observed. A similar result was also obtained from two independent experiments (i.e. number of independent experiments, $n = 2$). The vesicle with diameters less than 2 μm was eliminated because they were too many to count. In contrast, after 45 min purification of a GUV suspension at flow rate 2.0 mL/min, the histogram using $N = 314$ of the purified suspension is shown in Fig. 4.5D, in which a small number of GUVs with diameters smaller than 10 μm and a large number of GUVs with diameters 10–30 μm are observed. A similar result is also obtained from $n = 2$. Therefore, these results indicate that the purified suspension of GUVs contains only similar-size GUVs with diameters 10–30 μm .

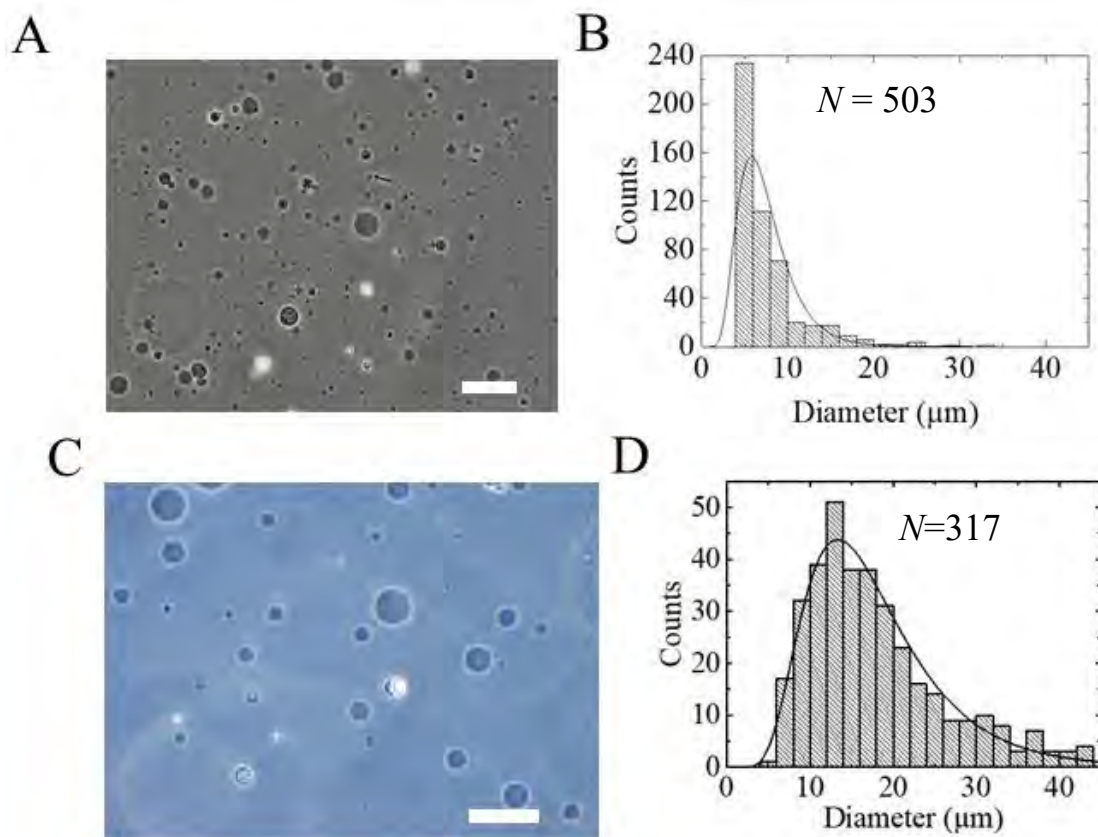


Fig. 4.5 Effects of filtering on the size distribution and average size of the 40%DOPG/60%DOPC-GUVs using non-electromechanical technique. (A) and (B) show a typical phase contrast image and a size distribution histogram of the GUVs suspension before the purification, respectively. (C) and (D) show a typical phase contrast image and a size distribution histogram of the GUVs suspension after the purification with flow rate 2.0 mL/min for 45 min, respectively. The bar in the images corresponds to 50 μm . The solid line of Fig. B and D corresponds to the lognormal distribution fit of eq. 1. N = Number of observed GUVs.

The histograms of Fig. 4.5B and 4.5D were fitted with equation (4.1) from which the average values of the GUVs were calculated. From the fitted curves, the average values of the GUVs using equation (4.2) are 8.4 and 19.98 μm for the unpurified and purified GUVs suspension, respectively. The best fit of the lognormal distribution was evaluated from the coefficient of determination, R^2 . The values of R^2 were 0.85 and 0.96 for the

unpurified and purified GUVs, respectively. The average sizes of the GUVs, $\overline{d_{\text{ave}}}$, from two independent experiments were (8.8 ± 0.4) and (20.1 ± 0.1) μm (\pm indicating the standard deviation) for the unpurified and purified GUVs suspension, respectively. These results can be set forth in the following way: that during purification most of the vesicles with diameters less than 10 μm pass through the pores of a polycarbonate membrane and therefore the average size of the GUVs is increased after purification. However, in Fig. 4.5D, some GUVs with diameters less than 10 μm are observed, perhaps, because lipid aggregates have obstructed their passage through the pores of the polycarbonate membrane.

4.6 Effects of filtering on the size distribution and average size of GUVs at flow rate 2.0 mL/min using membrane filtering method

A similar size distribution of GUVs is also got in the pump-driven membrane filtering method for 2.0 mL/min flow rate. To compare with the results of our new technique for 2.0 mL/min flow rate, an experiment was therefore performed using a compact mini peristaltic pump [34]. A typical phase contrast image of unpurified GUVs and their corresponding histogram of $N = 508$ with fitting (solid line) of equation 1 are presented in Fig. 4.6A and 4.6B, respectively. Similarly, a typical phase contrast image of purified GUVs suspension using pump-driven membrane filtrated and their corresponding histogram of $N = 315$ with fitting (solid line) of equation (4.1) are presented in Fig. 4.6C and 4.6D, respectively. From the fitting shown in Fig. 4.6B and 4.6D, the average values of the GUVs were 8.04 and 20.03 μm for the unpurified and purified suspensions of GUVs, respectively using equation (4.2). The values of R^2 are found to be 0.87 and 0.85 for the unpurified and purified GUV suspensions, respectively. The average sizes of the GUVs obtained from two independent experiments are (7.7 ± 0.3) and (20.0 ± 0.1) μm for the unpurified and purified GUV suspensions, respectively.

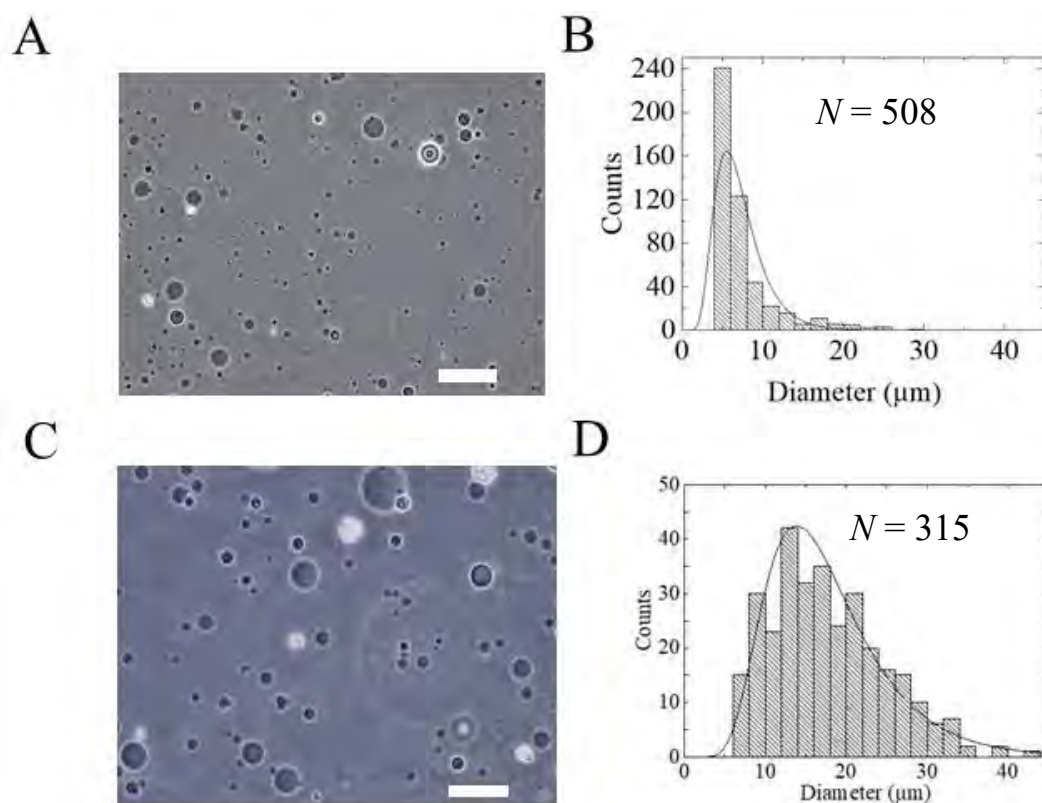


Fig. 4.6 Effects of filtering on the size distribution and average size of the 40%DOPG/60%DOPC-GUVs using membrane filtering method. (A) and (B) show a typical phase contrast image and a size distribution histogram of the GUVs suspension before the purification, respectively. (C) and (D) show a typical phase contrast image and a size distribution histogram of the GUVs suspension after the purification with a flow rate 2.0 mL/min for 45 min, respectively. The bar in the images corresponds to 30 μm . The solid line of Fig. B and D corresponds to the lognormal distribution fit of eq. 1. N = Number of observed GUVs.

Therefore, the results from our technique illustrated a high degree of similarity to that of the pump-driven membrane filtering method. The key point of this technique is that it provides a way to obtain enough GUVs of more or less similar size for subsequent experiments. The new purification technique has provided the required distribution as shown in Fig. 4.6(D). Without purification the size distribution width is probably narrow enough as shown in Fig. 4.6(B), but the presence of many small vesicles of sizes 2–10 μm and lipid aggregates in the observation chamber create challenges for studying membrane-active agents (peptides, proteins, nanoparticles, surfactants) interacting with

single GUVs and suspensions of GUVs. Therefore, it is important to remove the smaller vesicles and lipid aggregates from the GUVs suspension.

4.7 Effects of second purification on the size distribution and average size of GUVs using non-electromechanical method

To investigate the effects of a second purification on the size distribution and the average size of GUVs, 40%DOPG/60%DOPC-GUVs in buffer were again purified using the apparatus shown in Fig. 3.16. Fig. 4.7A shows a typical experimental result of the phase contrast image of the purified (first purification) GUVs suspension at flow rate 2.0 mL/min for 45 min. The histogram of $N = 323$ purified GUVs is shown in Fig. 4.7B. It shows a small number of GUVs with diameters smaller than 10 μm and a large number of GUVs with diameters 10–30 μm . The reproducibility is confirmed using $n = 2$. After the first purification, 2.0 mL of GUV suspension was filtered again using a new polycarbonate membrane with 10 μm pores and with same flow rate and duration. Fig. 4.7C shows a typical experimental result of the phase contrast image of the purified (second purification) GUVs suspension. In this case, the density of GUVs with diameters greater than 10 μm is increased over the result of the first purification. The histogram of $N = 316$ purified GUVs is shown in Fig. 4.7D. It shows a small number of GUVs with diameters smaller than 10 μm and that almost all the GUVs have diameters 10–30 μm after the second purification. The similar results are also obtained from $n = 2$. These results indicate that the second purification of a GUV suspension provides more similar-sized and concentrated GUVs with diameters of 10–30 μm as compared to the first purification. The histograms of Fig. 4.7B and 4.7D are fitted (solid line) with equation (4.1). The average values of the GUVs are 20.7 and 22.0 μm for the first and second purifications, respectively using equation (4.2). The values of R^2 are found to be 0.98 and 0.93 for Fig. 4.7B and 4.7D, respectively. The average sizes of the GUVs from two independent experiments are (20.5 ± 0.3) and (22.3 ± 0.5) μm for the first and second purifications, respectively. The average size of the GUVs is increased because the number of GUVs with diameters less than 10 μm is greatly reduced in the second purification as observed in Fig. 4.7D.

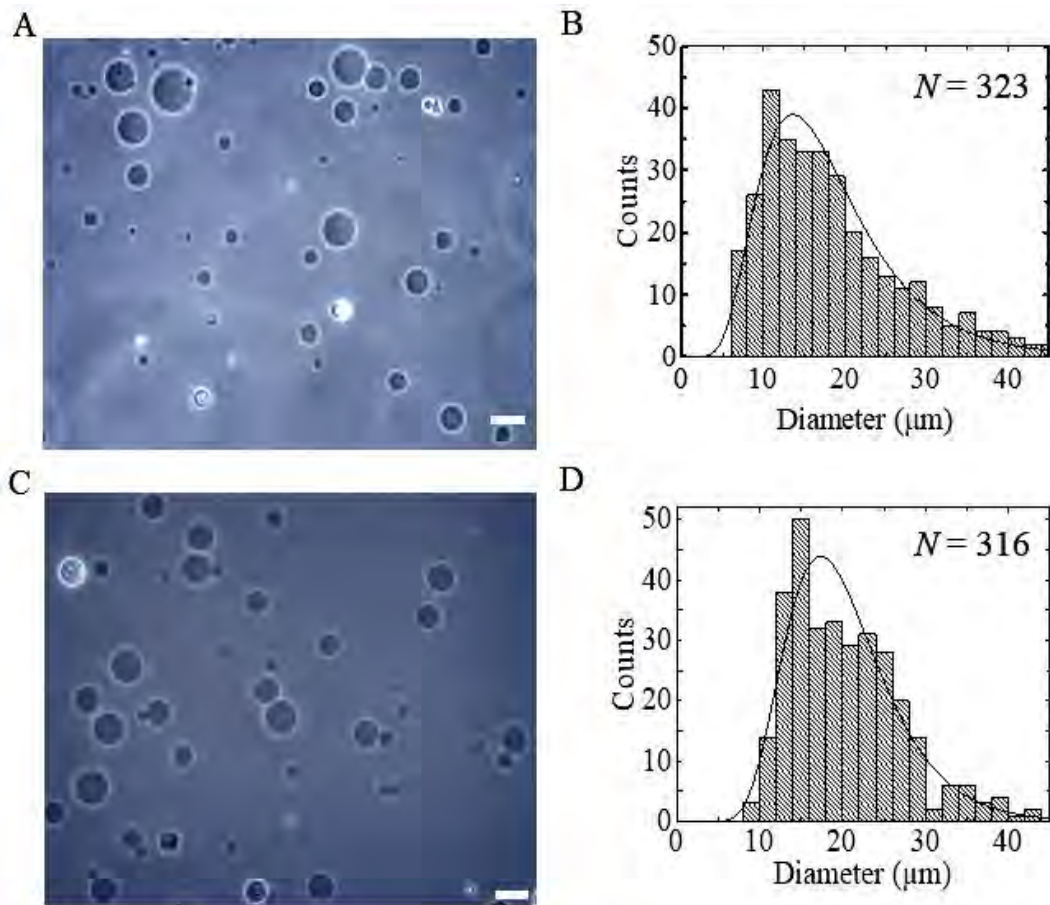


Fig. 4.7. Effects of second purification on the size distribution and average size of the 40%DOPG/60%DOPC-GUVs using non-electromechanical technique. (A) and (B) show a typical phase contrast image and a size distribution histogram of the GUVs suspension after the first purification with a flow rate 2.0 mL/min for 45 min, respectively. (C) and (D) show a typical phase contrast image and a size distribution histogram of the GUVs suspension after the second purification with a flow rate 2.0 mL/min for 45 min, respectively. The bar in the images corresponds to 30 μm . The solid line of Fig. B and D corresponds to the lognormal distribution fit of eq. 1. N = Number of observed GUVs.

4.8. Effects of flow rate on the size distribution and average size of GUVs using non-electromechanical technique

To investigate the effects of flow rate on the size distribution and average size of GUVs, 40%DOPG/60%DOPC-GUVs were purified using different flow rates such as 1.0, 1.5 and 2.0 mL/min for 45 min each. It is generally considered that an increase in flow rate may create extra pressure on the GUVs during the purification which can induce them to rupture [6]. In addition, a higher flow rate may remove the higher number of GUVs with diameters less than 10 μm by forcing their passage through the polycarbonate membrane pores. It was therefore important for us to test the effects of systematic increase in flow rate to identify an optimum flow rate for this purification method. In this regard, firstly the purification process is performed at flow rate 1 mL/min for 45 min. Fig. 4.8A shows a typical experimental result of the phase contrast image of GUVs suspension where a small number of GUVs are observed with diameter less than 10 μm . After measuring the diameters of $N = 317$, a histogram was prepared as shown in Fig. 4.8B. From this histogram, a large number of GUVs with diameters 10–25 μm and a small number of GUVs with diameters smaller than 10 μm was obtained. A similar purification was performed for GUVs at flow rates of 1.5 mL/min for 45 min. Fig. 4.8C shows a typical experimental result of the phase contrast image of the GUVs suspension where fewer GUVs with diameters smaller than 10 μm are observed than the GUVs obtained at flow rate 1.0 mL/min. In this case, the diameters of the GUVs are observed as 10–30 μm in the histogram using $N = 312$ as shown in Fig. 4.8D. Finally, the purification was performed at a flow rate 2.0 mL/min for 45 min. Fig. 4.8E shows a typical phase contrast image of the GUVs suspension for that and the histogram of the corresponding GUVs is shown in Fig. 4.8F using $N = 357$, where the diameters of the GUVs are obtained as 10–30 μm .

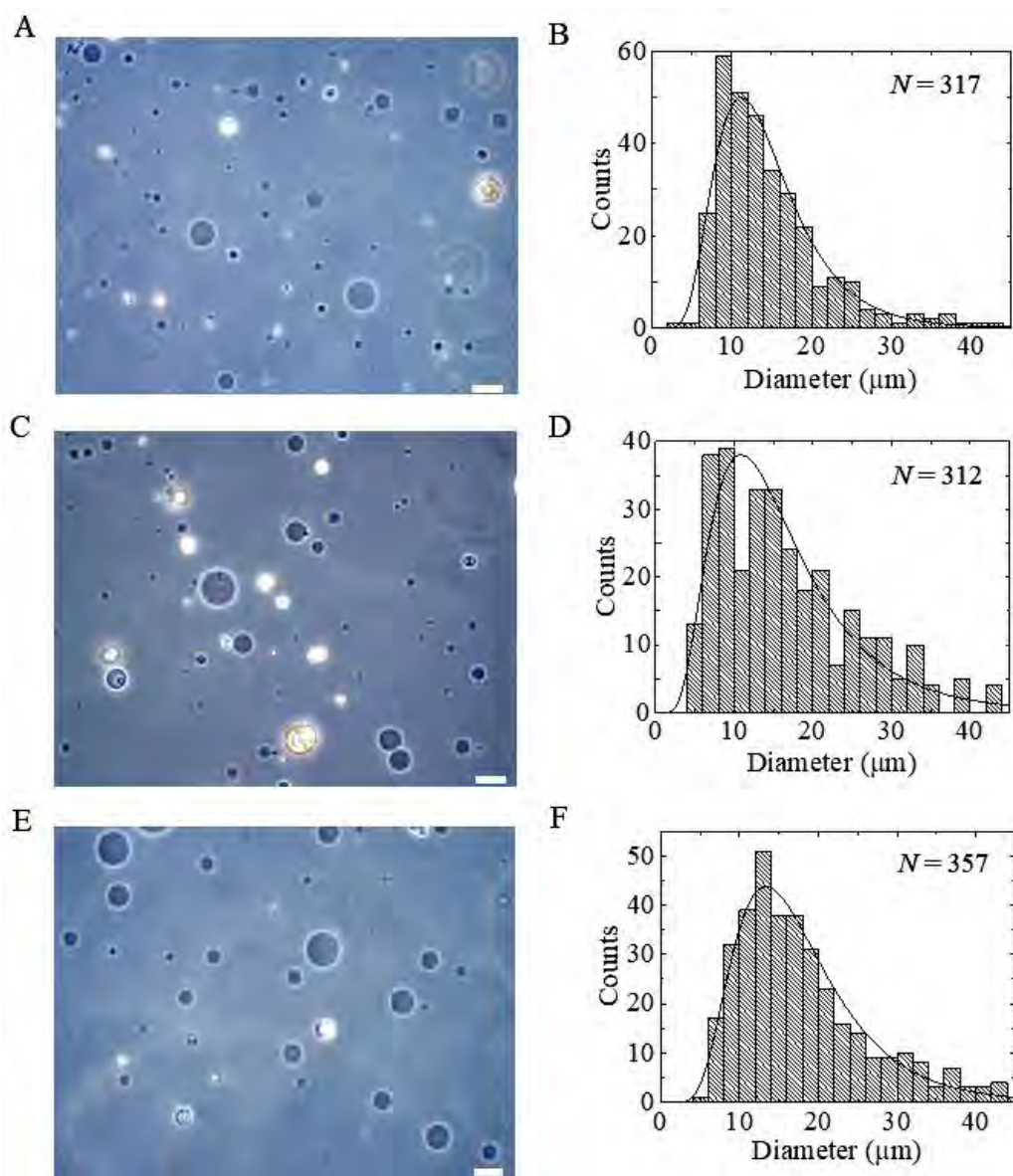


Fig. 4.8. Effects of flow rate on the size distribution and average size of the 40%DOPG/60%DOPC-GUVs using non-electromechanical technique. (A) and (B) show a typical phase contrast image and a size distribution histogram of the GUVs suspension with a flow rate 1.0 mL/min for 45 min, respectively. (C) and (D) show a typical phase contrast image and a size distribution histogram of the GUVs suspension with a flow rate 1.5 mL/min for 45 min, respectively. (E) and (F) show a typical phase contrast image and a size distribution histogram of the GUVs suspension with a flow rate 2.0 mL/min for 45 min, respectively. The bar in the images corresponds to 30 μm . The solid line of Fig. B, D and F corresponds to the lognormal distribution fit of eq. 1. N = Number of observed GUVs.

From the histograms of Fig. 4.8B, 4.8D and 4.8E, it is clearly visible that the distribution of GUVs with diameters greater than 10 μm is increased slightly with the increase in flow rate. The solid line of Fig. 4.8B, 4.8D and 4.8F corresponds to the fitting of equation (4.1) from where the average values of the GUVs are obtained as 16.4, 18.9 and 20.3 μm , respectively. The values of R^2 are found to be 0.95, 0.94 and 0.96 for Fig. 4.8B, 4.8D and 4.8F, respectively. The average sizes of the GUVs from $n = 2$ are (16.9 ± 0.8) , (18.7 ± 0.3) and (20.1 ± 0.1) μm for flow rates of 1.0, 1.5 and 2.0 mL/min, respectively using equation (4.3). Therefore, the hypothesis that the number of GUVs with diameters less than 10 μm passing through the pores of the polycarbonate membrane will increase with increasing flow rate (pressure inside the filter holder) is confirmed. At higher flow rate (3.0 mL/min), the proportion of GUVs with diameters greater than 25 μm is decreased compared to flow rate 2.0 mL/min. The average size of the GUVs at 3 mL/min is found to be (17.9 ± 0.5) using $n = 2$. This is because at this higher flow rate, some GUVs with diameters greater than 25 μm may pass through the pores of the polycarbonate membrane due to the distortion of spherical GUVs into prolate and cylindrical shapes at higher pressure [5-6]. The flow rate-dependent average size of the GUVs is presented in Fig. 4.9. Based on these analyses; the optimum flow rate is obtained as 1.0–2.0 mL/min for our new purification technique. Similar experiments were obtained using a compact peristaltic pump in the mechanical membrane filtering method [3]. The average sizes of the GUVs and the R^2 values for different flow rates using this new technique and the membrane filtering method are shown in table 1. In this paper, the average sizes of GUVs obtained are compared for various flow rates using a gravity-driven filtration method and (for comparison) using the established pump-drive membrane filtering approach. Since the value of R^2 indicates the quality of the fitting of a mathematical description of a distribution to the real histogram of data, the use of a lognormal distribution is supported by the values obtained which are ~ 1 .

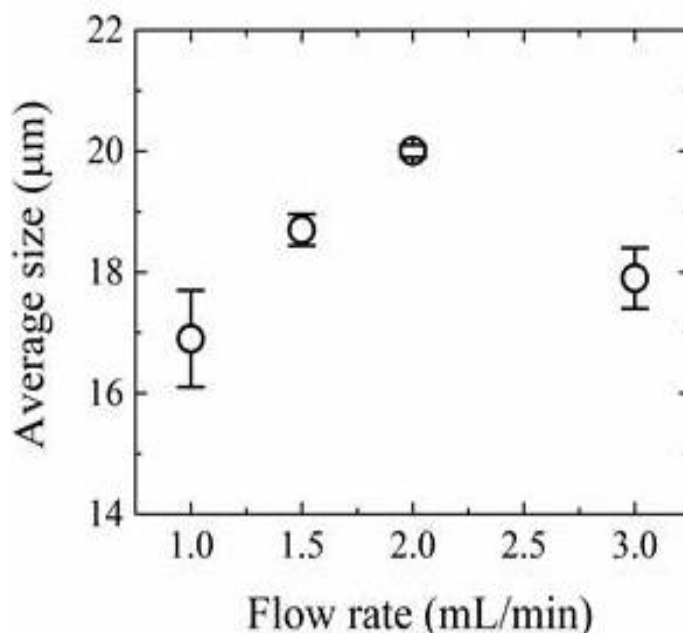


Fig. 4.9 Flow rate dependent average size of purified 40%DOPG/60%DOPC-GUVs.

4.9 Effects of higher flow rate on the size distribution and average size of GUVs in the non-electromechanical technique

To investigate the effects of higher flow rate on the size distribution and average size of GUVs in the new technique, 40%DOPG/60%DOPC-GUVs suspension was purified using flow rate 3.0 mL/min for 45 min. From two independent experiments ($n = 2$), two separate histograms are prepared using the GUVs of $N = 345$ and 367 (i.e. number of observed GUVs, N) as shown in Fig. 4.10A and 4.10B.

It is very clear that the number of GUVs with diameters greater than 25 μm is decreased for both the cases. The solid line of Fig. 4.10 corresponds to the lognormal distribution fitting of equation 1. From the fitting curves, the average values of the GUVs are obtained 18.2 and 17.5 μm for the first and second experiment, respectively. The values of R^2 are found 0.85 and 0.93 for the first and second experiment, respectively.

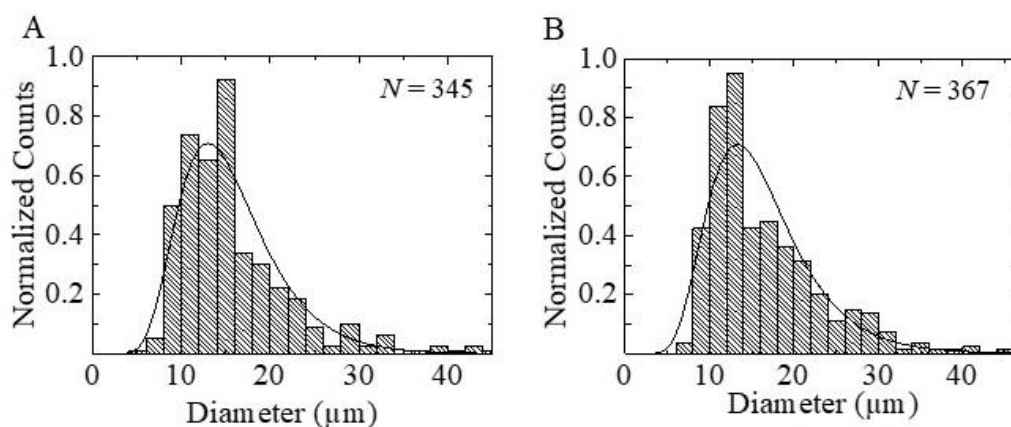


Fig. 4.10 Effects of filtering on the normalized size distribution histogram of the 40%DOPG/60%DOPC-GUVs using non-electromechanical technique. (A) First and (B) second experiment at flow rate 3.0 mL/min for 45 min in the non-electromechanical technique. The solid line of Fig. A and B corresponds to the equation 1. N = Number of observed GUVs.

The average size of the GUVs at flow rate 3.0 mL/min from $n = 2$ is obtained (17.9 ± 0.5) μm which is smaller than the average size of GUVs (20.0 ± 0.1 μm) obtained at 2.0 mL/min. At higher flow rate some GUVs with diameters greater than 25 μm may pass through the pores of polycarbonate membrane because spherical GUVs can change their shape into prolate and cylindrical shape GUVs [2-3] at higher pressure. Therefore, the average size of GUVs at 3.0 mL/min is decreased compared to 2.0 mL/min.

Table 1: Flow rate dependent average size of GUVs

Flow rate (mL/min)	Method for purification of GUVs	Average size $\overline{d_{ave}} \pm SD$ (μm)	Independent experiments (n)	R^2 values 1 st , 2 nd expt.
1.0	Non-electromechanical	16.9 ± 0.8	2	0.96, 0.95
	Membrane filtering	17.6 ± 2.1	2	0.93, 0.91
1.5	Non-electromechanical	18.7 ± 0.3	2	0.89, 0.94
	Membrane filtering	19.7 ± 1.2	2	0.89, 0.90
2.0	Non-electromechanical	20.1 ± 0.1	2	0.96, 0.80
	Membrane filtering	20.0 ± 0.1	2	0.86, 0.89

4.10 Flow rate dependent efficiency of the purification of GUVs

To evaluate the performance of this new technique, we investigated the flow rate dependent efficiency at various flow rates and compared to the pump-driven membrane filtering method [34]. The histograms in Fig. 4.8(B), 4.8(D) and 4.8(F) show a large number of GUVs with diameters 10–30 μm and a small number of vesicles with diameter smaller than 10 μm . The fraction of GUVs with diameters less than 10 μm for different flow rates in the new technique and pump-driven membrane filtration are presented in table 2. The efficiency of getting GUVs with diameters greater than 10 μm is 76, 80 and 83% for flow rate 1.0, 1.5 and 2.0 mL/min, respectively. Therefore, the efficiency of getting GUVs with diameters greater than 10 μm is increased with an increase in flow rate. This can be explained by the smaller vesicles with diameters less than 10 μm and lipid aggregates passing more easily through the pores of the polycarbonate membrane with increasing flow rate within the optimum range (i.e

1.0–2.0 mL/min). The average size of the GUVs increased with the increase of flow rate until 2.0 mL/min and then decreased (Fig. 4.9), meaning that GUVs with diameters greater than 10 μm were not lost until the flow exceeded 2.0 mL/min during the purification.

Table 2: Flow rate dependent efficiency of the purification of GUVs.

Flow rate (mL/min)	Method for purification of GUVs	Fraction of GUVs with sizes $<10 \mu\text{m}$ (%)	Independent experiments (n)	Efficiency of getting GUVs with sizes $\geq 10 \mu\text{m}$ (%)
1.0	Non-electromechanical	24 ± 5	2	76
	Membrane filtering	23 ± 4	2	77
1.5	Non-electromechanical	20 ± 5	2	80
	Membrane filtering	15 ± 4	2	85
2.0	Non-electromechanical	16 ± 3	2	84
	Membrane filtering	14 ± 1	2	86

4.11 Direct comparison of the present technique with other methods

A bar chart of the average sizes of the unpurified and purified GUVs using the new gravity-based purification technique and the pump-driven membrane filtering method for three flow rates are shown in Fig. 4.11. From this figure, it is obvious that the average size of unpurified GUVs for various flow rates are much smaller than those of purified GUVs. The average size of purified GUVs also increases slightly with an increase in flow rate. In addition, the average sizes of the GUVs using this new purification technique and the pump-driven method are almost the same for various

flow rates. Therefore, the new technique provides similar results to the pump-driven membrane filtering method, but with the advantage that our approach does not require any specialist electromechanical devices.

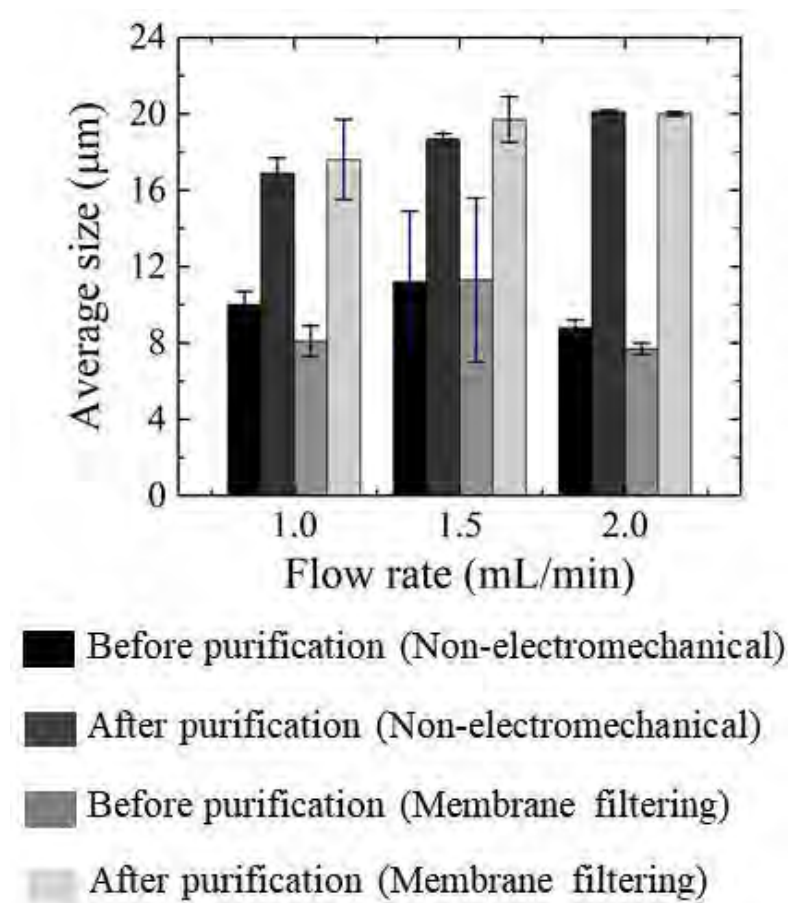


Fig. 4.11 Bar diagram of the average size of the unpurified and flow rate dependent purified 40%DOPG/60%DOPC-GUVs.

The advantages and disadvantages among different methods/techniques for the purification of GUVs are presented in the Table 3. From this table, it can be seen that all the methods require one or more electrical/mechanical equipment except the newly developed technique. The gravity-driven approach takes only about 45 min for the purification of GUVs. The recovery rate for getting the purified GUVs with diameters greater than 10 µm is quite high (efficiency > 76%) in the new technique compared to other methods.

Table 3: Comparison of methods for the purification of GUVs [34-35]

Main features	Dialysis	Centrifugation	Microfiltration	Membrane filtering	Non-electro mechanical
Electrical/ Mechanical equipments	Dialysis or cassette	Centrifuge Machine	Filter, vacuum pump, pressure regulator	Peristaltic pump	Not required
Purification Duration	Long (hours)	Short (10-30 min)	Very short (< 10 min)	Medium (40-50 min)	Medium (40-50 min)
Recovery-rate	Medium-High	Medium (> 50%)	Low (<50%)	Efficiency (> 77%)	Efficiency (> 76%)
Requirement	None	Density difference	Low lipid concentration	Low lipid concentration	Low lipid concentration
Cost	Expensive	Expensive	Expensive	Relatively expensive	Low cost
Advantage	Mild conditions	Easy	Easy and fast	Easy	Easy and simple
Drawback	Slow	Required density difference	Low recovery rate	Required pump and electricity	None

CHAPTER 5

CONCLUSIONS

The cell membrane is a complex structure which contains mainly proteins, lipids, cholesterol and lipopolysaccharides. To avoid the complexity, lipid membranes of giant unilamellar vesicles (GUVs) with diameters 10 μm or more have been used as a mimic of cell membrane for investigating various vesicle related experiments. In this thesis, it has been developed a membrane purification technique in which the gravity is used to flow the buffer in the purification unit and the flow rate of buffer is controlled by a locally available regulator. A polycarbonate membrane with pore size 10 μm pore is one of the important elements in the purification process. At first it is prepared the 40%DOPG/60%DOPC-GUVs (% indicates mole %) using the standard natural swelling method and then purifies them using the proposed technique. Both the unpurified and purified GUVs are analyzed statistically for getting the size distribution of GUVs. The size distributions are fitted with a well known lognormal distribution from where the mean and variance of the distribution are obtained. These two parameters are used to calculate the average sizes of GUVs. The results were evaluated by the values of average sizes of vesicles, fraction of GUVs with sizes $<10 \mu\text{m}$ (%), efficiency of getting GUVs with sizes $\geq 10 \mu\text{m}$ (%), purification duration etc in different flow rate. In each case, the results obtained in the proposed technique are compared with the well-established membrane filtering method.

Some existing techniques are used for the purification of GUVs, but all of them need one or more electromechanical devices which need continuous electrical or mechanical energy during the purification. Moreover, none of the techniques/methods investigated the statistical analysis for getting the average sizes of GUVs. This new technique purifies GUVs using gravity instead of any electromechanical devices without energy consumption. In this technique, due to gravity the potential energy of buffer which kept at a finite height is converted into kinetic energy that is enough to flow the buffer containing GUVs suspension in the purification system. The technique provides a large number of similar size GUVs with diameters 10–30 μm by removing LUVs and the

non-entrapped solutes like fluorescent probes. The GUVs are purified using different flow rate such as 1.0, 1.5, 2.0 and 3.0 mL/min. Before adding the GUVs suspension in the purification process, the buffer which flows through the tube due to gravity is taken into an eppendorf tube for one minute and then measured it using micropipette for calibrating the flow rate. The same procedure was repeated more than three times. Finally, the GUVs suspension was added to the flow of buffer for the purification. Before and after purification of GUVs, some phase contrast images have been taken using an inverted phase contrast microscope connected with CCD camera. The diameters of 300-400 GUVs have been measured from several phase contrast images for each flow rate and prepared a histogram using origin software. The histograms are fitted with a theoretical equation of lognormal distribution and checked out the best fitting by using the co-efficient of determination (R^2) of each histogram. In case of unpurified GUVs, the values of R^2 are 0.91, 0.89 and 0.95 for the flow rate 1.0, 1.5 and 2.0 mL/min. respectively. The average sizes of GUVs of two independent experiments are obtained ($10. \pm 0.7$), (11.2 ± 3.7) and (8.8 ± 0.4) μm for the flow rate 1.0, 1.5 and 2.0 mL/min, respectively. The average diameters of purified GUVs in first independent experiments are obtained 17.5, 18.9 and 20.3 μm for the flow rate 1.0, 1.5 and 2.0 mL/min, respectively. The R^2 values in this experiment are found 0.96, 0.89, and 0.96 for 1.0, 1.5 and 2.0 mL/min, respectively. In the second independent experiments the average diameters of GUVs are obtained 16.4, 18.5 and 19.9 μm for 1.0, 1.5 and 2.0 mL/min, respectively. The R^2 values in this experiment are found 0.95, 0.94 and 0.80 for 1.0, 1.5 and 2.0 mL/min, respectively. From these two independent experiments, the average size of GUVs after purification are obtained (16.9 ± 0.8), (18.7 ± 0.3) and (20.0 ± 0.1) μm for 1.0, 1.5 and 2.0 mL/min, respectively. It is clear that the average sizes of purified GUVs are increased compared with the unpurified GUVs in each flow rate. This is because the smaller GUVs whose diameters less than 10 μm are passed away through the pores of polycarbonate membrane during purification.

Using the well-known membrane filtering method, the average sizes of unpurified GUVs from two independent experiments are obtained (8.1 ± 0.8), (11.3 ± 4.3) and (7.7 ± 0.3) μm and the values of R^2 are 0.93, 0.85 and 96 for 1.0, 1.5 and 2.0 mL/min, respectively. In the same technique, the average diameters of purified GUVs in first

independent experiments are obtained 16.1, 18.8 and 20.0 μm for 1.0, 1.5 and 2.0, respectively. In this case, the values of R^2 are found 0.93, 0.89 and 0.86 for 1.0, 1.5 and 2.0 mL/min, respectively. Similarly, in the second independent experiments, the average diameters of purified GUVs are obtained 19.1, 20.5 and 19.9 μm for 1.0, 1.5 and 2.0 mL/min, respectively. The values of R^2 in this case are found 0.91, 0.90 and 0.89 for 1.0, 1.5 and 2.0 mL/min, respectively. From these two independent experiments, the average sizes of GUVs are obtained (17.6 ± 2.1) , (19.7 ± 1.2) and (20.0 ± 0.1) μm for 1.0, 1.5 and 2.0 mL/min, respectively. These investigations indicate that the average sizes of purified GUVs are also obtained higher than that of unpurified ones in membrane filtering method. This is because the smaller GUVs with diameter less than 10 μm are passed away through the polycarbonate membrane during purification. It illustrates that the new technique gives the similar results within the error bar to that of membrane filtering method. At higher flow rate (like 3.0 mL/min.), the average diameter for two independent experiments are decreased to 18.2 and 17.5 μm and the average size of GUVs is also decreased to 17.9 μm as compared to that of 2.0 mL/min. As a comparison of proposed technique and the membrane filtering method, both the cases the average sizes of GUVs increase with the increase of flow rate up to 2 mL/min, and then decrease above this flow rate. Therefore, the new technique purifies the GUVs by removing the non-entrapped solutes at optimum flow rate 1.0–2.0 mL/min. At higher flow rate some GUVs with diameter greater than 10 μm may rupture or pass away through the polycarbonate filter paper due to higher pressure of buffer flow and consequently the average sizes of GUVs decrease. Using the second (double) purification, it is possible to remove almost all the small vesicles to give concentrated similarly-sized GUVs. At flow rate 2.0 mL/min, the average sizes of purified GUVs are obtained (20.5 ± 0.3) and (22.3 ± 0.5) μm for single and double purification, respectively. In the proposed new technique, the efficiencies of getting the GUVs with diameters greater than 10 μm are obtained 76, 80 and 84% and in the membrane filtering method that are 77, 85 and 86% for 1.0, 1.5 and 2.0 mL/min, respectively. Increasing efficiency with increasing flow rate means that the number of GUVs with diameter less than 10 μm is decreased in the GUVs suspension after purification. Therefore, the new technique provides similar results to that of the

membrane filtering method but does not require any specialized electrical or mechanical devices. This technique can perform the purification of GUVs using only gravity without any electromechanical devices and the apparatuses are repeatedly usable except polycarbonate membrane. The technique can be applied to purify the GUVs prepared by any methods. In addition, this technique is eco-friendly, time saving and cost effective. Therefore, this simple and low cost non-electromechanical technique might be a promising tool for the purification of GUVs as model lipid membranes.

5.1 Recommendations

The following scopes are recommended for future work-

- In our experiment, only DOPC and DOPG lipids have used. The experiment can perform using various lipids in future.
- 40%DOPG and 60%DOPC-GUVs have used in this research work. In future, same work can perform using GUVs of different composition of lipid like 50%DOPG + 50%DOPC-GUVs, 60%DOPG + 40%DOPC-GUVs etc.
- Two different types of filter paper with different pore size can be used for getting a specific size distribution.
- This purification technique can use for the other GUV synthesis method.

CHAPTER 6

REFERENCES

- [1] Rawicz, W., Olbrich, K. C., McIntosh, T., Needham, D. & Evans, E. "Effect of Chain Length and Unsaturation on Elasticity of Lipid Bilayers." *Biophys. J.* 79, 328–339 (2000).
- [2] Tanaka, T., Tamba, Y., Masum, S. M., Yamashita, Y. & Yamazaki, M. "La³⁺ and Gd³⁺ induce shape change of giant unilamellar vesicles of phosphatidylcholine." *Biochim. Biophys. Acta BBA - Biomembr.* 1564, 173–182 (2002)
- [3] Yamashita, Y., Masum, S. Md., Tanaka, T. & Yamazaki, M. "Shape Changes of Giant Unilamellar Vesicles of Phosphatidylcholine Induced by a De Novo Designed Peptide Interacting with Their Membrane Interface." *Langmuir* 18, 9638–9641 (2002).
- [4] Karal, M. A. S., Levadnyy, V., Tsuboi, T., Belaya, M. & Yamazaki, M. "Electrostatic interaction effects on tension-induced pore formation in lipid membranes." *Phys. Rev. E* 92, (2015).
- [5] Karal, M. A. S. & Yamazaki, M. "Communication: Activation energy of tension-induced pore formation in lipid membranes." *J. Chem. Phys.* 143, 081103 (2015).
- [6] Karal, M. A. S., Levadnyy, V. & Yamazaki, M. "Analysis of constant tension-induced rupture of lipid membranes using activation energy." *Phys. Chem. Chem. Phys.* 18, 13487–13495 (2016).
- [7] Yamashita, Y., Oka, M., Tanaka, T. & Yamazaki, M. "A new method for the preparation of giant liposomes in high salt concentrations and growth of protein microcrystals in them." *Biochim. Biophys. Acta BBA - Biomembr* 1561, 129–134 (2002).
- [8] Baumgart, T., Hess, S. T. & Webb, W. W. "Imaging coexisting fluid domains in biomembrane models coupling curvature and line tension." *Nature* 425, 821–824 (2003).
- [9] Walde, P., Cosentino, K., Engel, H. & Stano, P. "Giant Vesicles: Preparations and Applications." *Chem. Bio. Chem.* 11, 848–865 (2010).

- [10] Vitkova, V., Mader, M. & Podgorski, T. "Deformation of vesicles flowing through capillaries." *Europhys. Lett. (EPL)* 68, 398–404 (2004).
- [11] Wick, R., Walde, P. & Luisi, P. L. Light microscopic investigations of the autocatalytic self-reproduction of giant vesicles." *J. Am. Chem. Soc.* 117, 1435–1436 (1995).
- [12] Menger, F. M. & Gabrielson, K. "Chemically-Induced Birthing and Foraging in Vesicle Systems." *J. Am. Chem. Soc.* 116, 1567–1568 (1994).
- [13] Takakura, K., Toyota, T. & Sugawara, T. "A Novel System of Self-Reproducing Giant Vesicles." *J. Am. Chem. Soc.* 125, 8134–8140 (2003).
- [14] Zhu, T. F. & Szostak, J. W. "Coupled Growth and Division of Model protocell Membranes." *J. Am. Chem. Soc.* 131, 5705–5713 (2009).
- [15] Peterlin, P., Arrigler, V., Kogej, K., Svetina, S. & Walde, P. "Growth and shape transformations of giant phospholipid vesicles upon interaction with an aqueous oleic acid suspension." *Chem. Phys. Lipids* 159, 67–76 (2009).
- [16] Li, Liang, X., Lin, M., Qiu, F. & Yang, Y. "Budding Dynamics of Multicomponent Tubular Vesicles." *J. Am. Chem. Soc.* 127, 17996–17997 (2005).
- [17] Staneva, G., Seigneuret, M., Koumanov, K., Trugnan, G. & Angelova, M. I. "Detergents induce raft-like domains budding and fission from giant unilamellar heterogeneous vesicles." *Chem. Phys. Lipids* 136, 55–66 (2005).
- [18] Zhou, Y. & Yan, D. "Real-Time Membrane Fusion of Giant Polymer Vesicles." *J. Am. Chem. Soc.* 127, 10468–10469 (2005).
- [19] Pantazatos, D. P. & MacDonald, R. C. "Directly Observed Membrane Fusion Between Oppositely Charged Phospholipid Bilayers." *J. Mem. Bio.* 170, 27–38 (1999).
- [20] Lei, G. & MacDonald, R. C. "Lipid Bilayer Vesicle Fusion: Intermediates Captured by High-Speed Microfluorescence Spectroscopy." *Biophys. J.* 85, 1585–1599 (2003).
- [21] Karal, M. A. S., Alam, J. Md., Takahashi, T., Levadny, V. & Yamazaki, M. "Stretch-Activated Pore of the Antimicrobial Peptide, Magainin 2." *Langmuir* 31, 3391–3401 (2015).
- [22] Moniruzzaman, Md., Alam, J. Md., Dohra, H. & Yamazaki, M. "Antimicrobial Peptide Lactoferricin B-Induced Rapid Leakage of Internal Contents from Single Giant Unilamellar Vesicles." *Biochem.* 54, 5802–5814 (2015).

- [23] Hasan, M., Karal, M. A. S., Levadnyy, V. & Yamazaki, M. "Mechanism of Initial Stage of Pore Formation Induced by Antimicrobial Peptide Magainin 2." *Langmuir* 34, 3349–3362 (2018).
- [24] Islam, Md. Z., Ariyama, H., Alam, J. Md. & Yamazaki, M. "Entry of Cell-Penetrating Peptide Transportan 10 into a Single Vesicle by Translocating Across Lipid Membrane and Its Induced Pores." *Biochem.* 53, 386–396 (2014).
- [25] Sharmin, S. *et al.* "Effects of Lipid Composition on the Entry of Cell-Penetrating Peptide Oligoarginine into Single Vesicles." *Biochem.* 55, 4154–4165 (2016).
- [26] Islam, Md. Z., Sharmin, S., Levadnyy, V., Alam Shibly, S. U. & Yamazaki, M. "Effects of Mechanical Properties of Lipid Bilayers on the Entry of Cell-Penetrating Peptides into Single Vesicles." *Langmuir* 33, 2433–2443 (2017).
- [27] Alam, J. Md., Kobayashi, T. & Yamazaki, M. "The Single-Giant Unilamellar Vesicle Method Reveals Lysenin-Induced Pore Formation in Lipid Membranes Containing Sphingomyelin." *Biochem.* 51, 5160–5172 (2012).
- [28] Laurencin, M., Georgelin, T., Malezieux, B., Siaugue, J.-M. & Ménager, C. "Interactions Between Giant Unilamellar Vesicles and Charged Core–Shell Magnetic Nanoparticles." *Langmuir* 26, 16025–16030 (2010).
- [29] Islam, Md. Z., Alam, J. Md., Tamba, Y., Karal, M. A. S. & Yamazaki, M. "The single GUV method for revealing the functions of antimicrobial, pore-forming toxin, and cell-penetrating peptides or proteins." *Phys. Chem. Chem. Phys.* 16, 15752–15767 (2014).
- [30] Sugiura S. "Novel Method for Obtaining Homogeneous Giant Vesicles from a Monodisperse Water-in-Oil Emulsion Prepared with a Microfluidic Device." *Langmuir* 24, 4581–4588 (2008).
- [31] Pautot, S., Frisken, B. J. & Weitz, D. A. "Production of Unilamellar Vesicles Using an Inverted Emulsion." *Langmuir* 19, 2870–2879 (2003).
- [32] Angelova, M. I. & Dimitrov, D. S. "Liposome Electroformation."
- [33] Baker, R. W. "*Membrane technology and applications.*" (McGraw-Hill, 2000).
- [34] Tamba, Y., Terashima, H. & Yamazaki, M. "A membrane filtering method for the purification of giant unilamellar vesicles." *Chem. Phys. Lipids* 164, 351–358 (2011).
- [35] Fayolle, D., Fiore, M., Stano, P. & Strazewski, P. "Rapid purification of giant lipid vesicles by microfiltration." *PLOS ONE* 13, e0192975 (2018).

- [36] Murate, M. & Kobayashi, T. "Revisiting transbilayer distribution of lipids in the plasma membrane." *Chem. Phys. Lipids* **194**, 58–71 (2016).
- [37] Biomembrane. Available: https://en.wikipedia.org/wiki/Biological_membrane.
- [38] Shohda, K., Takahashi, K. & Suyama, A. "A method of gentle hydration to prepare oil-free giant unilamellar vesicles that can confine enzymatic reactions." *Biochem. Biophys. Rep.* **3**, 76–82 (2015).
- [39] Altamura, E., Carrara, P., D'Angelo, F., Mavelli, F. & Stano, P. "Extrinsic stochastic factors (solute partition) in gene expression inside lipid vesicles and lipid-stabilized water-in-oil droplets: a review." *Synth. Biol.* **3**, (2018).
- [40] Kagan, B. L., Selsted, M. E., Ganz, T. & Lehrer, R. I. Antimicrobial Defensin Peptides Form Voltage-Dependent Ion-Permeable Channels in Planar Lipid Bilayer Membranes." *Proc. Natl. Acad. Sci. U. S. A.* **87**, 210–214 (1990).
- [41] Bretscher, M. S. "Membrane Structure: Some General Principles." *Science* **181**, 622–629 (1973).
- [42] Karal, M. A. S., Rahman, M., Ahamed, M. K., Shibly, S. A., Ahmed, M., Shakil, M. M., "Low cost non-electromechanical technique for the purification of giant unilamellar vesicles." *Eur. Biophys. J.* (2019). doi:10.1007/s00249-019-01363-6
- [43] Tanaka, T. & Yamazaki, M. "Membrane Fusion of Giant Unilamellar Vesicles of Neutral Phospholipid Membranes Induced by La^{3+} ." *Langmuir* **20**, 5160–5164 (2004).
- [44] Wesołowska, O., Michalak, K., Maniewska, J. & Hendrich, A. B. "Giant unilamellar vesicles - a perfect tool to visualize phase separation and lipid rafts in model systems." *Acta Biochim. Pol.* **56**, (2009).
- [45] Angelova, M. I., Soléau, S., Méléard, Ph., Faucon, F. & Bothorel, P. "Preparation of giant vesicles by external AC electric fields. Kinetics and applications. in *Trends in*

- Coll. and Int. Sci. VI*" (eds. Helm, C., Lösche, M. & Möhwald, H.) **89**, 127–131 (Steinkopff, 1992).
- [46] Reeves, J. P. & Dowben, R. M. "Formation and properties of thin-walled phospholipid vesicles." *J. Cell. Physiol.* **73**, 49–60 (1969).
- [47] Oku, N. & Macdonald, R. C. "Formation of giant liposomes from lipids in chaotropic ion solutions." *Biochim. Biophys. Acta BBA - Biomembr.* **734**, 54–61 (1983).
- [48] Higashi, K., Suzuki, S., Fujii, H. & Kirino, Y. "Preparation and Some Properties of Giant Liposomes and Proteoliposomes1." *J. Biochem. (Tokyo)* **101**, 433–440 (1987).
- [49] Menger, F. M. & Gabrielson, K. D. "Cytomimetic Organic Chemistry: Early Developments." *Angew. Chem. Int. Ed. Engl.* **34**, 2091–2106 (1995).
- [50] Menger, F. M. & Angelova, M. I. "Giant Vesicles: Imitating the Cytological Processes of Cell Membranes." *Acc. Chem. Res.* **31**, 789–797 (1998).
- [51] Nishimura, K., Suzuki, H., Toyota, T. & Yomo, T. "Size control of giant unilamellar vesicles prepared from inverted emulsion droplets." *J. Coll. Int. Sci.* **376**, 119–125 (2012).
- [52] Nishimura, K. *et al.* "Population Analysis of Structural Properties of Giant Liposomes by Flow Cytometry." *Langmuir* **25**, 10439–10443 (2009).
- [53] Szoka, F. & Papahadjopoulos, D. Comparative Properties and Methods of Preparation of Lipid Vesicles (Liposomes). *Annu. Rev. Biophys. Bioeng.* **9**, 467–508 (1980).
- [54] McIntosh, T. J., Simon, S. A. & MacDonald, R. C. "The organization of n-alkanes in lipid bilayers." *Biochim. Biophys. Acta BBA - Biomembr.* **597**, 445–463 (1980).
- [55] prieve1987.

- [56] Bibette, J. "Depletion interactions and fractionated crystallization for polydisperse emulsion purification." *J. Coll. Int. Sci.* **147**, 474–478 (1991).
- [57] Ferri, J. K. & Stebe, K. J. "Which surfactants reduce surface tension faster? A scaling argument for diffusion-controlled adsorption." *Adv. Coll. Int. Sci.* **85**, 61–97 (2000).
- [58] Jahn, A., Vreeland, W. N., Gaitan, M. & Locascio, L. E. "Controlled Vesicle Self-Assembly in Microfluidic Channels with Hydrodynamic Focusing." *J. Am. Chem. Soc.* **126**, 2674–2675 (2004).
- [59] de Souza, T. P. "Vesicle aggregates as a model for primitive cellular assemblies." *Phys. Chem. Chem. Phys.* **19**, 20082–20092 (2017).
- [60] Diamond, R. A. "Separation and enrichment of cell populations by centrifugal elutriation." *Methods* **2**, 173–182 (1991).
- [61] DOPG lipid structure. Available: <https://avantilipids.com/product/840475> (Access date: 05/08/2019)
- [62] DOPG lipid structure. <https://alphahelixproject.files.wordpress.com/2014/12/dopc2.jpg> (Access date: 05/08/2019)
- [63] BSA structure. Available: <https://www.mdpi.com/1420-3049/22/8/1258> (Access date: 05/08/2019)
- [64] EGTA structure. Available: <https://www.sigmaaldrich.com/catalog/product/sigma/e3889?lang=en®ion=BD> (Access date: 05/08/2019)
- [65] PIPES structure. Available: <https://en.wikipedia.org/wiki/PIPES#/media/File:PIPES.svg> (Access date: 05/08/2019)
- [66] Chloroform structure. Available: <https://my.all.biz/chloroform-g43844> (Access date: 05/08/2019)
- [67] Leipnik, R. B. "On lognormal random variables: I-the characteristic function." *J. Aust. Math. Soc. Ser. B Appl. Math.* **32**, 327–347, 1991.
- [68] Lognormal distribution. Available: https://upload.wikimedia.org/wikipedia/commons/a/ae/PDF-log_normal_distributions.svg (Access date: 05/08/2019)

[69] Georgiades P. "The flexibility and dynamics of the tubules in the endoplasmic reticulum." *Sci. Rep.* 7, 16474 (2017).

[70] Huang, C., Quinn, D., Sadovsky, Y., Suresh, S. & Hsia, K. J. "Formation and size distribution of self-assembled vesicles." *Proc. Natl. Acad. Sci.* 114, 2910–2915 (2017).

APPENDIX

Pear reviewed journal

Low cost non-electromechanical technique for the purification of giant unilamellar vesicles. *Eur. Biophys. J.* **48**, 349–359 (2019).

Authors: Mohammad Abu Sayem Karal, **Mostafizur Rahman**, Md. Kabir Ahamed, Sayed Ul Alam Shibly, Marzuk Ahmed and Md. Mostofa Shakil

Journal: European Biophysics Journal

<https://doi.org/10.1007/s00249-019-01363-6>

Publisher: Springer

Impact factor: **2.527**

Conference Presentations

1. **Mostafizur Rahman**, Mohammad Abu Sayem Karal, Md. Kabir Ahamed, Marzuk Ahmed, Md. Mostofa Shakil, Md. Nazmul Alam, Md. Mehedi Hasan, Shareef Ahammed. “**Non-Electromechanical Technique for the Purification of Giant Unilamellar Vesicles (GUVs).**” International Conference on Electronics and ICT - 2018, 25-26 November, 2018, Dhaka, Bangladesh.
2. **Mostafizur Rahman**, Mohammad Abu Sayem Karal, Md. Kabir Ahamed, Marzuk Ahmed, and Md. Mostofa Shakil “**Development of a Low Cost Technique for the Purification of Vesicles Working Without Electricity and Electromechanical Devices.**” National Conference on Physics-2019, 07-09 February, 2019, Dhaka, Bangladesh.

Collaborative Presentations

1. Mohammad Abu Sayem Karal, Md. Mostofa Shakil, Md. Mehedi Hasan, Marzuk Ahmed, **Mostafizur Rahman**, Md. Kabir Ahamed, Md. Sayful Islam “**Synthesis and Observations of Giant Unilamellar Vesicles (GUVs) of Lipid Membrane.**” International conference on nanotechnology and condensed matter physics, 11-12 January, 2018, Dhaka, Bangladesh.

2. Shareef Ahammed, Md. Mostofa Shakil, Mohammad Abu Sayem Karal, Md. Kabir Ahamed, **Mostafizur Rahman**, Md. Marzuk Ahmed, Md. Mehedi Hasan, and Mohammad Moniruzzaman. Biosynthesis of Magnetic “Nanoparticles and Investigations Its Interactions with Lipid Membranes of Vesicles” National Conference on Physics-2019, 07-09 February, 2019 Dhaka, Bangladesh.
3. Md. Kabir Ahamed, Mehedi Hasan, Mohammad Abu Sayem Karal, **Mostafizur Rahman**, Md. Marzuk Ahmed, and Md. Mostofa Shakil. “Development of Irreversible Electroporation (IRE) Technique for the Investigations of Rupture of Giant Unilamellar Vesicles” National Conference on Physics-2019, 07-09 February, 2019, Dhaka, Bangladesh.
4. Marzuk Ahmed, Mohammad Abu Sayem Karal, Md. Kabir Ahamed and **Mostafizur Rahman**. “Effects of Salt Concentrations and Surface Charge Density on the Size Distribution and Average Size of Giant Unilamellar Vesicles” National Conference on Physics-2019, 07-09 February, 2019, Dhaka, Bangladesh.
5. Md. Kabir. Ahamed, Mohammad Abu Sayem Karal, Marzuk Ahmed, **Mostafizur Rahman**, Mehedi Hasan, Md. Mostofa Shakil, Md. Nazmul Alam, and Md. Sayful Islam. “Irreversible Electroporation (IRE) Technique for the Study of Pore Formation in the Lipid Membranes of Giant Unilamellar Vesicles (GUVs)” International Conference on Electronics and ICT - 2018, 25-26 November, 2018, Dhaka, Bangladesh.
6. Marzuk Ahmed, Mohammad Abu Sayem Karal, Md. Kabir Ahamed, **Mostafizur Rahman**, Mostofa Shakil, and Md. Nazmul Alam “Effects of Electrostatic Interaction on the Sizes of Giant Unilamellar Vesicles (GUVs)” International Conference on Electronics and ICT - 2018, 25-26 November, 2018, Dhaka, Bangladesh.
7. Mohammad Abu Sayem Karal, Md. Kabir Ahamed, Md. Mostofa Shakil, Marzuk Ahmed, **Mostafizur Rahman**, Md. Mehedi Hasan, Md. Nazmul Alam, and Sayed Ul Alam Shibly. “Edge Detection of Peptide-Induced Submicron Pores in the Lipid Membranes through ImageJ” International Conference on Electronics and ICT - 2018, 25-26 November, 2018, Dhaka, Bangladesh.